TP 6681E

german & milne inc.

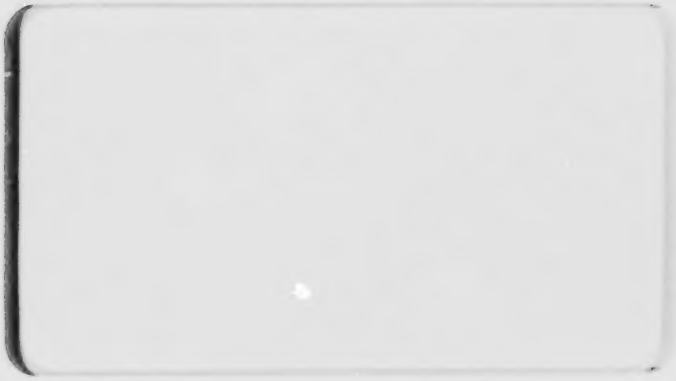

Prepared for the
Transportation Development Centre
Transport Canada

July 1985

CA1
DTC 820
85
S58
c.2

Montreal, Quebec
Ottawa, Ontario

TP 6681E

SMALL WATERPLANE AREA TWIN HULLED (SWATH) VESSEL ICE TESTS

For the
Transportation Development Centre
Contract No: OSD 83-00033

Prepared by:
J. E. Carter
D. B. Colbourne
GERMAN & MILNE INC.
Ottawa, Ontario, Canada

Canada Institute for Scientific and Technical Information (CISTI)
REÇU LE
OCT 8 1985
Government Publication Officielle
Transport Canada / Transports Canada

July 1985

The contents of this report reflect the view of the Contractor and not necessarily the official views or policies of the Transportation Development Centre, Transport Canada.

REPORT DOCUMENTATION FORM

1. Transport Canada Report No.	2. TDC Project No.	3. Recipient's Catalogue No.
TP 6681E	4915	

4. Title and Subtitle	5. Report Date
Small Waterplane Area Twin Hulled (SWATH) Vessel Ice Tests	July 1985
	6. Performing Organization Report No. 7070/R.01

7. Author(s)	8. Transport Canada File No.
J.E. Carter, B. Colbourne	D1460-157-2

9. Performing Organization Name and Address	10. DSS File No.
German & Milne Inc. Place de Ville, 112 Kent Street, 15th Floor, Tower 'B' Ottawa, Ontario, K1P 5P2	10SD.T8200-2-2574
	11. DSS or Transport Canada Contract No. 0SD83-00033

12. Sponsoring Agency Name and Address	13. Type of Report and Period Covered
Transportation Development Centre (TDC) Complexe Guy Favreau, Suite 601, West Tower 200 Dorchester Blvd., West Montreal, Quebec, H2Z 1X4	14. Sponsoring Agency Code 4915

15. Supplementary Notes	16. TDC Project Officer
	J.E. Laframboise

17. Abstract

A series of model tests was carried out on Small Waterplane Area Twin Hull (SWATH) vessels to determine the icebreaking resistance relative to a conventional monohull icebreaker of similar displacement. The tests were carried out in open water, pre-sawn ice and continuous level ice in order to determine the relative magnitudes of the icebreaking and ice clearing components of resistance in addition to the absolute ice resistance. An attempt was also made to determine the degree of interference between the SWATH vessel hulls with regard to icebreaking.

The results of the tests indicate that the ice resistance of a SWATH vessel would be significantly higher than that of the resistance of a similar monohull. The ice breaking component was determined to represent 80 - 85% of the total resistance for a SWATH vessel in ice. In addition, the tests indicated that there are interference effects between the hulls which become worse as speed increases.

A further significant conclusion of the study is that traditional icebreaking formulations do not seem to be valid except within a very narrow range for monohull vessels.

18. Key Words	19. Distribution Statement
SWATH, Ice Resistance, Ice Testing Model Testing	Limited number of copies available from TDC

20. Security Classification (of this report)	21. Security Classification (of this page)	22. No. of Pages	23. Price
Nil	Nil		

TDC/CDT 79-005

FORMULE DE DOCUMENTATION POUR RAPPORT

1. N° du rapport Transports Canada	2. N° de l'étude — CDT	3. N° de catalogue du destinataire
TP 6681E	4915	

4. Titre et sous-titre	5. Date du rapport
Small Waterplane Area Twin Hulled (SWATH) Vessel Ice Tests	juillet 1985
	6. N° du rapport de l'organisme exécutant: 7070/R.01

7. Auteur(s)	8. N° de dossier Transports Canada
J.E. Carter, B. Colbourne	D1460-157-2

9. Nom et adresse de l'organisme exécutant	10. N° de dossier — ASC
German & Milne Inc. Place de Ville, 112 rue Kent, 15e étage Tour 'B', Ottawa, Ontario, K1P 5P2	10SD.T8200-2-2574
	11. N° de contrat — ASC ou Transports Canada: 0SD83-00033

12. Nom et adresse de l'organisme parrain	13. Genre de rapport et période visée
Centre de développement des transports (CDT) Complexe Guy Favreau, suite 601, tour ouest 200 boul. Dorchester, ouest, Montréal, Québec, H2Z 1X4	14. Code de l'organisme parrain: 4915

15. Remarques additionnelles	16. Agent de projet — CDT
	J.E. Laframboise

17. Résumé

Des navires à double coque à plan d'eau réduit (SWATH) ont subi une série d'essais par le biais de modèles réduits dans le but de déterminer la résistance de déglaçage par rapport à un brise-glace conventionnel de type monocoque et de déplacement similaire. Les essais ont été effectués en eau libre, dans des glaces pré-coupées, et dans des glaces uniformes en vue de déterminer l'ampleur relative des composants de résistance engendrée par la rupture et le dégagement des glaces, en plus de la résistance totale de déglaçage. On a également tenté de déterminer le degré d'interférence entre les coques des navires SWATH durant le déglaçage.

Les résultats des essais indiquent que la résistance aux glaces d'un navire SWATH serait beaucoup plus élevée que celle d'un monocoque similaire. Le composant rupture s'élèverait à 80 - 85% de la résistance totale pour un navire SWATH dans la glace.

Une autre conclusion significative de l'étude est que les théories traditionnelles de résistance des glaces ne semblent être valides que dans une étendue très restreinte et pour des navires monocoques.

18. Mots-clés	19. Diffusion
SWATH, Résistance de déglaçage, Essais dans des glaces, Essais de modèles	Le CDT dispose d'un nombre limité d'exemplaires

20. Classification de sécurité (de ce rapport)	21. Classification de sécurité (de cette page)	22. Nombre de pages	23. Prix
Néant	Néant		

CDT/TDC 78-005

PROJECT TEAM

John Carter
Bruce Colbourne
Nozer Dadachanji

SUMMARY

This report details the results and analysis of a series of model trials carried out on 1:20 scale Small Waterplane Area Twin Hulled (SWATH) vessels. The purpose of these model tests was to compare the ice resistance of the SWATH type vessel to a monohull vessel of similar displacement. Based on conventional ice breaking theories it has been hypothesized that the lower effective beam of the SWATH would result in lower ice resistance.

The test were carried out for a SWATH model with two different bow configurations in open water, pre-sawn ice and continuous level ice. This allowed the resistance of the models to be separated into ice breaking, ice clearing and open water components.

The results of the test show that the resistance of a SWATH vessel is substantially higher in ice than a monohull vessel of similar displacement. This indicates that the conventional icebreaking theory predicting strong beam dependence is invalid. From the trials it appears that the resistance associated with breaking the ice cover is the dominant component of ice resistance. This component is not strongly beam dependent and the higher resistance of the SWATH stems from breaking ice at two locations i.e., the forward part of each hull.

Serious problems in ice testing were also identified. It is clear that major improvements are needed in the areas of model ice properties particularly Elastic Modulus and Fracture Toughness. In addition a means of stabilizing the ice at a given state where properties can be maintained is required. These items would improve the reliability and repeatability of ice model tests.

Although these tests did not validate the original hypothesis they did provide valuable information on ice breaking and model testing.

SOMMAIRE

Ce rapport décrit les résultats et l'analyse d'une série d'essais effectués sur modèles réduits à l'échelle 1:20 de navires catamaran à plan d'eau réduit (SWATH). L'objectif de ces essais était de comparer la résistance aux glaces d'un tel navire par rapport à celle d'un navire monocoque de déplacement similaire. Fondé sur des théories conventionnelles de déglaçage, on a supposé que la largeur plus étroite effective du SWATH résulterait en une résistance plus faible aux glaces.

Les essais ont eu lieu en eau libre, dans des glaces pré-coupées, et dans des glaces uniformes, en utilisant un modèle de navire SWATH avec deux formes de proue. Cette démarche a permis la séparation de la résistance des modèles en composants: déglaçage, dégagement, et eau libre.

Les résultats des essais démontrent que la résistance dans des glaces d'un SWATH est bien plus élevée que celle d'un navire monocoque de déplacement similaire. Cette situation invalide la théorie conventionnelle de déglaçage qui prévoit une dépendance élevée de la largeur. A partir des résultats d'essais, il apparaît que la résistance associée à la rupture de la couverture des glaces soit le composant dominant de la résistance de la glace. Ce composant ne dépend pas de la largeur de façon marquée, et la résistance plus élevée du SWATH découle du fait de briser des glaces à deux endroits, soit à la partie avant de chaque coque.

On a également identifié des problèmes sérieux liés aux essais dans la glace. Il est évident que des améliorations majeures sont nécessaires quant aux propriétés de la glace des bassins d'essais, surtout celles relatives au module d'élasticité et à la résistance à la rupture. De plus, il faut développer un moyen pour stabiliser les propriétés de la glace à un état donné. Ces points amélioreraient la fiabilité et la reproduction des essais de modèles.

Bien que ces essais n'aient pas validé l'hypothèse initiale, ils ont fourni des renseignements précieux sur le déglaçage et sur les essais de modèles réduits.

TABLE OF CONTENTS

SUMMARY

SOMMAIRE

1.0	Introduction		1
2.0	Selection of Hull Forms		3
3.0	Object of Tests		8
4.0	Test Outline		9
5.0	Results		10
	5.1	Phase 1 - Results	10
	5.2	Phase 2 - Results	10
	5.3	Control Results	13
6.0	Analysis		14
	6.1	Analysis for Level Continuous Ice	15
	6.2	Analysis for Icebreaking Components	20
7.0	Conclusions and Recommendations		24

Appendix 1 NRC Model Test Report LTR-SH-389

Appendix 2 ARCTEC Model Test Report 1904C

Appendix 3 NRC Model Test Report LTR-SH-383

LIST OF FIGURES AND TABLES

Figure 1	SWATH Model Configuration	5
Figure 2	Lines Plan R-SWATH	6
Figure 3	Lines Plan S-SWATH	7
Figure 4	Specific Ice Resistance vs Speed Phase 1	18
Figure 5	Specific Ice Resistance vs Speed Phase 2	19
Figure 6	Sample Resistance Trace	22
Table 1	Phase 1 - Test Results	11
Table 2	Phase 2 - Test Results	12
Table 3	Control Test Results	13
Table 4	Normalized Test Results	16

1.0 INTRODUCTION

The Small Waterplane Area Twin Hull (SWATH) type vessel has received a degree of attention in recent years for applications requiring a stable platform in rough seas. The SWATH vessel is similar to a catamaran except that the bulk of the displacement of the vessel is provided by large underwater pontoons. These pontoons are connected to the above water hull by relatively slim struts resulting in a low but widely separated waterplane area. The low waterplane area of these vessels results in a reduced sensitivity to wave action thus reducing motions in a seaway. It has been hypothesized that the small waterplane and low beam of these vessels would offer advantages for icebreaking.

The purpose of the research detailed in this report was to investigate the applicability of SWATH vessels to icebreaking. Traditional formulations for icebreaking resistance predict a strong dependance on vessel beam. In theory then, the much smaller effective beam of the SWATH vessel should offer considerable advantage in terms of resistance in ice. Even though there are two hulls, the width of each hull is on the order of 25% of the width of a conventional monohull vessel of the same displacement. This results in an effective beam of half that of a conventional vessel, which should give significant reduction in icebreaking resistance.

In order to assess the potential benefit of a SWATH configuration a series of model tests was performed on a twin hulled form. (A general arrangement drawing of the SWATH model used in the tests is given in Figure 1. This model does not include the pontoons normally found on conventional SWATH vessels for reasons explained later in the report.) Two different bow shapes were tested for comparison and one of the hulls (A half SWATH) was tested by itself to attempt to identify potential interference effects between the hulls. The results of these tests were then compared with results for a conventional monohull.

The testing was performed in open water, pre-sawn ice and level continuous ice at various thicknesses, ice strengths and two vessel speeds. This served to identify the relative magnitudes of the icebreaking, ice clearing and open water resistance for the SWATH form.

In general the results of the test were not as expected but did illustrate interesting and beneficial points about icebreaking resistance and model testing.

2.0 SELECTION OF HULL FORMS

The Canadian Coast Guard R-Class icebreaker hull form is a relatively recent design which has been successful in operation and extensively studied at both model and full scale. Because a reasonable base of data exists for this hullform it was selected as the control monohull for comparison with the SWATH tests.

To provide a degree of similarity, the R-Class bow form was used on the first SWATH model. For the SWATH, the forward outboard side of each hull was given an R-Class bow form with the inboard side a flat vertical surface. This arrangement is similar in effect to splitting a narrowed and deepened monohull longitudinally with each half forming one hull of the SWATH vessel. A flat vertical face was maintained on the inboard side of each hull to minimize the breaking action between the hulls. The form is illustrated in Figure 2 and the hydrostatic particulars of the Model are given in the NRC Report in Appendix A.

For comparison with the more conventional R-Class bow a simplified WAAS or shearing bow was developed. This bow consisted of a flat inclined front face and flat vertical sides. Ice knives or reamer blades were fitted at each side of the inclined front face. This type of bow induces shear failure in the ice at the reamer blades, providing a different mechanism of failure in the ice sheet. The bow form of this model is illustrated in Figure 3. Early in the program this was designated as the sled bow.

The use of these two bow types on the SWATH model provided a comparison between icebreaking by conventional bending of the ice sheet and the recently introduced shearing method which has been claimed to be a substantial improvement over conventional icebreaking.

In order to isolate the effect of vessel beam on the icebreaking mechanism, the SWATH hulls used in the model tests differ from a normal SWATH form in that the underwater pontoons have been deleted. The required displacement has been supplied by making the hulls abnormally deep but no wider than the beam at the waterplane. This measure was taken to eliminate resistance effects from ice interacting with the wider pontoons

below the water surface. It was hoped that, through observation, it would be possible to determine the best location and arrangement of pontoons to reduce interference. This later became an academic point.

Throughout the report the vessel configurations are referred to as follows:

R-Class - Hullform control model	R - Monohull
R-Class - Bow SWATH model	R - SWATH
Sled type bow - SWATH Model	S - SWATH

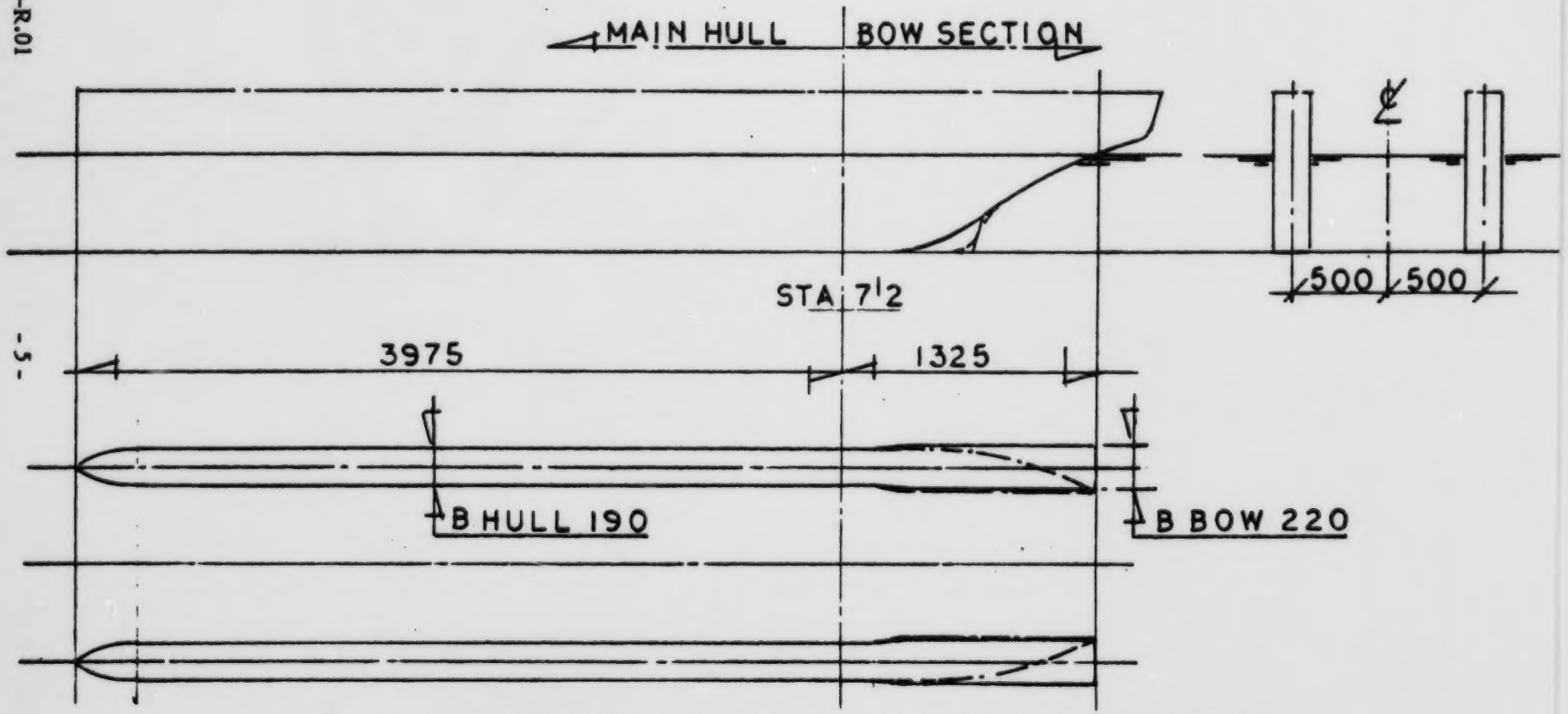

FIG 1 : SWATH MODEL CONFIGURATION

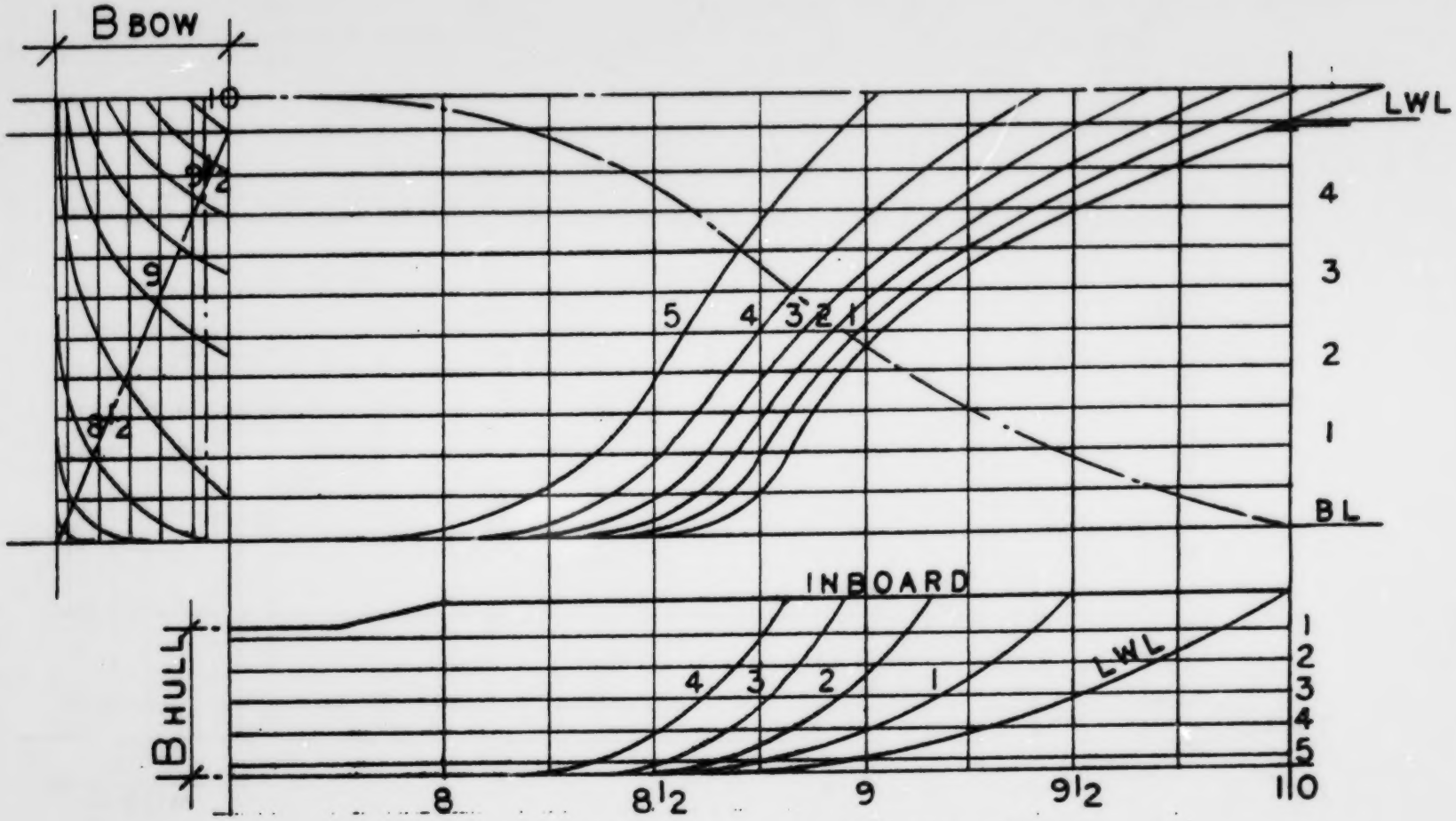

FIG 2: LINES PLAN- R SWATH

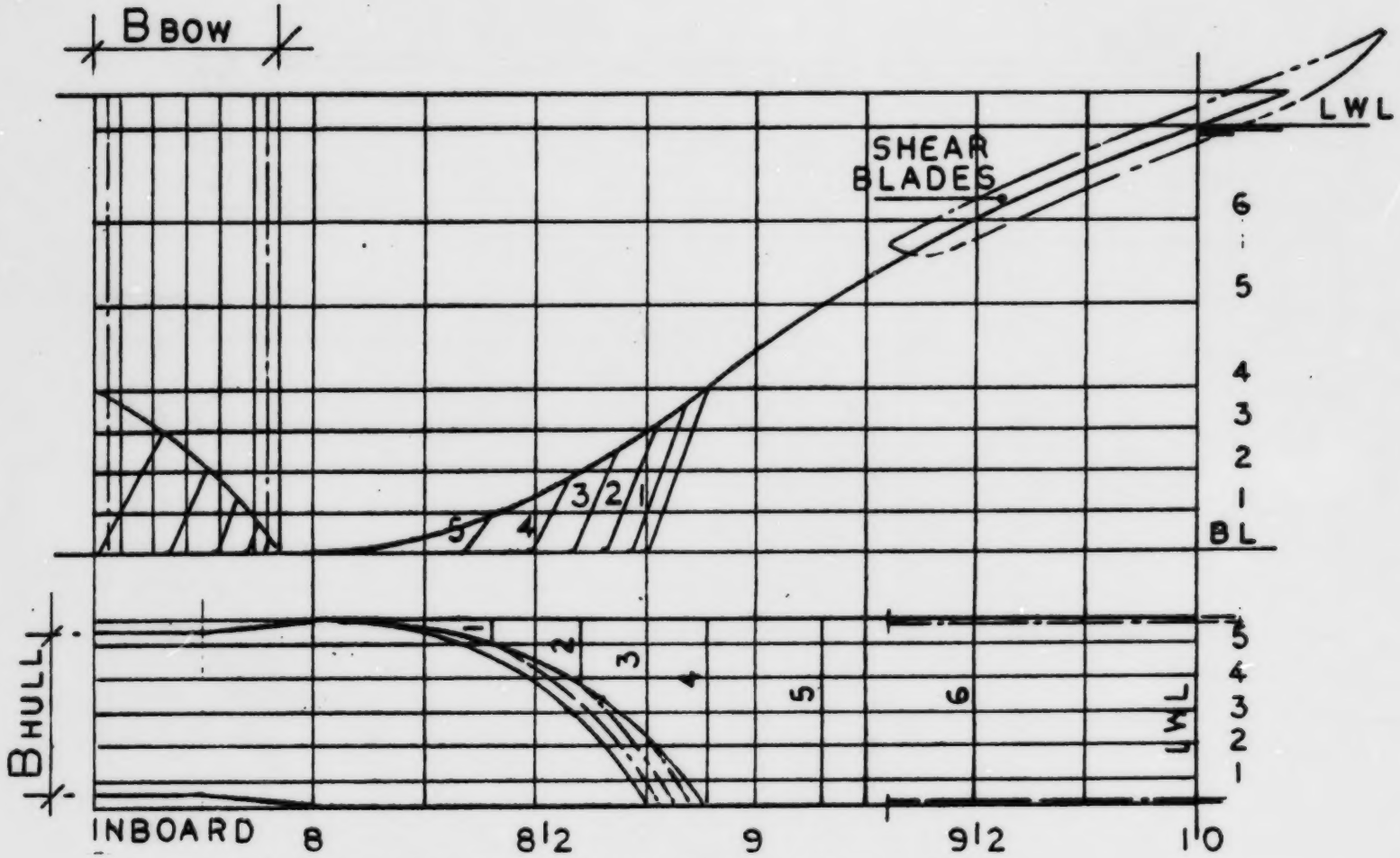

FIG 3 : LINES PLAN - S SWATH

3.0 OBJECT OF TESTS

The overall objective of the model test program was to determine whether in fact, a SWATH type vessel offered lower resistance in ice than a conventional monohull icebreaker of the same displacement.

As parts of this overall objective a number of secondary objectives were set. The first of these was the determination of the relative magnitudes of the components of the total in-ice resistance of the SWATH vessel. A second objective was to compare the effect of speed on the ice resistance of the SWATH to that of the monohull.

In addition, it was hoped to better understand the ice breaking process by observing the bending action of the conventional R-SWATH bow and the shearing action of the S-SWATH bow. It was intended that the test should demonstrate which type offered superior icebreaking and perhaps offer some insight into the failure mechanisms of model ice.

Finally, it was also planned to project the model tests results to full scale (20 to 1). This , in order to estimate the resistance of a SWATH replacement for an icebreaking patrol vessel and, to make a corresponding estimate for higher scale (60 to 1) SWATH which would be roughly equivalent to an icebreaking Arctic tanker. It was later decided that scaling the SWATH Model test results would not be practical as the icebreaking mechanism did not seem comparable to the monohull.

Part way through the test program an additional objective was added, that being the determination of possible interference effects between the hulls of the SWATH vessel while operating in ice. This objective was dealt with in the second phase of the model test program.

4.0 TEST OUTLINE

The model tests were conducted in two phases with the second phase to answer questions raised during the first series of tests. Unfortunately it became necessary to conduct the second phase of the trials at a different tank thus slightly complicating the comparison of results. Throughout the series the tests were run at a scale of 1:20.

The first phase tests were conducted at the Hydraulics Laboratory of the National Research Council of Canada. These tests are fully documented in Appendix 1 and involved open water runs, runs in pre-sawn ice and runs in continouus level ice for both the R-SWATH and S-SWATH models.

The control model tests on the R-Monohull had been performed at the NRC Laboratory previous to the SWATH tests. These tests are documented in Appendix 3. Unfortunately, runs in pre sawn ice were not performed as part of these tests and thus the breaking and clearing components of the icebreaking resistance cannot be separated for the R-Monohull. Although a predictor equation was developed for the vessel from which resistances could be calculated for zero flexural strength ice, this equation was not judged to be valid for low values of ice strength. The tests were performed over a range of ice strengths from 15 to 42 kPa (model scale) and a regression analysis performed over this range. Results calculated outside this range were judged to be of dubious reliability.

As a result of the unexpectedly high resistance values obtained in the phase one trials a second series of tests to identify interference effects between the SWATH hulls was proposed. Because of a tight schedule at the NRC facility the tests were carried out at the Arctec Ice Model Basin. These tests are documented in Appendix 2. This series involved runs in pre-sawn ice and continuous level ice the R-SWATH and for a single hull of the R-SWATH. The R-SWATH trials were repeated at the Arctec tank to provide a reference level for comparison with the NRC trials.

5.0 RESULTS

The test results from the Phase 1, Phase 2, and Control model tests are given in Tables 1, 2 and 3 respectively. These results and observations from the tests are discussed in detail in the following sections.

5.1 PHASE 1 (NRC) RESULTS

The phase 1 results shown in Table 1 cover a number of trial conditions ranging from open water to continuous ice. The open water tests (Runs 1121, 1122, 1127 and 1128) illustrate the expected poor hydrodynamic performance of the S-SWATH in comparison to the R-SWATH. Because open water tests are not subject to the high variability of ice tests these runs were not repeated and the obtained values were used for analysis purposes on all subsequent trials.

Runs 5/1118 A and 5/1118 B were tests run in relatively high strength ice. For the A part of the test. the ice was pre-sawn to reduce its flexural strength to zero thus isolating the ice clearing resistance. The B part of the test involved the same sheet of ice without pre-sawing. It is unfortunate that the ice strength was not closer to the target value of 30 kPa, as this would allow a better evaluation of the relative magnitudes of the ice clearing and ice breaking resistance. It is expected that the higher ice strength would make the breaking resistance appear disportionately large in comparison to the ice clearing resistance.

The remaining runs are for level continuous ice for the R-SWATH and the S-SWATH. In general the runs seem to be reasonable although ice strengths vary from 20 kPa to 46 kPa and E/ (Elastic Modulus/Flexural Strength) ratios are even more variable. Given the problems inherent in model ice testing the results are acceptable.

5.2 PHASE 2 (ARCTEC) RESULTS

The 01 series runs of the phase two tests (Table 2) were done for the R-SWATH to duplicate the Phase 1 R-SWATH tests. This was intended to provide a standard for comparison. Generally the resistance results were

much lower than the Phase 1 results. For two of the three cases this can be explained by the much weaker ice but the remaining case remains unexplained.

TABLE 1 - PHASE 1 TEST RESULTS

Sheet /Run	V (m/s)	h (mm)	σ_f (KPa)	E (MPa)	R (N)	Model	Comments
1/1104	0.3	28	31	6.5	149	R-Swath	
1/1107	0.6	29	22	17.6	148	R-Swath	
3/1111	0.3	38	46	19.0	196	R-Swath	
4/1115	0.3	45	20	50.5	236	R-Swath	
5/1118	0.3	38	0	-	46	R-Swath	Pre-Sawn Ice
5/1118	0.3	39	78	-	310	R-Swath	
-/1121	0.3	0	-	-	6.4	R-Swath	Open Water
-/1122	0.6	0	-	-	22	R-Swath	Open Water
6/1125	0.3	34	28	26.0	121	S-Swath	
-/1127	0.3	0	-	-	9.3	S-Swath	Open Water
-/1128	0.6	0	-	-	34.3	S-Swath	Open Water
7/1130	0.6	32	28	17.2	173	S-Swath	

V = Model velocity
h = ice thickness
σ_f = ice flexural strength
E = ice elastic modulus
R = model resistance

Note: Cases where the same Run Number appears twice in the table indicate that two sets of data were taken during the length of the run.

TABLE 2 - PHASE 2 TEST RESULTS

Test No.	Run No.	V (M/s)	h (m)	σ_f (KPa)	E (MPa)	R (N)	Model	Comments
01	01A	.27	.0260	35.4	14.8	10.1	R-Swath	Pre-Sawn Ice
01	01B	.27	.0251	34.1	14.3	56.1	R-Swath	
01	01B	.27	.0254	10.3	4.3	47.1	R-Swath	
01	02	.57	.0246	8.4	3.5	62.4	R-Swath	
02	01A	.29	.0279	28.9	57.6	6.7	R-Swath 1 Hull	Pre-Sawn Ice
02	01B	.29	.0312	26.7	53.2	57.9	R-Swath 1 Hull	
02	02	.57	.0263	25.4	50.6	76.2	R-Swath 1 Hull	
02	03A	.28	.0283	26.0	53.0	75.9	R-Swath 1 Hull	
02	03A	.28	.0302	49.1	97.9	139.0	R-Swath 1 Hull	
02	03B	.56	.0265	27.2	54.2	59.2	R-Swath 1 Hull	

The 02 series runs were done for single hull of the R-SWATH and in absolute terms these show much higher resistance values than the two hulls together. This is best explained by the considerably higher ice strength and somewhat higher thickness used in the second set of trials. The explanation of boundary effects and combined point loads given in the discussion section of the Arctec Report (Appendix 2) seems to overlook the higher ice strengths and thicknesses used for the second set of trials. This is particularly important in that the ice resistance is generally proportional to the thickness squared.

In addition to this the combined point load explanation is discredited further in that the SWATH is not in any way a pair of static point loads nor is the ice sheet infinite. At best it approximates a semi infinite sheet. For these reasons this explanation is not judged to be valid.

5.3 CONTROL (NRC) RESULTS

The Control results for the R-Monohull are given in Table 3. With the exception of Run 3 where the flexural strength (σf) of the ice is low, the results show good consistency in terms of both ice strength and thickness. These tests were performed for three vessel speeds, two of which are directly comparable to the SWATH tests. Unfortunately Elastic Modulus (E) values are not given and thus E/σ values cannot be compared.

TABLE 3 - CONTROL TEST RESULTS

Run No.	V (M/sec)	H_i (cm)	σf (KPa)	E (MPa)	R_{it} (N)	R_{ow} (N)	R_i (N)
C1	0.15	3.64	37	-	75.5	0.6	74.9
C2	0.6	3.61	40	-	121.6	4.3	117.3
C3	0.15	3.73	15	-	66.8	0.6	66.2
C4	0.3	3.33	42	-	78.0	1.5	76.5
C5	0.3	2.46	38	-	52.5	1.5	51.0
C6	0.3	4.08	25	-	97.0	1.5	95.5
C7	0.6	2.47	30	-	61.1	4.3	56.8
C8	0.6	3.77	20	-	85.0	4.3	80.7
C9	0.15	2.19	36	-	36.7	0.6	36.1

6.0 ANALYSIS

The analysis of the test results presented a number of problems. Comparisons between three sets of values performed under differing conditions is subject to interpretation. In addition the high cost of ice testing has limited the number of data points available for anlaysis.

The initial problem was to deal with the wide degree of variation in ice strength and thickness. In order to compensate for these variations a non-dimensional resistance was used. This was termed the specific resistance where:

$$R_S = R/\sigma h^2$$

R_S = Specific Resistance
R = Model Resistance
σ = Ice flexural strength
h = Ice thickness

This formulation in addition to being non dimensional is further justified by the fact that ice resistance has been shown to be proportional to flexural strength and ice thickness squared. For each trial the factor σh^2 was used to normalize the resistance to the point where the results were more directly comparable.

The second issue was whether the results from the two tanks could be compared at model scale, full scale or not at all. The reference tests performed on the R-SWATH indicate that there is reasonable agreement between the tanks after normalization. The slight difference may be explained through different ice formulations or testing methods. Because the SWATH results were so much higher than the Monohull it was considered to be risky to attempt to scale the results based on a traditional monohull scaling formulations and then do a comparison. Thus it was decided to compare models to models only. Comparisons between tanks were avoided because there were very few points on which to base the comparison.

6.1 ANALYSIS FOR LEVEL CONTINUOUS ICE

The normalized results for the level continuous ice are given for all three sets of trials in Table 4. Open water resistances have been subtracted based on the results of the Phase I trials. This is the only case where the results from one tank have been carried over to the other. The tabulated results were grouped by trial speed and model type, (R-SWATH, S-SWATH, R-monohull) and the specific resistance averaged, where possible, for each group. The results for this data reduction are plotted in Figure 4 for the Phase 1 and Control Trials and Figure 5 for the Phase 2 trials. Even without comparing results between tanks the results reveal some interesting points.

The Phase 1 results show that the SWATH models have resistances on the order of 2 to 2.5 times as high as the R-Monohull. The higher resistance for the SWATH was clearly not the expected result. However, on examination of the relative magnitudes of the breaking and clearing components (see Section 6.2) it would seem that the resistance from breaking ice is the dominant component. On this basis, the SWATH models are in essence, breaking ice at two locations while the monohull is only breaking ice at one. This would lead to the expectation of higher resistance.

The S-SWATH showed considerably better icebreaking performance than the R-SWATH. This indicates that the shearing action of the S-SWATH is more efficient at inducing failure in the model ice than the bending action of the R-SWATH. Observations from the model tests did however indicate that the S-SWATH was more difficult to keep on a straight line track than the R-SWATH.

It is also interesting to note that the SWATH models show a greater increase in resistance with speed than the monohull. Speed dependency is generally relatable to inertial effects in clearing broken ice pieces and this higher dependence on speed would lead one to believe that there are interference effects between the two hulls in the clearing of the ice after breaking.

The Phase 2 tests were intended to determine possible interference in icebreaking between the SWATH hulls. The plots shown in Figure 5 show

TEST	ICE thk(m)	E (MPa)	σ (KPa)	SPEED (m/sec)	R_T (N)	R_I (N)	R_{OW} (N)	E/σ	R_I/h^2
PHASE I									
1/1104	.028	6.46	31	.30	149	142.6	6.4	208.4	5.867
2/1107	.029	17.62	22	.60	148	126.0	22	800.9	6.810
3/1111	.038	14.00	46	.30	196	189.6	6.4	413.0	2.854
4/1115	.045	50.51	20	.30	236	214.0	22	2525.5	5.284
5/1118B	.039	--	78	.30	310	303.6	6.4	--	2.559
6/1125	.034	26.00	28	.30	121	111.7	9.3	928.6	3.451
7/1130	.032	17.17	28	.60	173	138.6	34.4	613.2	4.834
PHASE 2									
0101B	.0251	14.3	34.1	.27	56.14	50.3	5.8*	419.4	2.341
0101B	.0254	4.3	10.3	.27	47.06	41.3	5.8*	417.5	6.215
0102	.0246	3.5	8.4	.57	62.45	41.5	21.0*	416.7	8.164
0201B	.0312	53.2	26.7	.29	57.87	54.8	3.1*	1992.5	2.108
0202	.0263	50.6	25.4	.57	76.27	65.8	10.5*	1992.1	3.745
0203A	.0283	53.0	26.6	.28	75.87	72.9	3.0*	1992.5	3.422
0203A	.0302	97.9	49.1	.28	139.01	136.0	3.0*	1993.9	3.304
0203B	.0265	54.2	27.2	.56	59.24	48.9	10.3*	1992.6	2.560
CONTROL									
C1	.0364	--	37	.15	75.5	74.9	0.6	--	1.528
C2	.0361	--	40	.60	121.6	117.3	4.3	--	2.250
C3	.0373	--	15	.15	66.8	66.2	0.6	--	3.172
C4	.0333	--	42	.30	78.0	76.5	1.5	--	1.643
C5	.0246	--	38	.30	52.5	51.0	1.5	--	2.218
C6	.0408	--	25	.30	97.0	95.5	1.5	--	2.295
C7	.0247	--	30	.60	61.1	56.8	4.3	--	3.103
C8	.0377	--	20	.60	85.0	80.7	4.3	--	2.839
C9	.0219	--	36	.15	36.7	36.1	0.6	--	2.091

*Estimated from Phase 1 values.

TABLE 4: NORMALIZED TRIAL RESULTS

that the resistance of the single SWATH hull is considerably lower than the full SWATH vessel. It should however be borne in mind that the Phase 2 R-SWATH ice trials were performed in ice with a flexural strength considerably below the target value. This would tend to inflate the specific resistance values. Based on the results as they stand, it would appear that there are some interference effects between hulls and that these effects are beneficial at low speeds but become detrimental at the higher speeds. Generally due to the poor results obtained for the full SWATH vessel confidence in the results and the conclusion is low .

At the conclusion of the final test runs it was observed that there was some distortion in the bow of the SWATH hull. It has been suggested that the inward distortion of both hulls would cause increased frictional resistance on the flat inside face of the hulls. It is difficult to estimate what effect, if any, this would have on the results but it is judged that frictional effects were relatively minor and thus a slight increase in model friction would not have a significant effect on the overall results.

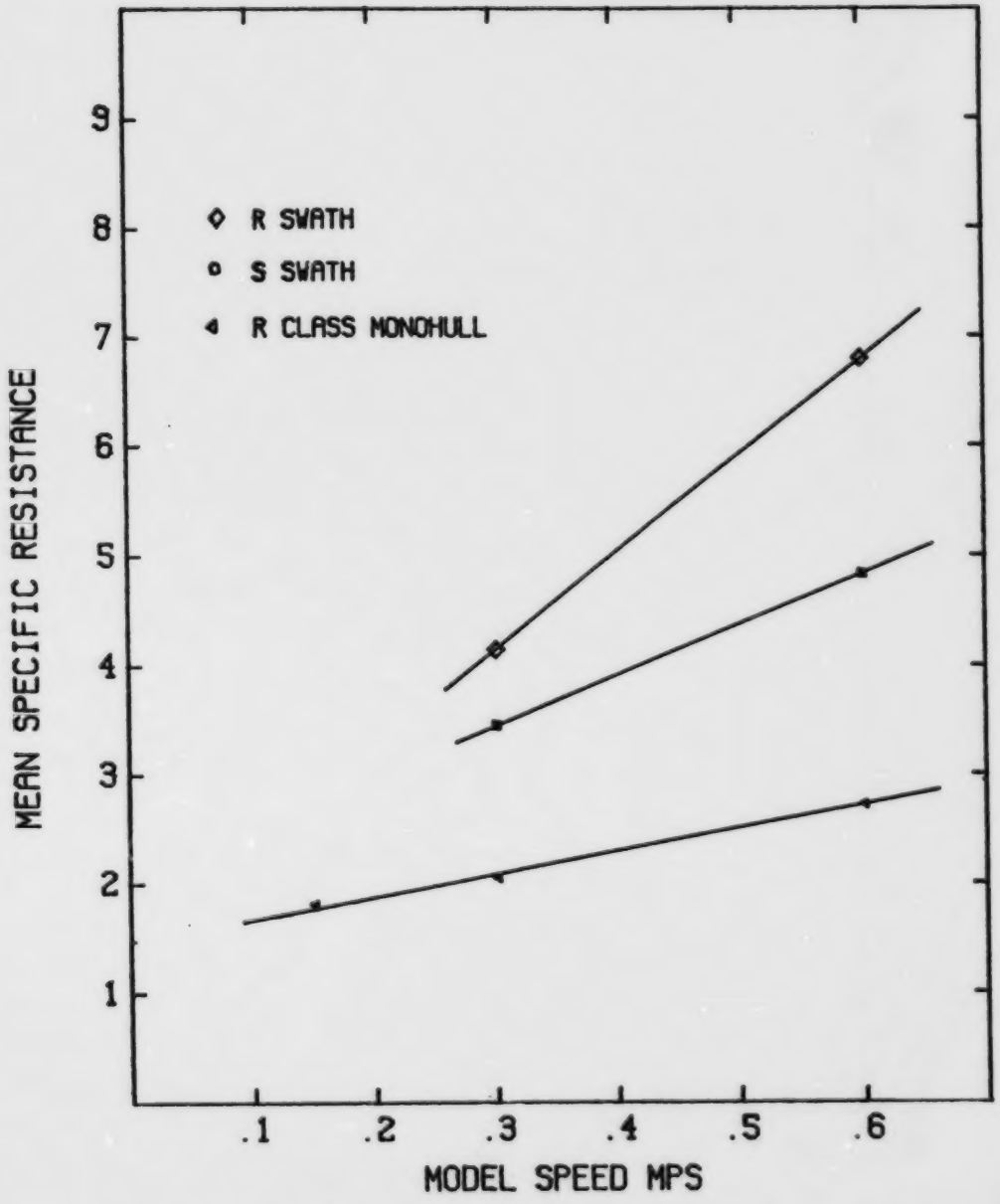

FIGURE 4 - SPECIFIC ICE RESISTANCE VS SPEED - PHASE 1

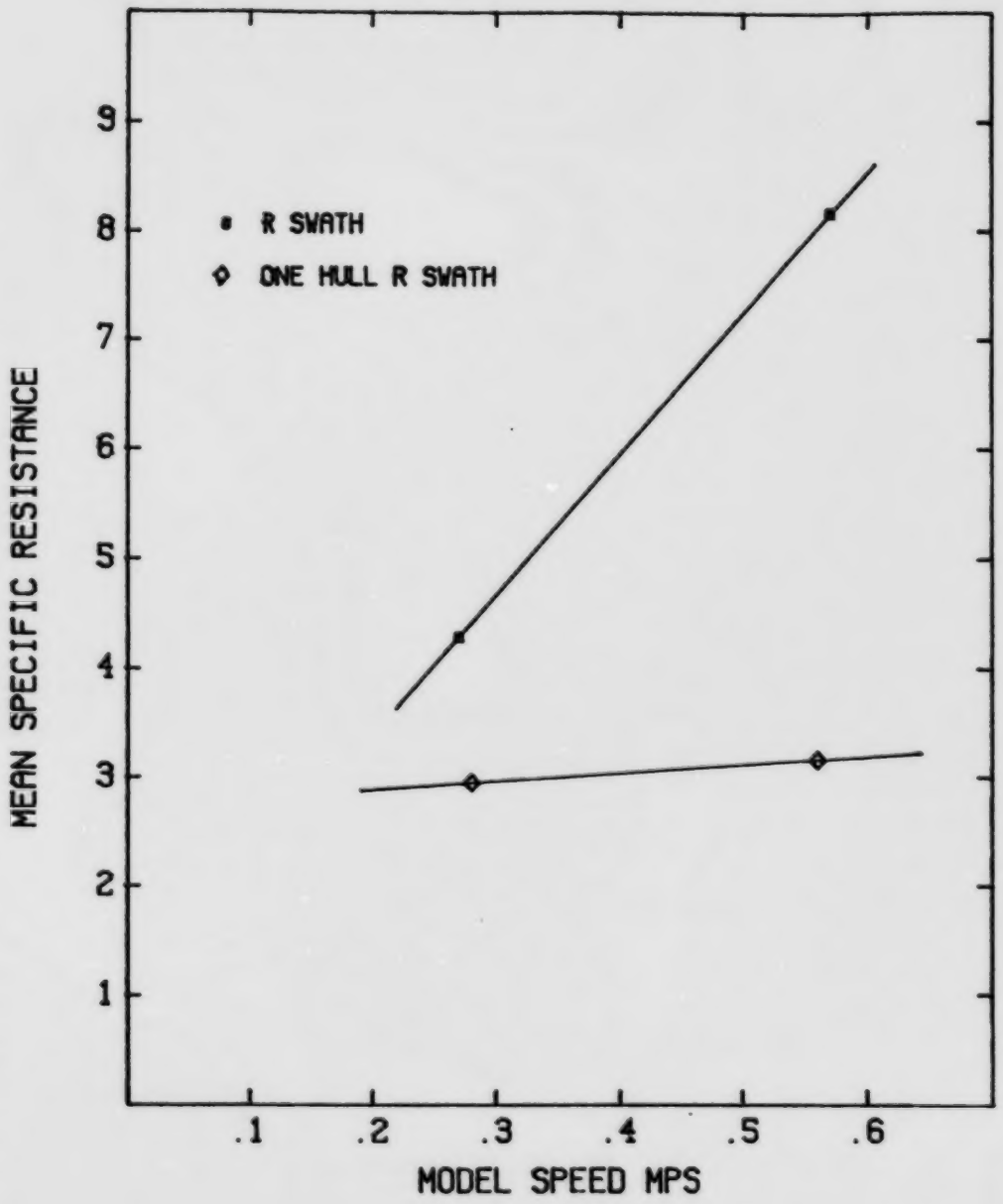

FIGURE 5 - SPECIFIC ICE RESISTANCE VS SPEED - PHASE 2

6.2 ANALYSIS FOR ICEBREAKING COMPONENTS

Runs in both phases were performed in pre-sawn ice followed immediately by continuous ice. These runs combined with the open water trials performed during Phase 1 were done to allow the vesel resistance to be spearated into ice breaking, ice clearing and open water components.

These trials were not performed on the control model so no comparison can be made with the monohull. In addition, the Phase 1 trials were run in ice much stronger than the target value while the Phase 2 trials were run in ice at about the target value. It was expected that this would skew the results but this does not appear to be the case. The results are as follows:

Case 1 Phase 1 - Run 5-1118 A&B R-SWATH

Speed = .3 m/sec	σ = 78 kPa
Resistance in open water (from Run 1121)	6.4N
Resistance in Pre-sawn ice	46 N
Resistance in Continuous ice	310 N

Total resistance	310 N	100%
Breaking Resistance	264 N	85%
Clearing Resistance	39.6 N	13%
Open water resistance	6.4 N	2%

Case 2 Phase 2 - Run 0101 A&B R-SWATH

Speed - .27 m/sec	σ = 34.1
Resistance in Open water (from Run 1121 less 10%))	5.8 N
Resistance in pre-sawn ice	10.1 N
Resistance in Continuous ice	56.1 N

Total resistance	56.1	100%
Breaking resistance	46.0	82%
Clearing resistance	4.3	8%
Open water resistance	5.8	10%

Case 3 Phase 2 Run 0201 A&B 1 Hull - R-SWATH

Speed = .29 m/sec		σ = 26.7
Resistance in Open water (50% x (run 1121 less 3%)	3.1 N	
Resistance in pre-sawn ice	6.7 N	
Resistance in continuous ice	57.9 N	
Total resistance	57.9 N	100%
Breaking resistance	51.2 N	88%
Clearing resistance	3.6 N	6%
Open water resistance	3.1 N	6%

Based on these results it is clear that the major component of resistance for a SWATH vessel is the breaking resistance. The fact that this component is even higher for the single SWATH hull indicates that there is some interference between hulls in the clearing of broken ice pieces which increases the clearing resistance of the SWATH vessel.

The high percentage resistance going into the ice breaking also supports the analysis of section 6.1 and it would seem to indicate that the energy required to actually break ice is a more significant part of the icebreaking equation than previously thought.

A further attempt was made to estimate the resistance related to initializing fracture in the ice sheet. This component of the resistance can be seen as the mean amplitude of the oscillating component of the total resistance (see Figure 6). For the NRC results these values were scaled from the supplied results. Unfortunately the small scale of the supplied traces left this method very subject to error. The Arctec results listed both a mean value and a standard deviation for each run and the standard deviation was taken as the average amplitude of the oscillating component. For the three cases covered previously the results are as follows:

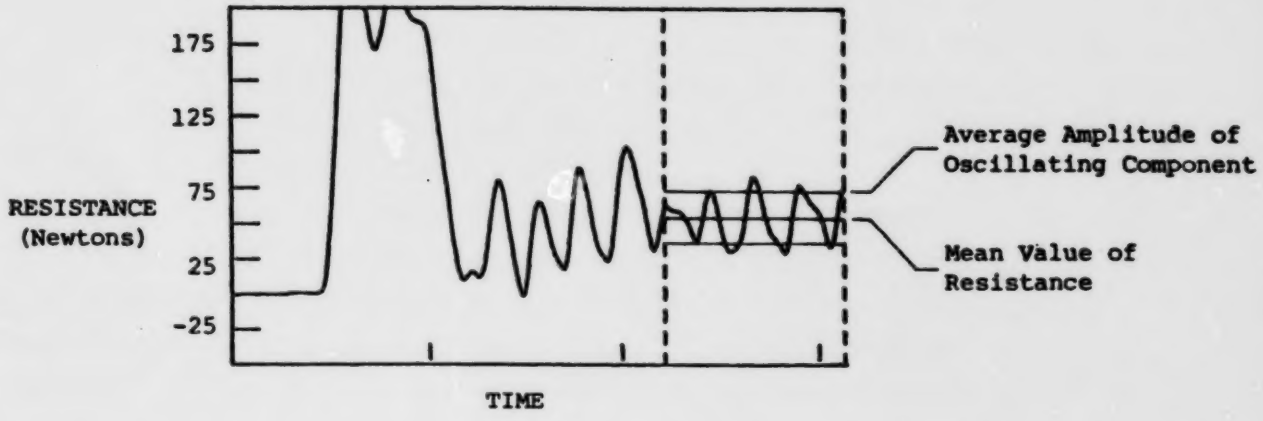

FIGURE 6 - SAMPLE RESISTANCE TRACE

Case 1

Mean Resistance	= 310 N
Amplitude of Oscillating Component	= 165 N
Fracturing Resistance as % of total	= 53%
as % of breaking	= 63%

Case 2

Mean Resistance	= 56.1 N
Amplitude of Oscillating Component	= 19.4 N
Fracturing Resistance as % of total	= 35%
as % of breaking	= 42%

Case 3

Mean Resistance	= 57.9 N
Amplitude of Oscillating Component	= 14.0 N
Fracturing Resistance as % of total	= 24%
as % of breaking	= 27%

Unfortunately these results do not indicate any clear trends except to show that the fracturing component of ice breaking in model ice represents somewhere between 25 and 55% of the total resistance. This conclusion is further devalued by the fact that the model ice is known to have a much higher fracture toughness than full scale ice.

7.0 CONCLUSIONS AND RECOMMENDATIONS

In conclusion it would appear that the SWATH vessel does not exhibit lower resistance than an equivalent monohull icebreaker. Within the limitations of the data generated for this study the SWATH does not offer potential as a viable icebreaking or ice transiting vessel.

The tests however did reveal a number of interesting and potentially important points.

In the first case it would seem that considerable effort should be devoted to improvements in Ice Model Testing. There are severe problems in obtaining and maintaining desired ice properties thus leading to inconsistent and somewhat unreliable data. Examples of areas needing improvement are more consistent flexural strength, elastic modulus and fracture toughness. These are areas of investigation more related to material science than naval architecture but the success of future ship research will depend on them.

In a related area it would be desirable generally to perform more tests for a given series. A larger base of data would allow a higher degree of confidence in the results and allow obviously suspect points to be discarded.

As a final point these tests have illustrated that the dependence of total ice transiting resistance on vessel beam is not as strong as previously believed. In addition it appears that the energy expended in inducing failure in the ice sheet is a dominant factor in the resistance of vessels in ice. These findings should induce a thorough re-evaluation of presently held theories on icebreaking and methods of scaling test results.

Although these tests did not support the original hypothesis they did illustrate potential problems in current icebreaking theories and have thus served a valuable purpose in furthering understanding of ships in ice.

APPENDIX 1

NRC Model Test Report LTR-SH-389

REPORT
RAPPORT

LIMITED

REPORT
RAPPORT LTR-SH-389

DATE January 1985

LAB ORDER
COMM. LAB. 22509

FILE
DOSSIER 7862

PAGES 12

FIG.

DIAG. 15

TABLES 6

Institute for Marine Dynamics
(IMD)

Institut de dynamique marine
(IDM)

FOR German & Milne Ltd.
POUR

REFERENCE Letters June 11, 1984; September 24, 1984; October 10, 1984.
REFERENCE

LTR-SH-389

SWATH IN ICE

RESISTANCE EXPERIMENTS WITH MODEL 377

SUBMITTED BY
PRESENTE PAR

Section Head
Chef de section

AUTHOR
AUTEUR

E. EMERY
S. NEWBURY
M. WILLIAMS

APPROVED
APPROUVE

This report may not be published wholly or in part without the written consent of the IMD.

Ce rapport ne doit pas être reproduit, ni en entier ni en partie, sans une autorisation écrite de IDM.

Copy No.
Copie No. 1

TABLE OF CONTENTS

		PAGE
	LIST OF SYMBOLS	ii
	LIST OF TABLES	iii
	LIST OF FIGURES	iv
1.0	INTRODUCTION	1
2.0	SHIP MODEL DESCRIPTION	1
3.0	TEST FACILITIES	2
4.0	ICE PROPERTIES	3
5.0	ICE-HULL FRICTION COEFFICIENT	5
6.0	PRESAWN ICE AND CLEARWATER	5
7.0	TEST RESULTS	6
8.0	DISCUSSION OF RESULTS	8
9.0	VISUAL OBSERVATIONS	10
	REFERENCES	12

LIST OF SYMBOLS

B	Waterline beam at maximum section, m
E	Strain modulus for model ice, kPa
IMD	Institute for Marine Dynamics
L	Length of cantilever ice beams, m
L_c	Characteristic length of plate in flexure, m
LWL	Length on waterline, m
P	Vertical load on ice, N
R	Resistance, N
T	Tangential force, N
W	Normal force, N
b	Width of cantilever ice beams, m
d	Distance from north end of tank, m
f	Coefficient of dynamic friction, f = T/W
f.w.	Fresh water
g	Gravitational acceleration, m/s^2
h	Thickness of ice sheet, mm
r	Distance from point load on plate, m
t	Run time, sec
v	Model speed, m/s
δ	Deflection of point load on plate, mm
ν	Poisson's ratio for ice
σ_f	Flexural strength, kPa
ρ	Density of water, = 999.96 kg/m^3

LIST OF TABLES

1. MODEL 377 - SWATH ICEBREAKER - HYDROSTATIC PARTICULARS FOR MODEL OF SCALE 1:20 WITHOUT APPENDAGES

2. SUMMARY OF ICE SHEET DATA

3. ICE-HULL FRICTION VALUES

4. ZERO VALUES

5. SUMMARY OF MODEL TEST RESULTS

6. SUMMARY OF MODEL MOTIONS

LIST OF FIGURES

1 Swath model - general arrangement

2 Swath model - lines plans

3 Presawn ice pieces

4 Run 1104

5 Run 1107

6 Run 1111

7 Run 1115

8 Run 1118

9 Run 1125

10 Run 1130

11 Resistance vs flexual strength

12 Resistance vs thickness, R-Class bow

13 Resistance vs thickness, R-Class and sled bows

14 Resistance and yaw, v = 0.3 m/s

15 Resistance and yaw, u = 0.6 m/s

1.0 INTRODUCTION

This report describes ice resistance experiments carried out by the Institute for Marine Dynamics at the request of German & Milne Inc. The model represented a simplified ice transiting SWATH ship. The tests were conducted in the ice tank at the Hydraulics Laboratory, NRC. The objective of the tests was to determine the performance in ice of the SWATH concept.

2.0 SHIP MODEL DESCRIPTION

The model, designated 377, was made of wood with a steel beam frame connecting the two hulls, and finished in polyurethane paint. It was built to lines supplied by German & Milne, drawings 1-7070-07,08,09, dated March, 1984.

Since the test program required the testing of two different bow designs, the model was constructed in such a way that the bow sections were removable. The bows for 377A were similar to an R-Class icebreaker bow cut down the centreline. Model 377B had a pair of sled bows. A body plan is shown in Figure 1, and bow lines in Figure 2.

The model was tested in the bare hull condition (i.e. no propellers, shafts or rudders were fitted). The displacement was set to 0.957 tonnes f.w., the same as that of the 1:20 scale R-Class model previously tested in ice at the IMD [1].

The model was too large to fit in the swinging frame so the distribution of ballast weights was arranged while the model was floating in the water. The ballast was arranged to correspond to a longitudinal radius of gyration for the model of approximately 0.25 LWL, and a transverse radius of gyration of approximately 0.38 B. The vertical centre of gravity was specified at 0.50 m above the base line, and was checked experimentally by inclining the model. The hydrostatic particulars for 377 A and 377 B are listed in Table 1.

The model was towed from a point at the longitudinal centre of gravity, about 0.755 m above the base. This is the closest the tow point could be situated to the centre of gravity while keeping the towing apparatus above the water level.

3.0 TEST FACILITIES

The model tests were performed in the ice tank of the Hydraulics Laboratory, National Research Council, Ottawa. The tank, enclosed in a refrigerated room, has dimensions 21 m x 7 m x 1.2 m. The model was towed at constant speed by a motorized carriage.

The IMD towing system attaches to the model at or near the centre of gravity. The model was restrained in surge, sway and yaw motions. The measured resistance was the horizontal centreline component of the forces on the model at the attachment point. The model was free in pitch, roll and heave, and these motions were measured at the attachment point by the towing system. The position of the carriage was also measured during the tests.

The ship model data was scanned at 0.05 sec. intervals, digitized, and stored on magnetic tape. The data acquisition was controlled by a Transduction 11/Blue 7 microcomputer. Data analysis was carried out on a Digital VAX.

Video recordings were made of each run with a video camera mounted a fixed distance ahead of the model, directed to observe ice behaviour at the bow.

4.0 ICE PROPERTIES

During the test program a total of seven ice sheets were grown. The sheets were seeded when the 0.5% urea solution was sprayed with airborne water droplets at an air temperature of -16°C and a solution temperature between -0.1 and -0.2°C. (The freezing point of the urea solution is -0.155°C.) The growth rate was approximately 3 mm per hour at -16°C.

When the correct thickness was achieved the air temperature was increased to 2°C and the flexural strength of the ice declined from its maximum level of approximately 200 kPa. The flexural strength was monitored by a series of in situ cantilever beam tests. The strength thus calculated was plotted against warm-up time. The stiffness of the ice sheet, in terms of the characteristic length and elastic modulus, was determined by applying a point load and measuring the corresponding plate deflection. The time plots for strength and stiffness are included in Appendix A.

The following standard formulae [6] were used to calculate the ice properties:

$$\sigma_f = \frac{6 \times 10^3 \, PL}{bh^2} \qquad (1)$$

$$L_c^2 = \frac{-P \times 10^3}{2\pi\rho g \delta} \, kei(r/L) \qquad (2)$$

$$kei(r/L)_{r=0} = -\pi/4 \qquad (3)$$

$$L_c = \left[\frac{P \times 10^3}{2\pi\rho g \delta} \, \frac{\pi}{4} \right]^{\frac{1}{4}} \qquad (4)$$

$$E = 10^3 [12\rho g(1-\nu^2) L_c^4]/h^3, \quad \nu = 0.3. \qquad (5)$$

The ice properties for each ice sheet at test time are summarized in Table 2. The σ_f and the L_c at the time of the run were interpolated from the time plots of the test results. The average thickness was calculated from the thickness profile taken along both sides of the track at the end of each run. The E was calculated from the average h and the L_c.

It must be noted that there was some variation in σ_f and h throughout an ice sheet. The thickness can vary as much as 5 mm in the extreme, and flexural strengths varied across the ice sheet due to slight differences in freezing and warm up conditions. Accurate σ_f values were difficult to obtain below 40 kPa because the ice was too weak for precise cantilever beam tests.

5.0 ICE-HULL FRICTION COEFFICIENT

The paint on the model was sprayed on and finished with no. 600 sandpaper. The coefficient of dynamic friction between the model and the ice was measured experimentally during the tests at approximately the same time as the test run.

A 15 x 15 cm sample was cut from the ice sheet in the test basin and inserted into the sample holder. The side of one of the bows not in use, held level, was used as the test surface. The sample was loaded with a normal force, W, of 225 N and manually pulled along the surface at a rate of about 10 cm/sec. The pulling force, T, was measured with a push/pull gauge. The coefficient of friction, f, was calculated as:

$$f = T/W$$

Both top and bottom surfaces of the ice were tested, under wet and dry conditions, with very little variation in f. The coefficient values are given in Table 3. The differences in the friction measurements between the two bows was significant. The overall average f measured on Bow B was 0.12, while that measured on Bow A was 0.06.

6.0 PRESAWN ICE AND CLEARWATER

After each test, the dimensions of the broken channel and the size and shape of the broken ice pieces were noted.

Part of Sheet #5 was sawn by hand into pieces as shown in Figure 3. These pieces were geometrically simple representations of the observed pieces from the previous tests. Experience at other ice tanks [2] indicated that the resistance results are not sensitive to the details of the piece shapes. Since the model is not required to break the ice, σ_f for the presawn ice is 0.

Runs 1121, 1122, 1127 and 1128 were in clear water. Hence both the σ_f and the h are 0.

7.0 TEST RESULTS

The time records of the ship model data for each run are shown in Figues 4 to 10. The channel records give relative values for the measured quantities; the zero values, or values for the model at rest, are given in Table 4. Carriage travel was measured through a pulley running on a wire, which results in a sawtooth signal. Heave was positive upwards, except for run 1104, where it was positive down. Roll was positive for starboard down. Pitch was positive for bow up. Pitch and roll are unavailable for run 1104, and the carriage position transducer was nonfunctional for run 1107.

For runs 1104, 1107, 1111, and 1115, the ice conditions and the model condition were uniform for the entire run. For run 1118, the ice between the 6 m and 12 m marks was presawn, while the ice between 12 m and 18 m was intact, with high flexural strength. On both icebreaking runs with the sled bow, the model yawed to starboard as the run progressed, and the resistance level increased as the yaw increased.

The carriage speed, and hence the model average speed, was constant between the initial and final accelerations. The model motions were small. Heave was, on the average, positive while the model was breaking ice. The roll was so small that the vibrations of the towing system, seen as sharp spikes on the roll record, dominated the output of the transducer. The pitch was also small, but consistently positive, and increasing with increasing ice resistance. Over the test section, the resistance oscillated about a smoothly varying average.

Detailed examination of the time records showed that steady state was not reached until the entire length of the model had entered the ice sheet. For simple runs, the record for a consistent interval along the tank, between 13 and 16 m, was analysed. Otherwise, the interval selected for analysis was that in which the data record showed the least variation. For the presawn and high strength ice sheet, averages were calculated for a short interval near the end of the test section. For the two runs in which the model yawed, averages were calculated for an interval in which the yaw, measured by the position of the starboard edge of the track, was small and increasing slowly.

The test results are summarized in Table 5. The resistance R is the average over the time interval t_1-t_2, with the bow of the model moving through d_1-d_2. The thickness h is the average over d_1-d_2, and may differ from the average for the ice sheet, given in Table 2. The model data for the same run segments is collected in Table 6. In Table 6, the heave for all runs, including 1104, is positive upwards.

8.0 DISCUSSION OF RESULTS

During the tests, the parameters which were varied were bow shape, v,h, and σ_f. The resistance depends on each of these, but the test program was not extensive enough to determine the form of that dependence. The trends in the results, however, are reasonable.

The ice-breaking resistance equations in the literature, which specify the dependence of R on the above parameters, are all for conventional hull forms, and hence do not apply to the SWATH. However a number of these equations, from a variety of sources, [3], [4] and [5], have, for a given hull form and a fixed v, the common form:

$$R(h, \sigma_f) = A(h) + ch\,\sigma_f \qquad (6)$$

for total, dimensional resistance. The function A(h) depends on v and includes the open water resistance, and c is a constant.

For the R-class bow at v = 0.3 m/s and h = 38 mm(runs 1111 and 1118), the variation of R with σ_f is shown by the points in Figure 11. The linear relation which best fits these points:

$$R(38, \sigma_f) = 44.5 + 3.38\,\sigma_f \qquad (7)$$

is shown in the same figure.

If Equation (7) is a special case of Equation (6), then the resistance values for various σ_f, for one bow and one speed, may be adjusted to the equivalent R at σ_f = 30 kPa, through:

$$R(h,30) = R(h,\sigma_f) + 0.889h(30\,\sigma_f) \qquad (8)$$

Resistance is plotted against h, for σ_f = 30 kPa and v = 0.3 m/s, in Figure 12. The second order curve which best fits the points is :

$$R(h,30) = 9.12 + 1.52h + 0.09h^2 \qquad (9)$$

The h^2 dependence is a feature of the resistance formulations given in [3], [4] and [5].

The average R for the R-class bow at v = 0.6 m/s with σ_f = 22 kPa, and for the sled bow at v = 0.3 m/s and 0.6 m/s with σ_f = 28 kPa, are compared with the curve (9) in Figure 13.

To examine the effect of yaw on the measured R for the sled bow, both R and yaw were tabulated at selected distances along the tank. The R is the average over approximately 1 m of travel, and is influenced by the length of the model in the ice sheet, as well as the yaw. The values are plotted in Figure 14 for v = 0.3 m/s, and in Figure 15 for v = 0.6 m/s. The scatter in the R values at 0.3 m/s shows the effect of several sharp roll motions. The sudden motions may have occured when the yaw restraint structure failed. Both R and yaw are increasing, with increasing slope, suggesting directional instability.

Before the run at v = 0.6 m/s, the yaw restraint was repaired and strengthened. During the test, the yaw restraint deformed elastically, then snapped back toward the neutral position, thrusting the model as it did so. This effect can be seen in both the R and yaw plots.

9.0 VISUAL OBSERVATIONS

The video record, and observations during the tests, provide further information on the icebreaking process for the hull form tested.

A significant feature of the SWATH performance is the absence of model rotations. The pitch jumped as the model entered the ice and remained steady during the run. No roll was noticeable except for the isolated sudden changes in roll due to model or ice assymetry. In comparison, the R-Class model of the same displacement in similar ice conditions showed regular roll motion. The difference is evident in the run records for the SWATH and the R-Class [1].

Ice was broken by the conventional R-Class on alternate sides of the bow as the model rolled. The cusps were formed well forward on the shoulders. Since the SWATH model was not rolling, the weight of the model was brought to bear on the ice sheet only after the contact point had moved aft and been submerged by the local curvature.

As the SWATH with R-Class bow was breaking ice, the ice ahead of the bow became white and heaved slightly. As the cusps formed, they separated quickly from the ice sheet and rotated to a vertical position. These observations suggest that there was in-plane pressure in the ice sheet in the region of the bow. The track was approximately 1.4 m wide, with an undisturbed tongue between the hulls and extending aft up to one model length. The primary breaking piece size was approximately 140 mm x 300 mm. Pieces came to rest underneath the ice up to 0.5 m from the track, upside down. It appeared that the pieces were accelerated by contact with the water line.

The SWATH with sled bow showed similar pitch and roll behaviour to the SWATH with R-Class bow. The sled bow did not appear to cause pressure or buckling in the ice sheet, except when the yaw was large. The track was the width of the two hulls, with intact tongue between the hulls. The pieces were rectangular, 100 mm x 200 mm, and came to rest under the ice about 200 mm from the track, top side up.

REFERENCES

1. Newbury, S., "R-class Icebreaking Experiments with Model 327 and Comparison with 1:40 Scale and Full Scale Results", Institute for Marine Dynamics, National Research Council of Canada, Publication No. LTR-SH-383, (1985).

2. Enkvist, E., "A Survey of Experimental Indications of the Relation Between the Submersion and Breaking Components of Level Ice Resistance to Ships", Proceedings POAC 83, Vol. I, 484 - 493 (1983).

3. Enkvist, E., "On the Ice Resistance Encountered by Ships Operating in the Continuous Mode of Icebreaking", The Swedish Academy of Engineering Sciences in Finland, Report No. 24, Helsinki, 1972.

4. Milano, V.R., "Comparison of Several Analytical Models for the Prediction of Total Ship Resistance in Level Ice", Special Report to the ITTC Ice Committee, 1983.

5. Edwards, R.Y. Jr., "Modeling the Interaction Between Ice and Ships", in Physics and Mechanics of Ice, Ed. Per Tryde, IUTAM Symposium, Copenhagen, 1979.

6. Wyman, M., "Deflections of an Infinite Plate", Canada J. Res., A 28, 293 - 302 (1950).

MODEL 377

SWATH ICEBREAKER

HYDROSTATIC PARTICULARS FOR MODEL OF SCALE 1:20

WITHOUT APPENDAGES

	377A	377B
Length overall (LOA), m	5.576	5.572
Length between perpendiculars (LBP), m	5.300	5.300
Length on waterline (LWL), m	5.354	5.322
Waterline beam at midships, m	0.190	0.190
Waterline beam at maximum section, m	0.220	0.220
Hull separation, m	1.000	1.000
Level keel draft, m	0.530	0.518
Maximum section fwd of midships, m	1.590	1.590
Parallel middle body, aft of midships, m	2,385	2.385
to, fwd of midships, m	1.325	1.325
Centre of buoyancy, fwd of midships, m	-0.206	-0.150
Centre of buoyancy above keel, m	0.274	0.266
Volume of displacement, m^3	0.957	0.957
Displacement, tonnes of fresh water	0.957	0.957
Centre of gravity above keel, m	0.500	0.500
Centre of flotation fwd of midships, m	-0.005	0.117
Area of waterplane, m^2	1.959	2.062
Transverse metacentric radius (BM), m	0.497	0.528
Longitudinal metacentric radius (BM_L), m	4.540	5.077

SUMMARY OF ICE SHEET DATA

Ice Sheet Number	1	2	3	4	5	6	7
Date (DD-MM-YY)	06.11.84	08.11.84	13.11.84	16.11.84	19.11.84	23.11.84	26.11.84
Freeze Time (HRS)	11.0	11.0	18.0	18.0	17.0	11.0	11.0
Warm-Up Time (HRS)	12.27	12.75	14.12	13.42	7.58	10.63	10.60
Desired Thickness (mm)	30	30	50	50	35	30	30
Desired Flexural Strength (kPa)	30.0	30.0	30.0	30.0	N.A.	30.0	30.0
Actual Average Thickness (mm)	27.7	29.0	38.0	44.3	38.0	35.4	33.7
Actual Flexural Strength (kPa)	31.0	22.0	46.0	20.0	78.0	28.0	28.0
Elastic Modulus (MPa)	6.46	17.62	19.00	50.51	-	26.00	17.17
Characteristic Length (m)	0.188	0.250	0.312	0.447	-	0.32	0.278
E/σ_f	210	800	410	2530	-	930	610
L_c/hav.	6.79	8.62	8.21	10.09	-	9.04	8.25
Bow	A	A	A	A	A	B	B
Carriage Speed (m/sec)	0.3	0.6	0.3	0.3	Pre-Sawn	0.3	0.6

Table 2
LTR-SH-389
LIMITED

ICE-HULL FRICTION VALUES

Sheet	Surface	Condition	σ_f kPa	T N	f T/W
1	top	dry	32.0	35.6	0.16
1	top	wet	32.0	32.9	0.15
1	bottom	dry	32.0	38.2	0.17
1	bottom	wet	32.0	38.2	0.17
2	top	dry	22.0	28.9	0.13
2	top	wet	22.0	30.7	0.14
2	bottom	dry	22.0	27.6	0.12
2	bottom	wet	22.0	30.2	0.13
3	top	dry	48.0	26.2	0.12
3	top	wet	48.0	21.8	0.10
3	bottom	dry	48.0	24.5	0.11
3	bottom	wet	48.0	24.9	0.11
4	top	dry	53.0	24.0	0.11
4	top	wet	53.0	22.2	0.10
4	bottom	dry	53.0	26.7	0.12
4	bottom	wet	53.0	29.8	0.13
4	top	dry	20.0	24.9	0.11
4	top	wet	20.0	26.2	0.12
4	bottom	dry	20.0	28.0	0.12
4	bottom	wet	20.0	30.2	0.13
5	top	dry	78.0	21.8	0.10
5	top	wet	78.0	21.8	0.10

ICE-HULL FRICTION VALUES CONT'D

Sheet	Surface	Condition	σ_f kPa	T N	f T/W
5	bottom	dry	78.0	22.2	0.10
5	bottom	wet	78.0	24.0	0.11
6	top	dry	32.0	13.3	0.06
6	top	wet	32.0	13.8	0.06
6	bottom	dry	32.0	13.3	0.06
6	bottom	wet	32.0	15.1	0.07
7	top	dry	33.0	12.0	0.05
7	top	wet	33.0	11.1	0.05
7	bottom	dry	33.0	12.4	0.06
7	bottom	wet	33.0	13.3	0.06

Table 4
LTR-SH-389
LIMITED

ZERO VALUES

Run #	Heave mm	Roll deg	Pitch deg	R N
1104	282.58	-1.75	17.61	- 1.42
1107	113.33	2.30	19.24	9.52
1111	-0.03	-0.03	0.00	0.70
1115	-13.36	-1.42	0.27	18.04
1118	-22.17	-0.98	0.37	3.81
1121	-22.93	0.32	0.23	-17.87
1122	-22.93	0.32	0.23	-17.87
1125	0.06	0.14	-0.01	-2.31
1127	-0.23	0.14	-0.03	-12.79
1128	-0.23	0.14	-0.03	-12.79
1130	-2.87	-0.13	0.13	4.50

Table 5
LTR-SH-389
LIMITED

SUMMARY OF MODEL TEST RESULTS

Date Nov.	Sheet /Run	t_1-t_2 sec	d_1-d_2 m	h mm	σ_f kPa	v m/s	R N	Bow
6	1/1104	21-23	12-16	28	31	0.3	149	R-Class
8	2/1107	13-19	13-16	29	22	0.6	148	R-Class
13	3/1111	23-35	12-16	38	46	0.3	196	R-Class
16	4/1115	24-36	12.5-16	45	20	0.3	236	R-Class
19	5/1118	12-21	9.4-12	38	0	0.3	46	R-Class
19	5/1118	30-36	15-17	39	78	0.3	310	R-Class
20	-/1121	23-34	13-16	0	-	0.3	6.4	R-Class
20	-/1122	10-16	13-16	0	-	0.6	22	R-Class
23	6/1125	14-16	10-11	34	28	0.3	121	sled
23	-/1127	21-31	12-14	0	-	0.3	9.3	sled
23	-/1128	9-15	13-16	0	-	0.6	34.4	sled
26	7/1130	10-12	10-11	32	28	0.6	173	sled

SUMMARY OF MODEL MOTIONS

Run #	t_1-t_2 sec	h mm	σ_f kPa	v m/s	Heave mm	Roll deg	Pitch deg	R N
1104	21-33	28	31	0.3	5.1	0.07	0.18	149
1107	13-19	29	22	0.6	1.4	-.69	0.32	148
1111	23-35	38	46	0.3	2.7	0.11	0.35	196
1115	24-36	45	20	0.3	5.1	0.05	0.47	236
1118	12-21	38	0	0.3	0.5	0.07	0.10	46
1118	30-36	39	78	0.3	7.5	0.08	0.85	310
1121	23-34	0	-	0.3	0.1	-.12	0.01	6.4
1122	10-16	0	-	0.6	-1.6	-.09	0.01	22
1125	14-16	34	28	0.3	3.0	-.10	0.36	121
1127	21-31	0	-	0.3	0.1	0.00	0.01	9.3
1128	9-15	0	-	0.6	-1.0	0.00	0.10	34.4
1130	10-12	32	28	0.3	1.5	0.03	0.42	173

FIGURE 1

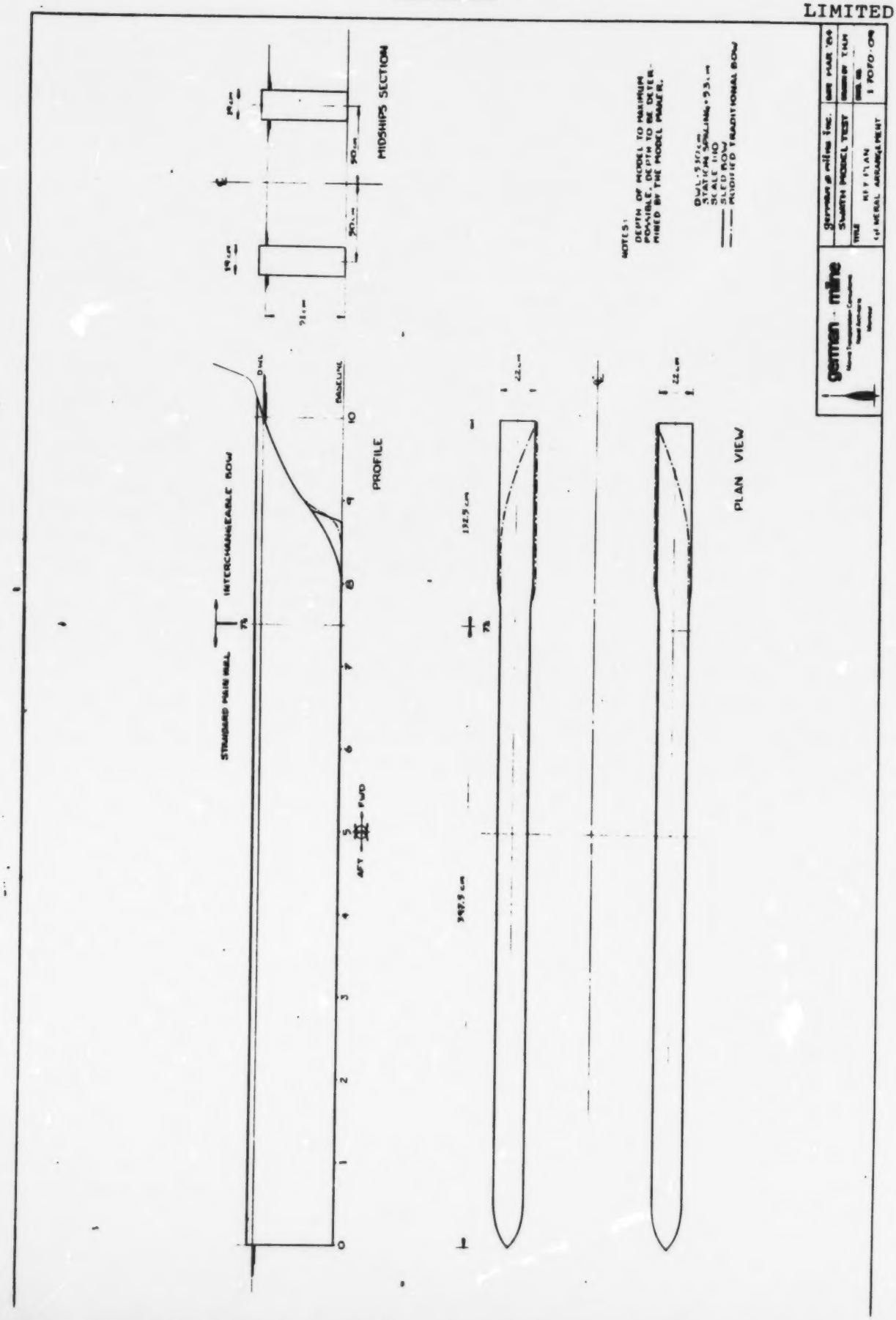
MIDSHIPS SECTION
PROFILE
PLAN VIEW
STANDARD PAIR REEL
INTERCHANGEABLE ROW
NOTES:
DEPTH OF MODEL TO MAXIMUM POSSIBLE, DEPTH TO BE DETERMINED BY THE MODEL MAKER.
SCALE 1:40
MODIFIED TRADITIONAL BOW
german - milne
SMITH MODEL TEST

FIGURE 2a

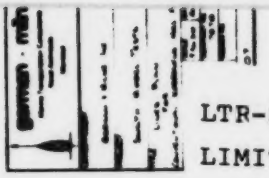

FIGURE 2b

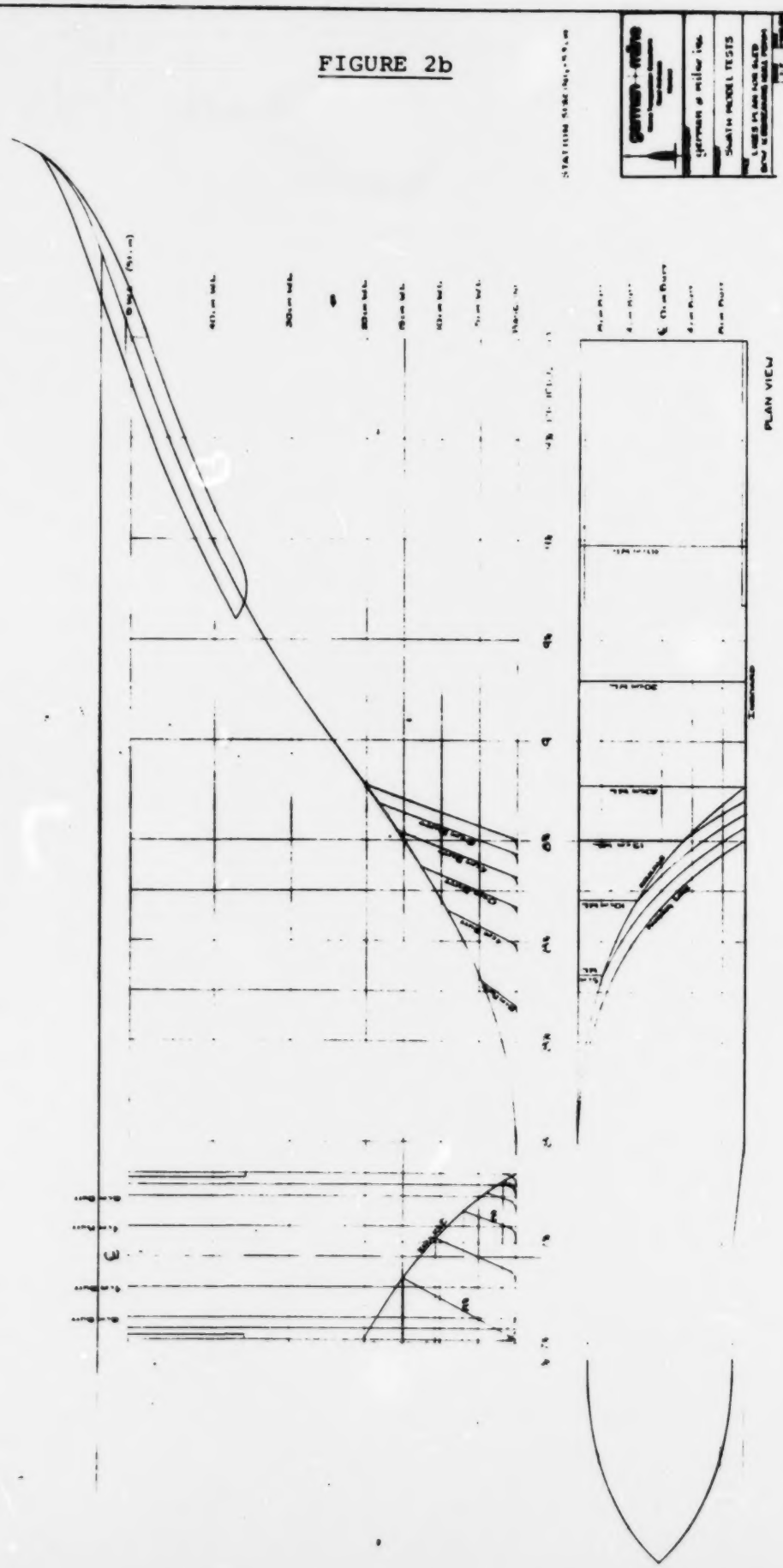

FIGURE 3

PRESAWN ICE PIECES

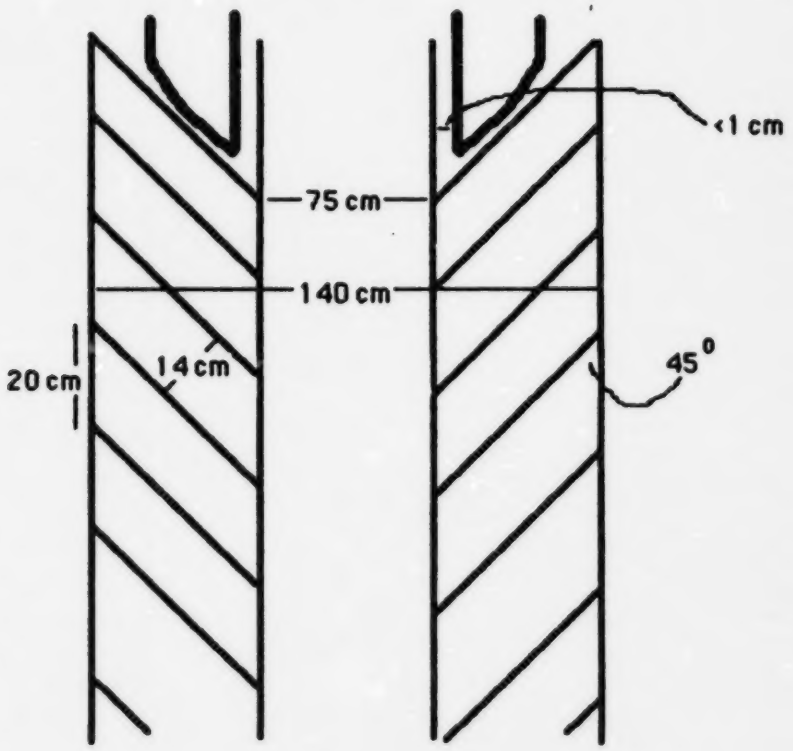

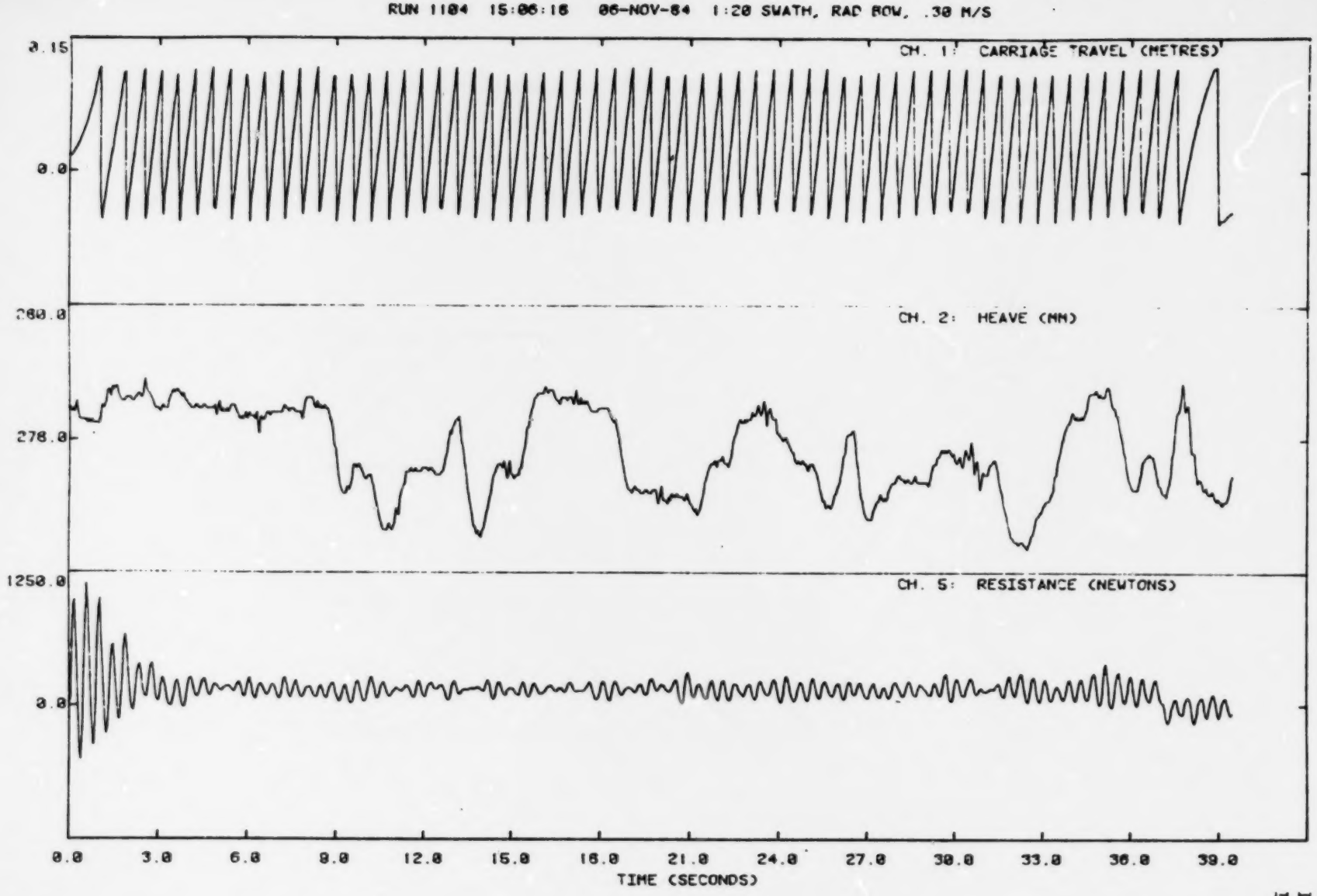

FIGURE 4

LIR-SI-339
LIMITED

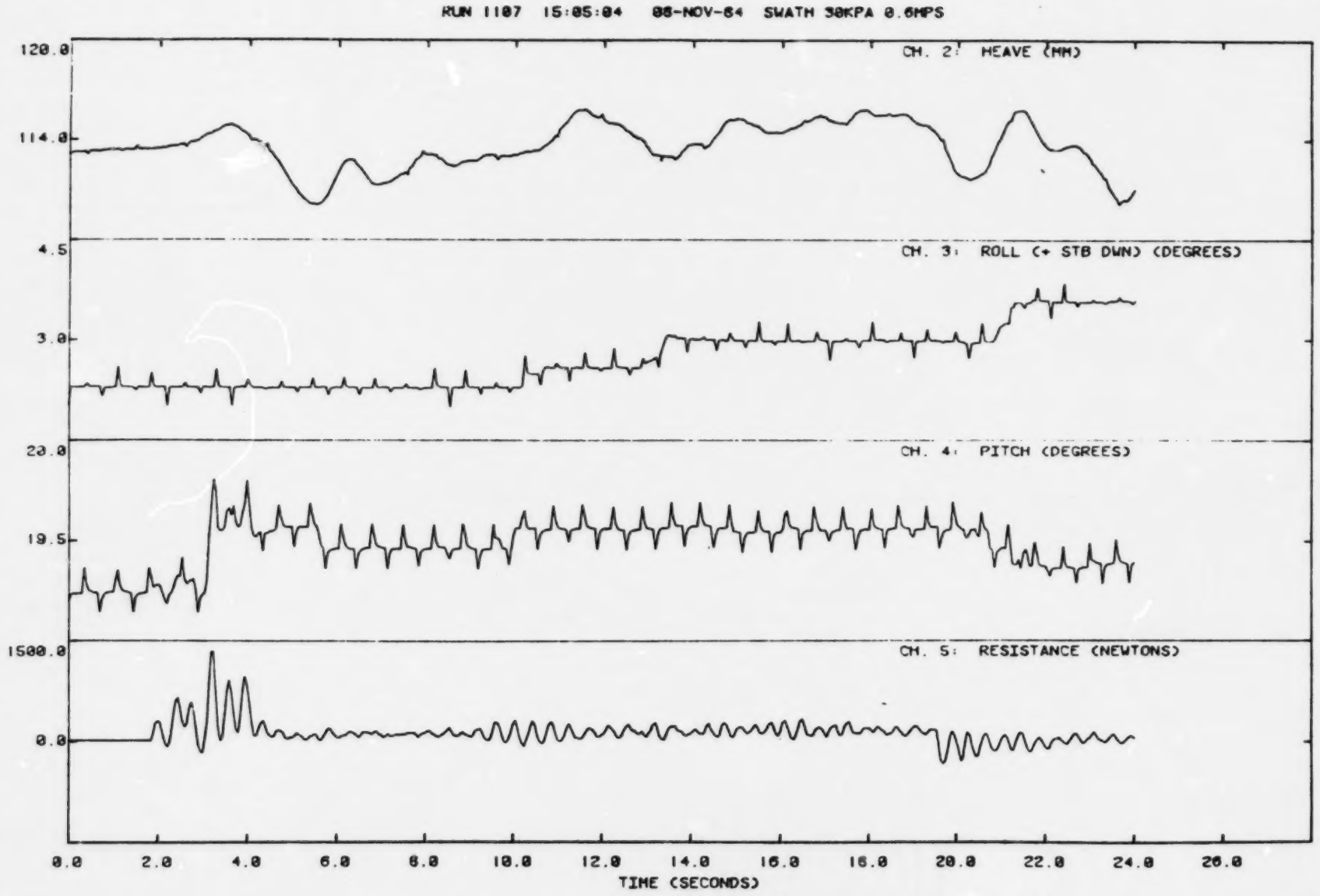

FIGURE 5

LTR-SR-389
LIMITED

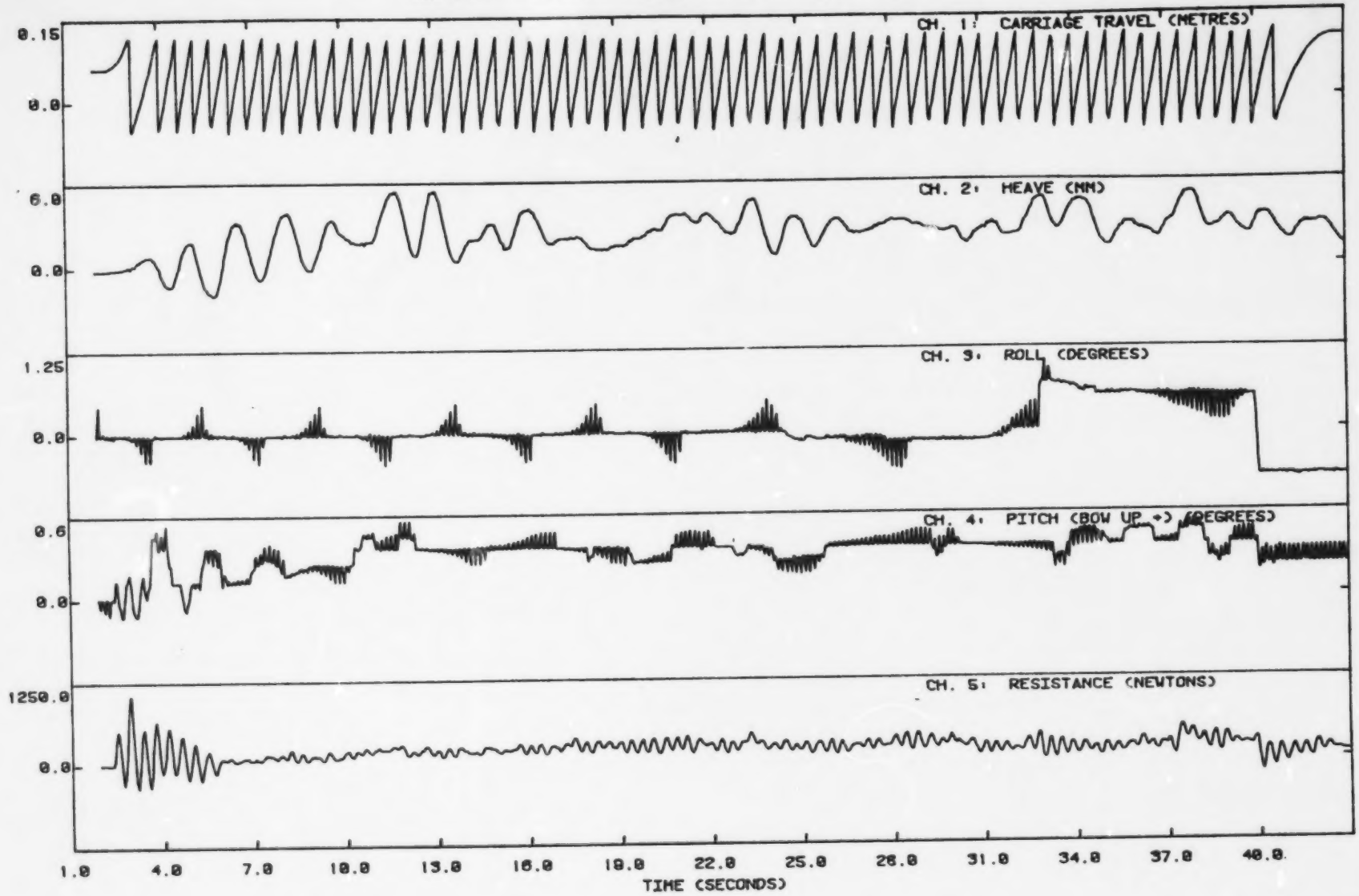

FIGURE 6

LTR-SH-339
LIMITED

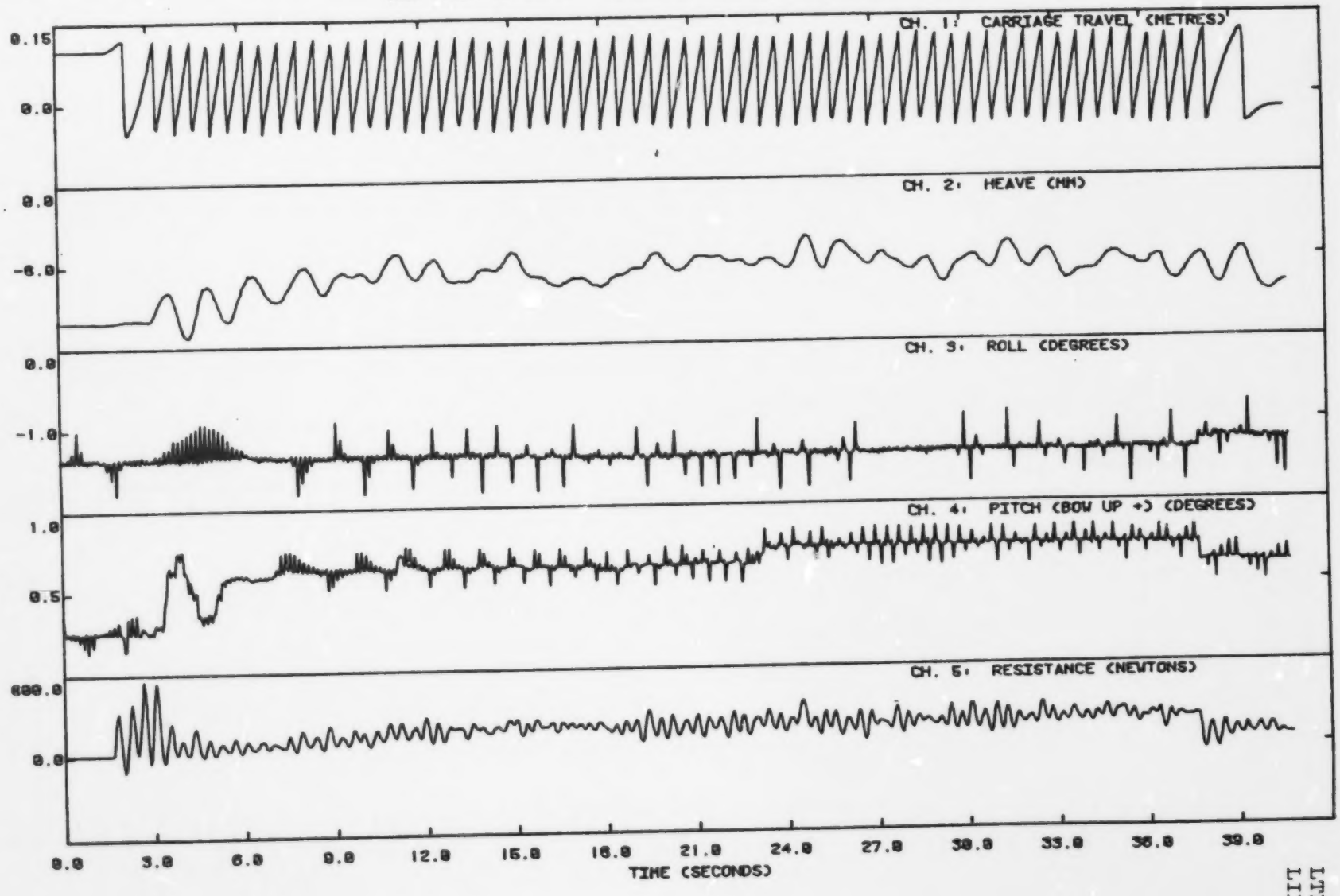

FIGURE 7

LTR-SI-309
LIMITED

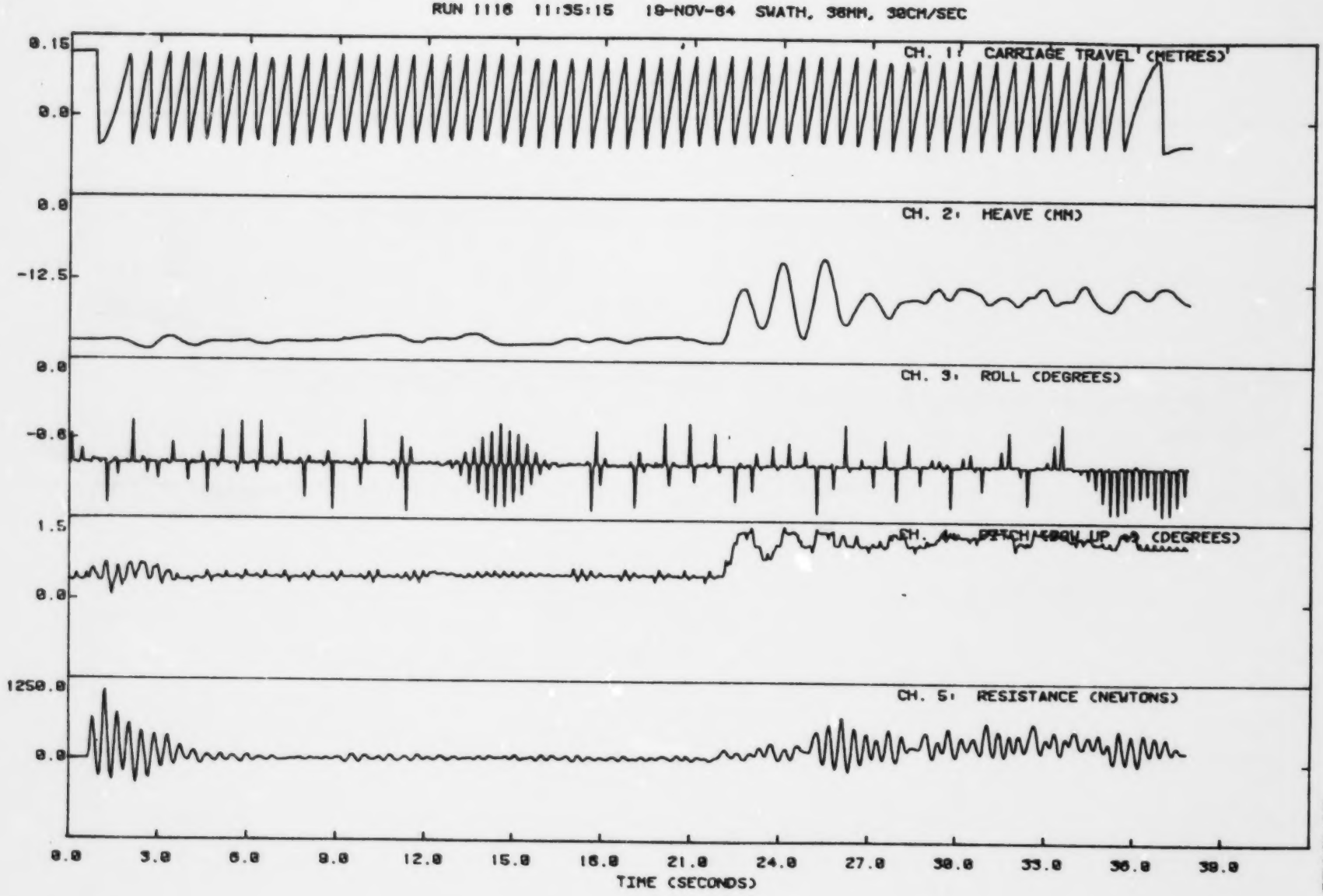

FIGURE 3

LTR-SI-339
LIMITED

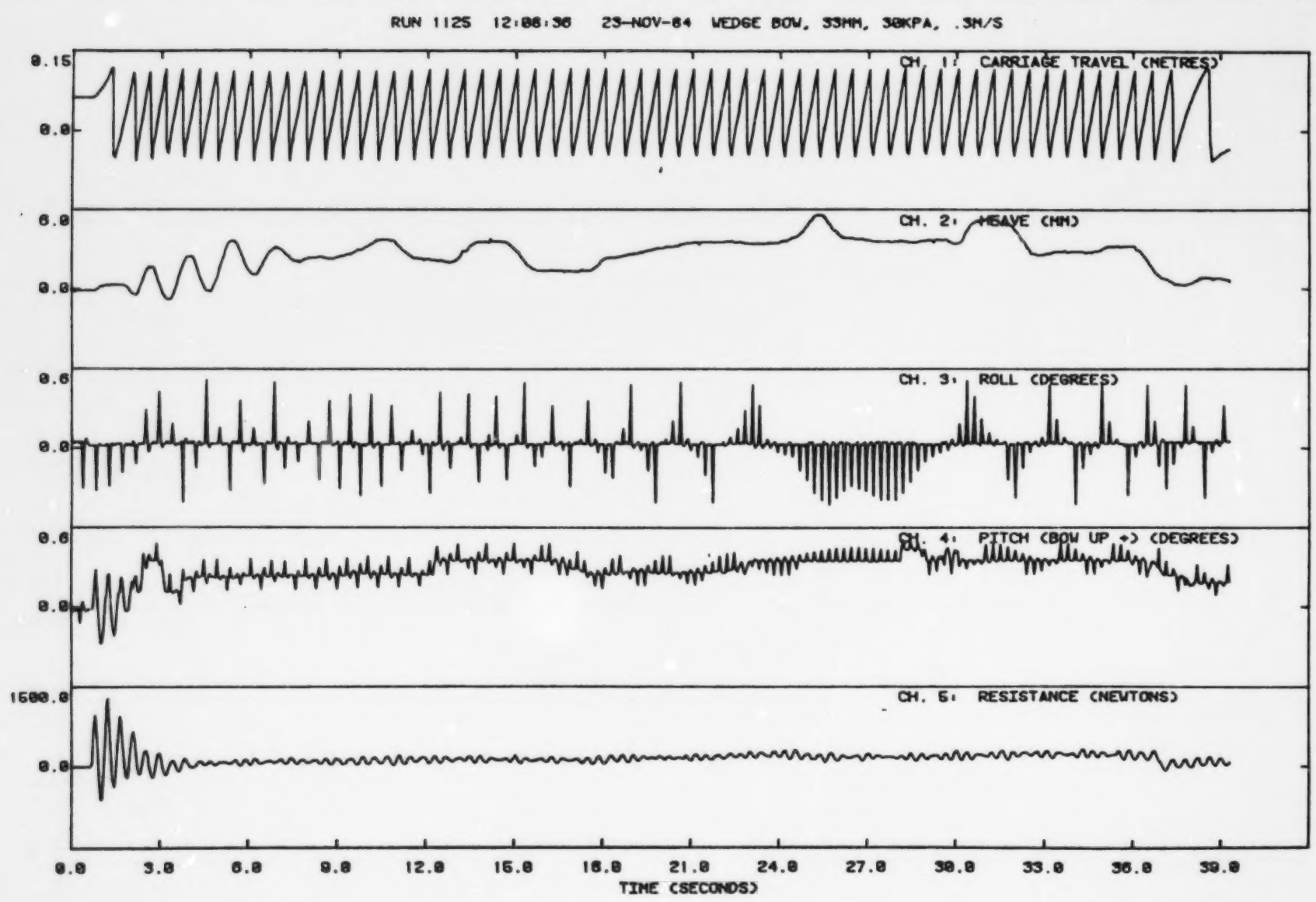

FIGURE 9

LTR-CI-389
LIMITED

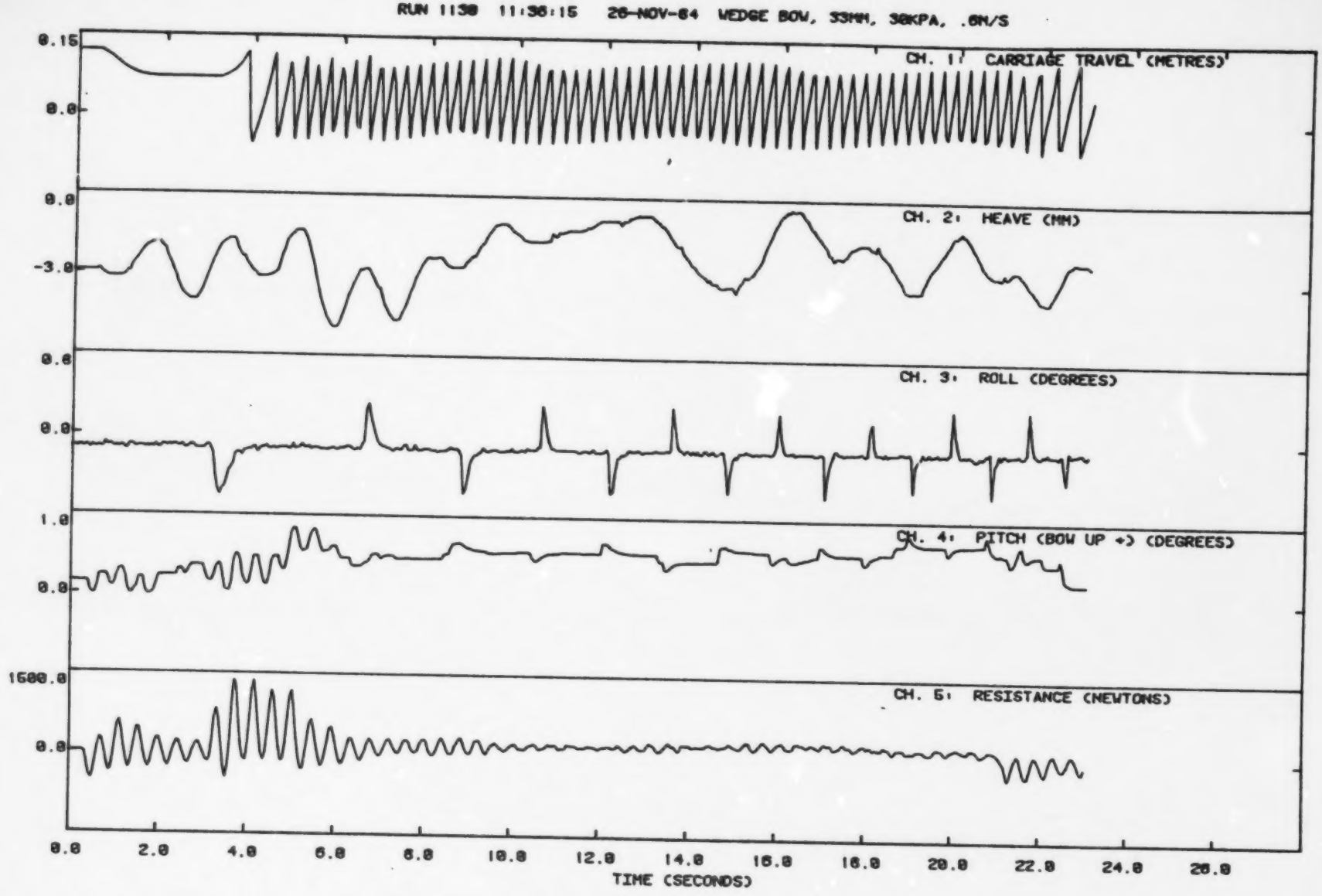
RUN 1130 11:36:15 26-NOV-84 WEDGE BOW, 33MM, 30KPA, .6M/S
0.15
0.0
CH. 1: CARRIAGE TRAVEL (METRES)
0.0
-3.0
CH. 2: HEAVE (MM)
0.0
0.0
CH. 3: ROLL (DEGREES)
1.0
0.0
CH. 4: PITCH (BOW UP +) (DEGREES)
1500.0
0.0
CH. 5: RESISTANCE (NEWTONS)
0.0 2.0 4.0 6.0 8.0 10.0 12.0 14.0 16.0 18.0 20.0 22.0 24.0 26.0
TIME (SECONDS)

FIGURE 10

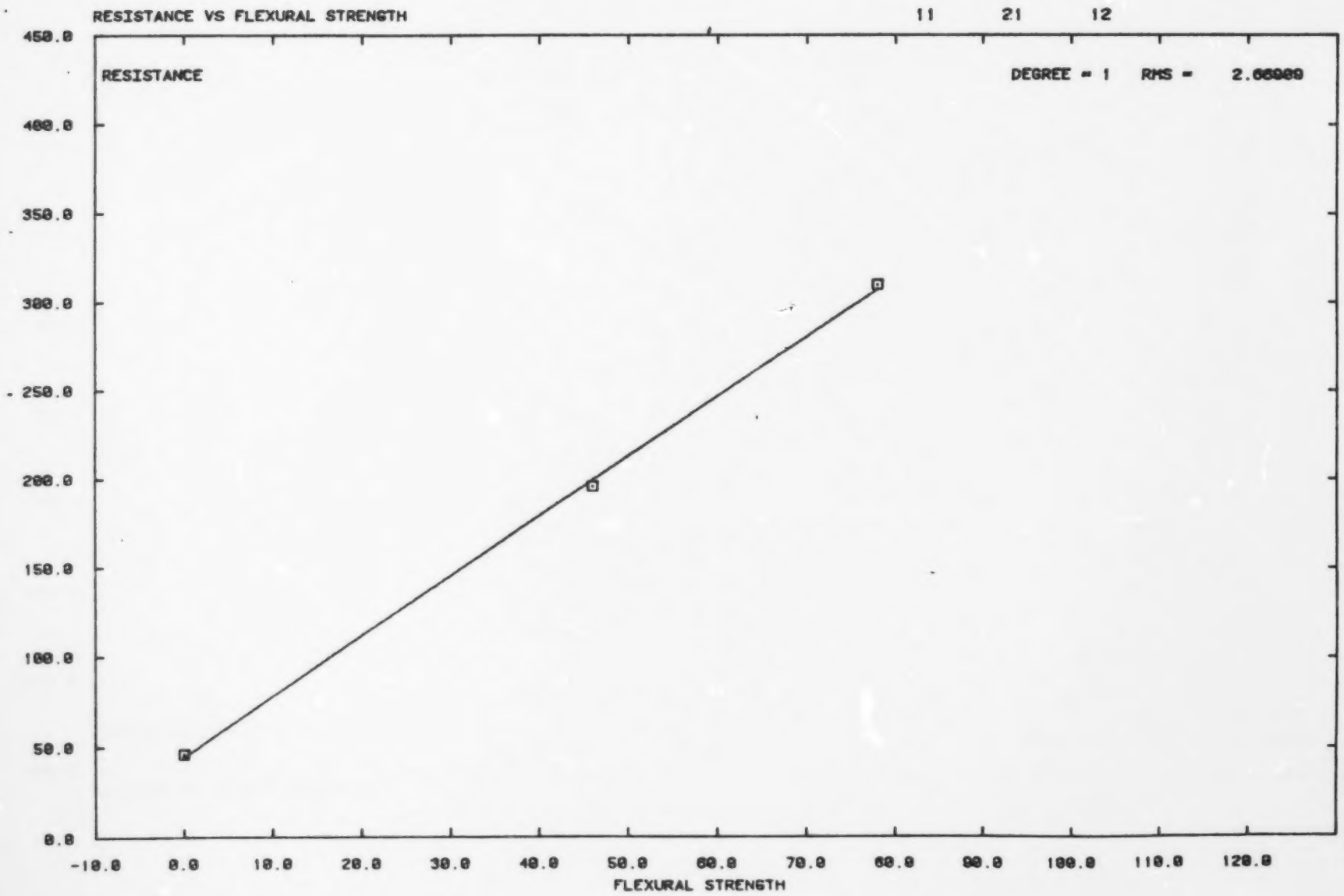

FIGURE 11

LTR-SI-339
LIMITED

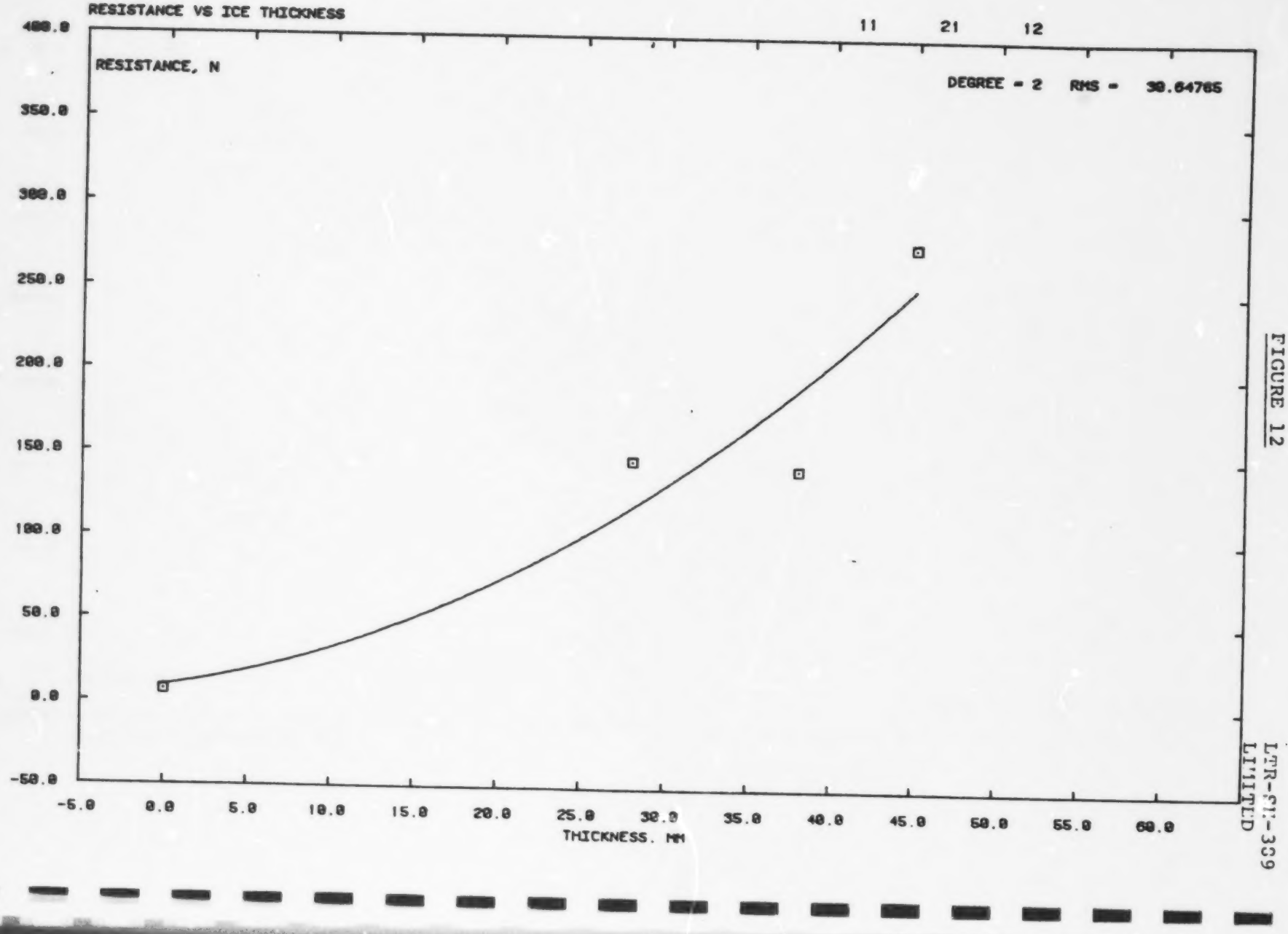

FIGURE 12

LTR-SI-339
LIMITED

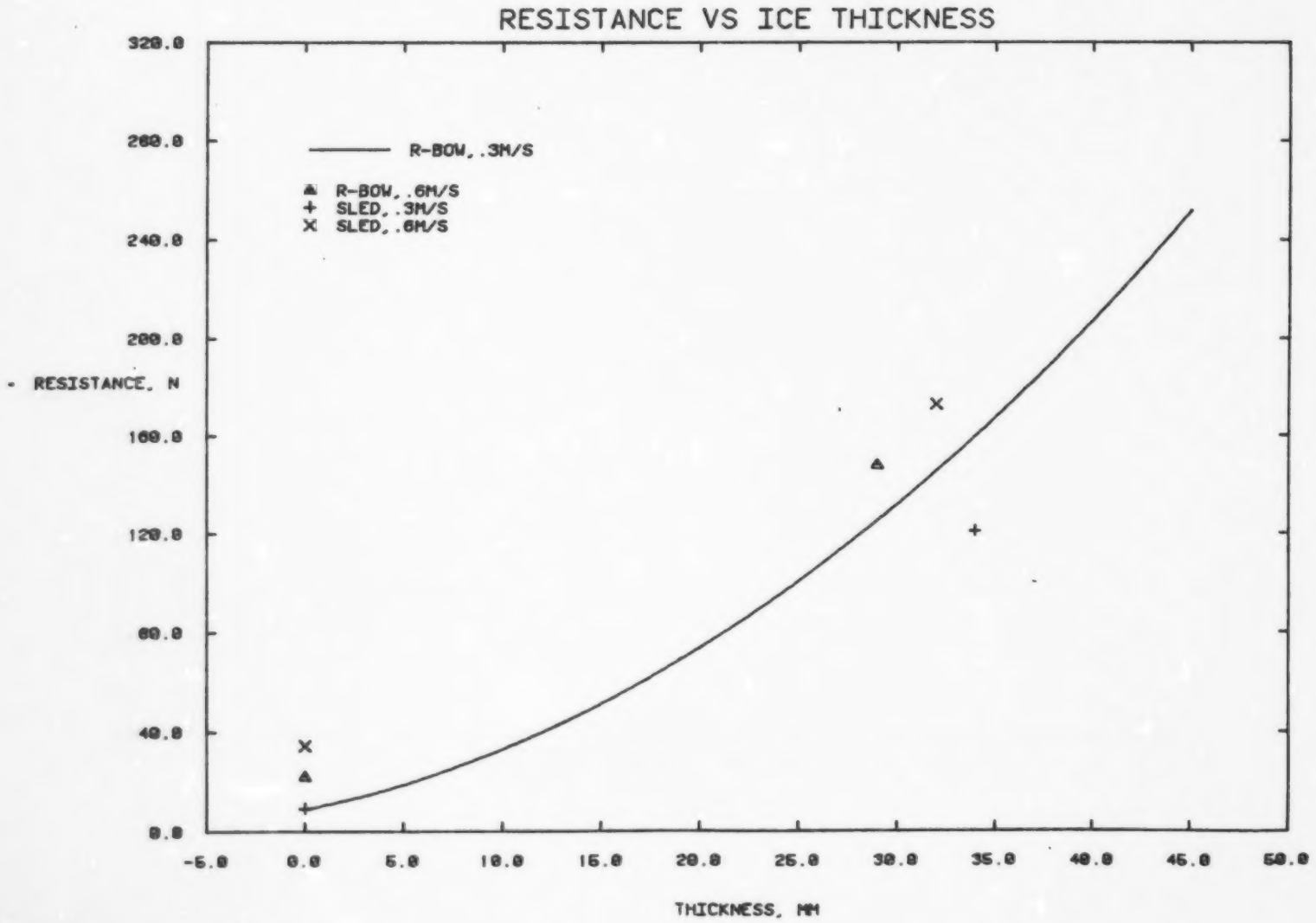

FIGURE 13

LTR-SI-339
LIMITED

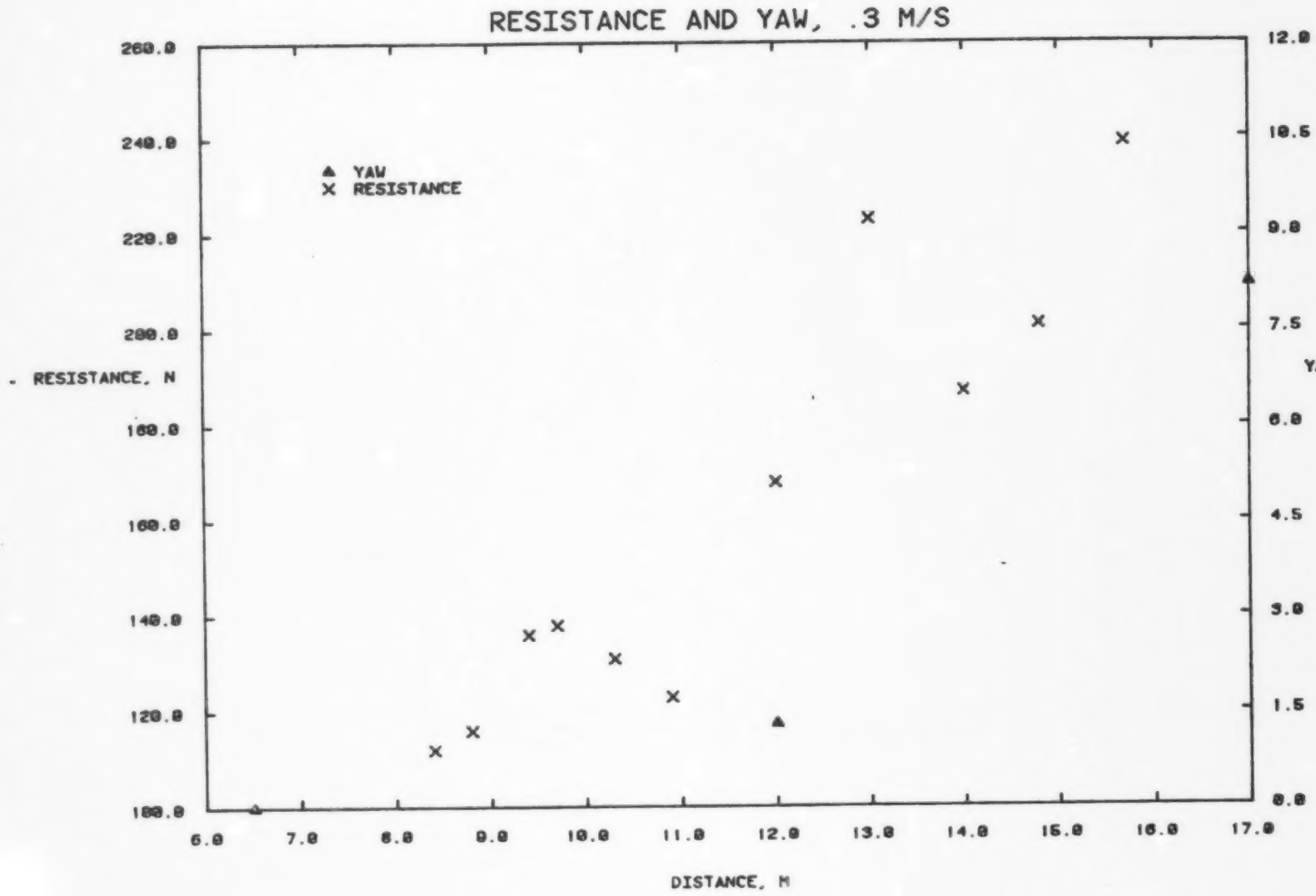

FIGURE 14

LTR-CC-339
LIMITED

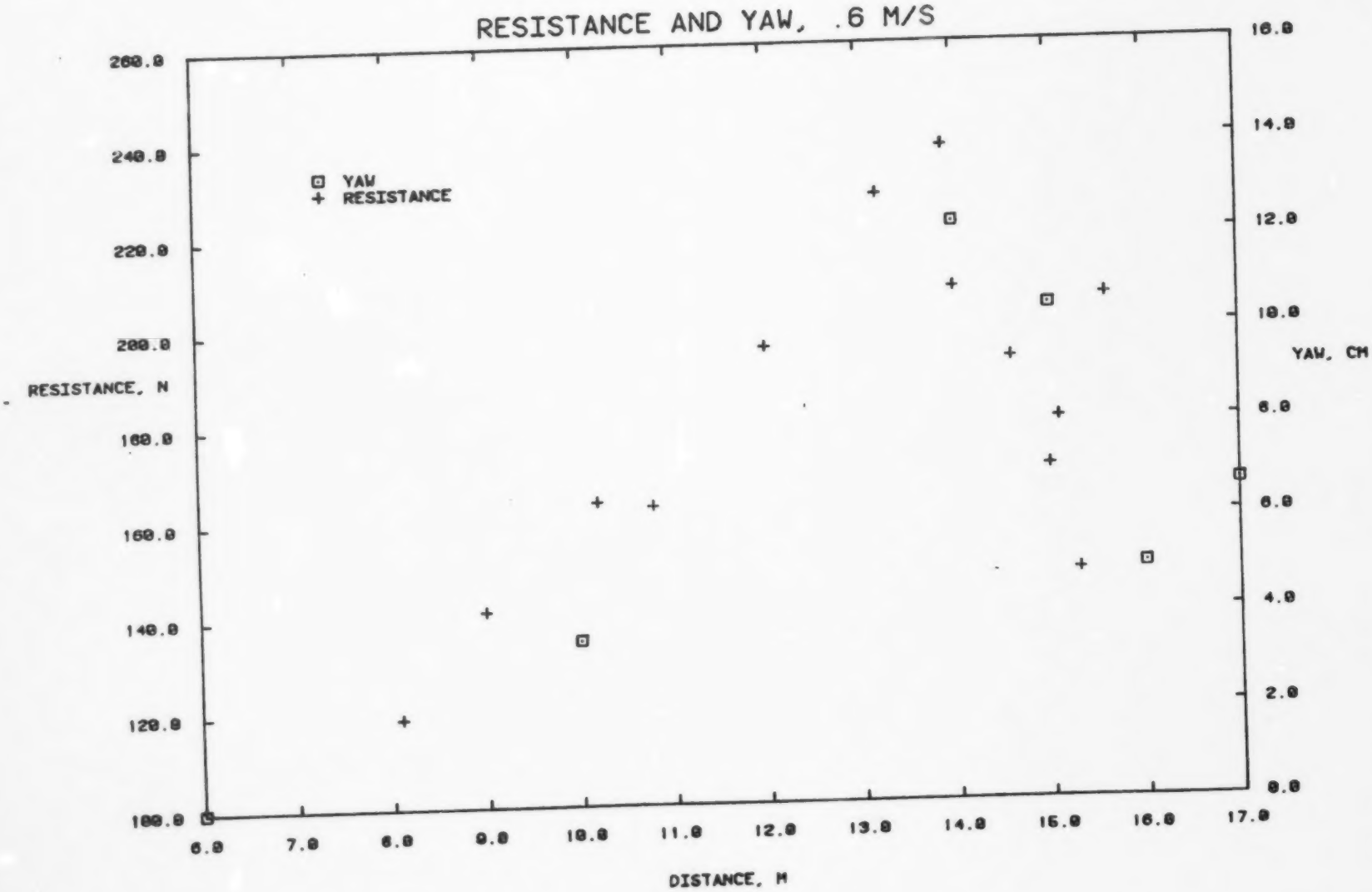

FIGURE 15

LTR-SH-309
LIMITED

APPENDIX A

K·E 10 X 10 TO ½ INCH 7 X 10 INCHES KEUFFEL & ESSER CO MADE IN U.S.A.

Strength is gaining with time

REFRIDGERATION OFF AT 3:00 am NOV. 5

ICE SHEET NO. 1

16E

16W

14E 14W

12E

12W

9E

TEST AT 3:10 pm

180 100 90 80 70 60 50 40 30 20 10 0

1-0 2-0 3-0 4-0 5-0 6-0 7-0 8-0 9-0 10-0 11-0 12-0

HOURS

K·E 10 T CM INCH KEUFFEL & ESSER CO MADE IN U.S.A.

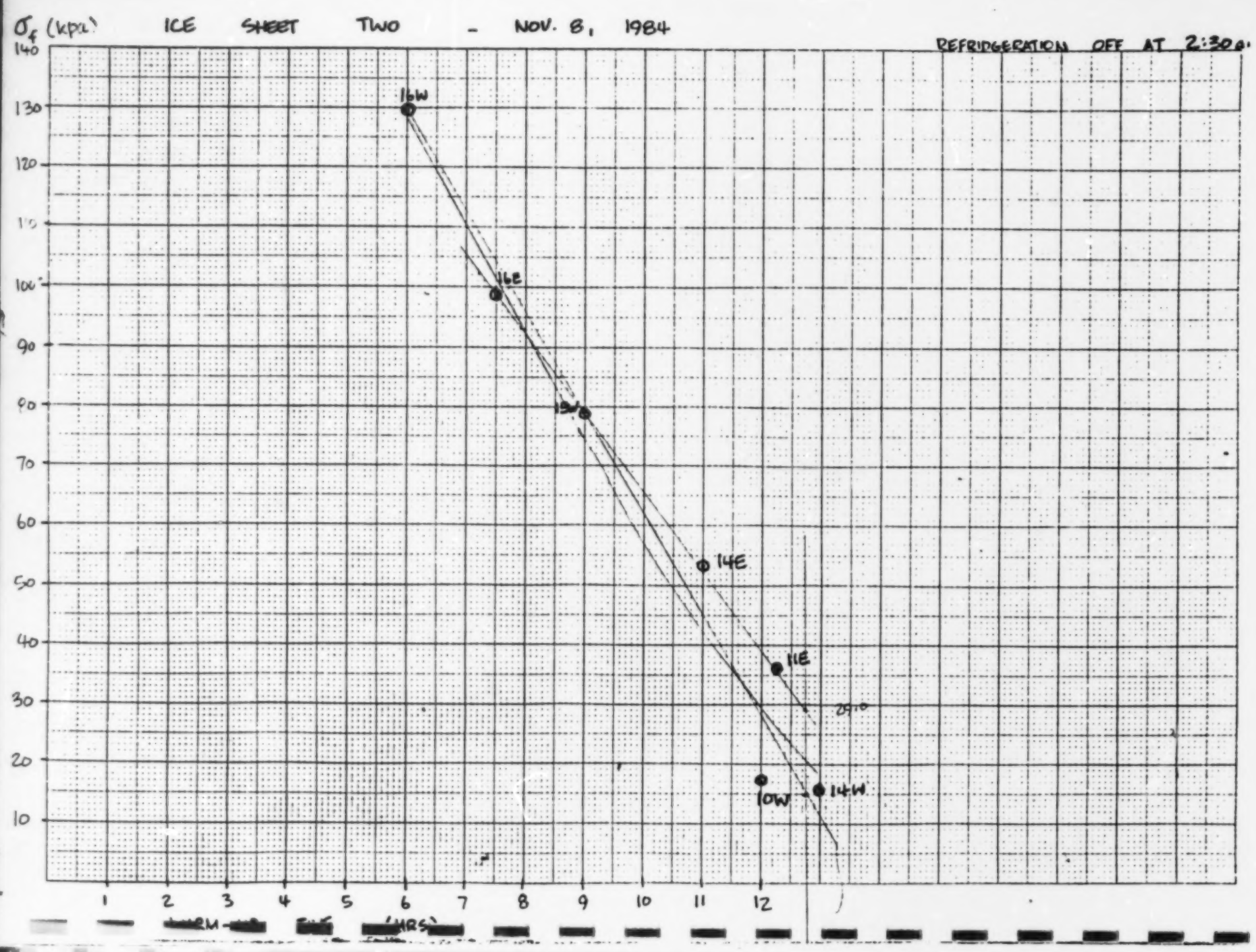

K·E 10 X 10 TO ½ INCH 7 X 10 INCHES KEUFFEL & ESSER CO MADE IN U.S.A.

σ_f (kPa)

ICE SHEET NO 3 FLEXURAL STRENGTH VS. TIME

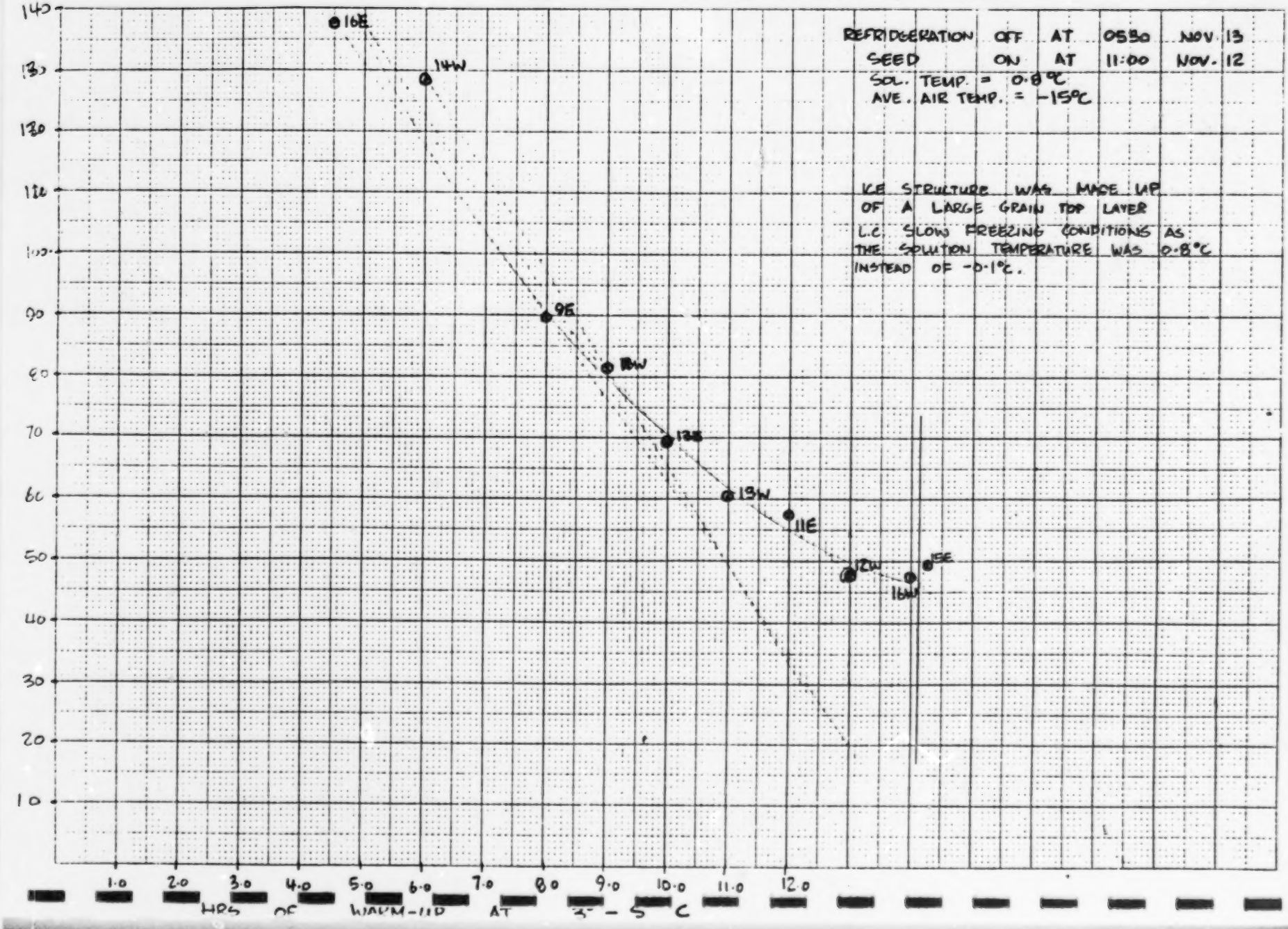

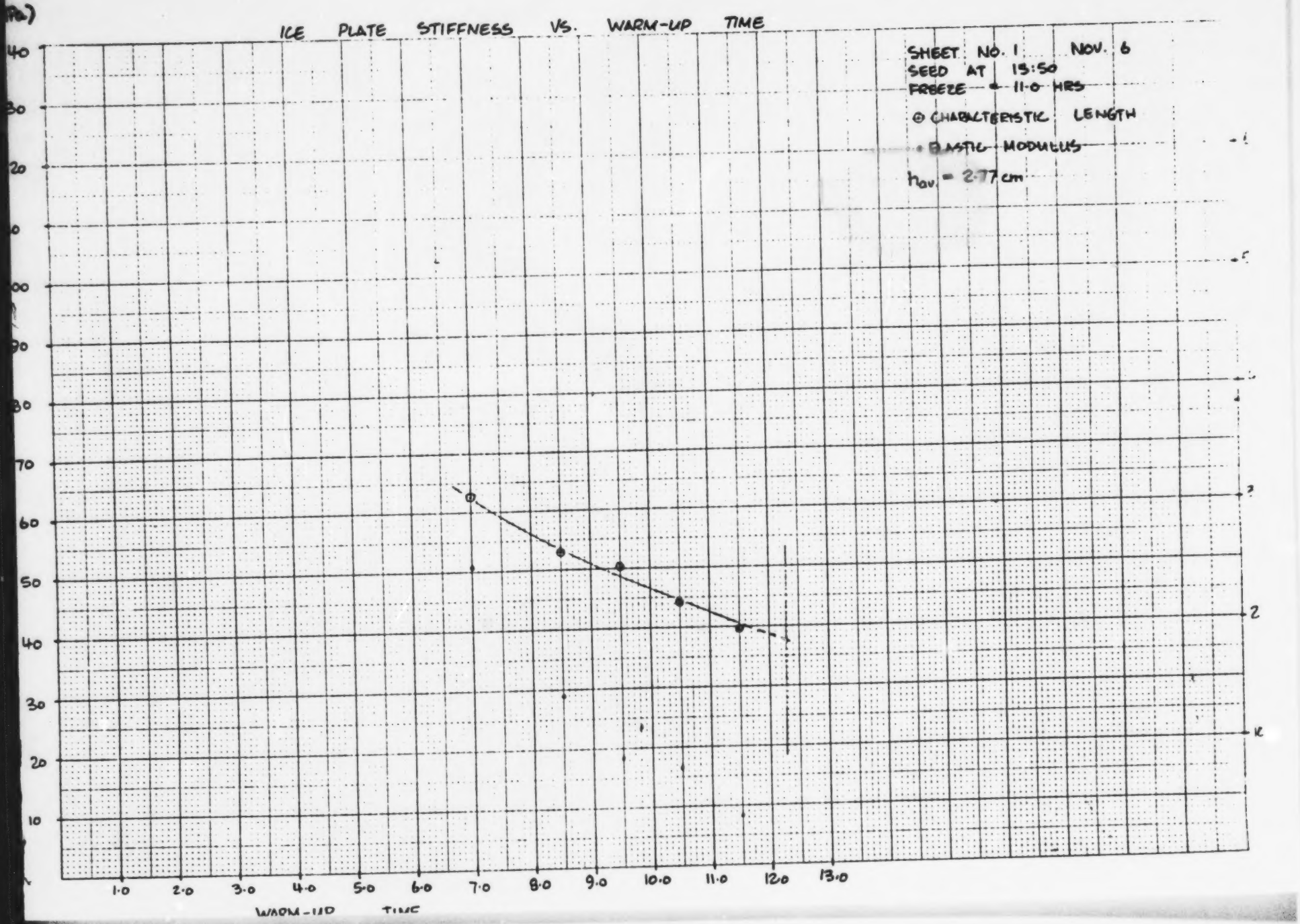
ICE PLATE STIFFNESS VS. WARM-UP TIME
SHEET NO. 1 NOV. 6
SEED AT 15:50
FREEZE + 11.0 HRS
⊕ CHARACTERISTIC LENGTH
• ELASTIC MODULUS
$h_{av.}$ = 2.77 cm
40
30
20
70
60
50
40
30
20
10
1.0
2.0
3.0
4.0
5.0
6.0
7.0
8.0
9.0
10.0
11.0
12.0
13.0
WARM-UP TIME

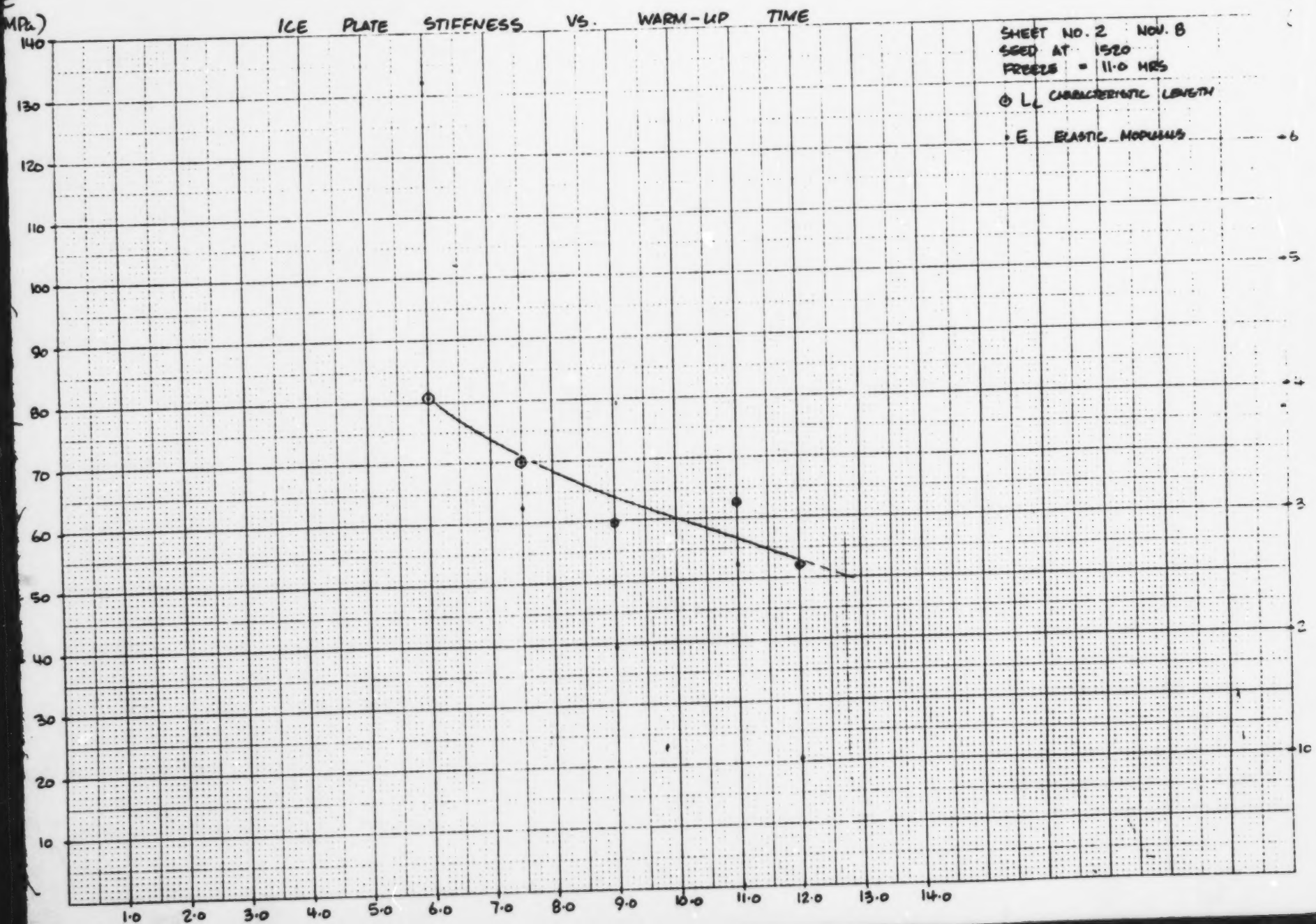
ICE PLATE STIFFNESS VS. WARM-UP TIME
(MPa)
SHEET NO. 2 NOV. 8
SEED AT 1520
FREEZE = 11.0 HRS
Φ L_c CHARACTERISTIC LENGTH
• E ELASTIC MODULUS
140
130
120
110
100
90
80
70
60
50
40
30
20
10
6
5
4
3
2
1
1.0
2.0
3.0
4.0
5.0
6.0
7.0
8.0
9.0
10.0
11.0
12.0
13.0
14.0

K·E 10 X 10 TO ½ INCH 7 X 10 INCHES
KEUFFEL & ESSER CO MADE IN U.S.A.

σ_f (Kp a)

130
120
110
100
90
80
70
60
50
40
30
20
10

REFRIGERATION OFF AT 0945
TEST AT 4:45 PM NOV

14W
16E
12W
14E
10E 10W
9E

1.0 2 3 4 5.0 6.0 7.0 8.0 9.0 10.0 11.0 12.0

LOG AT LIABILITY AT 20 - 4° C

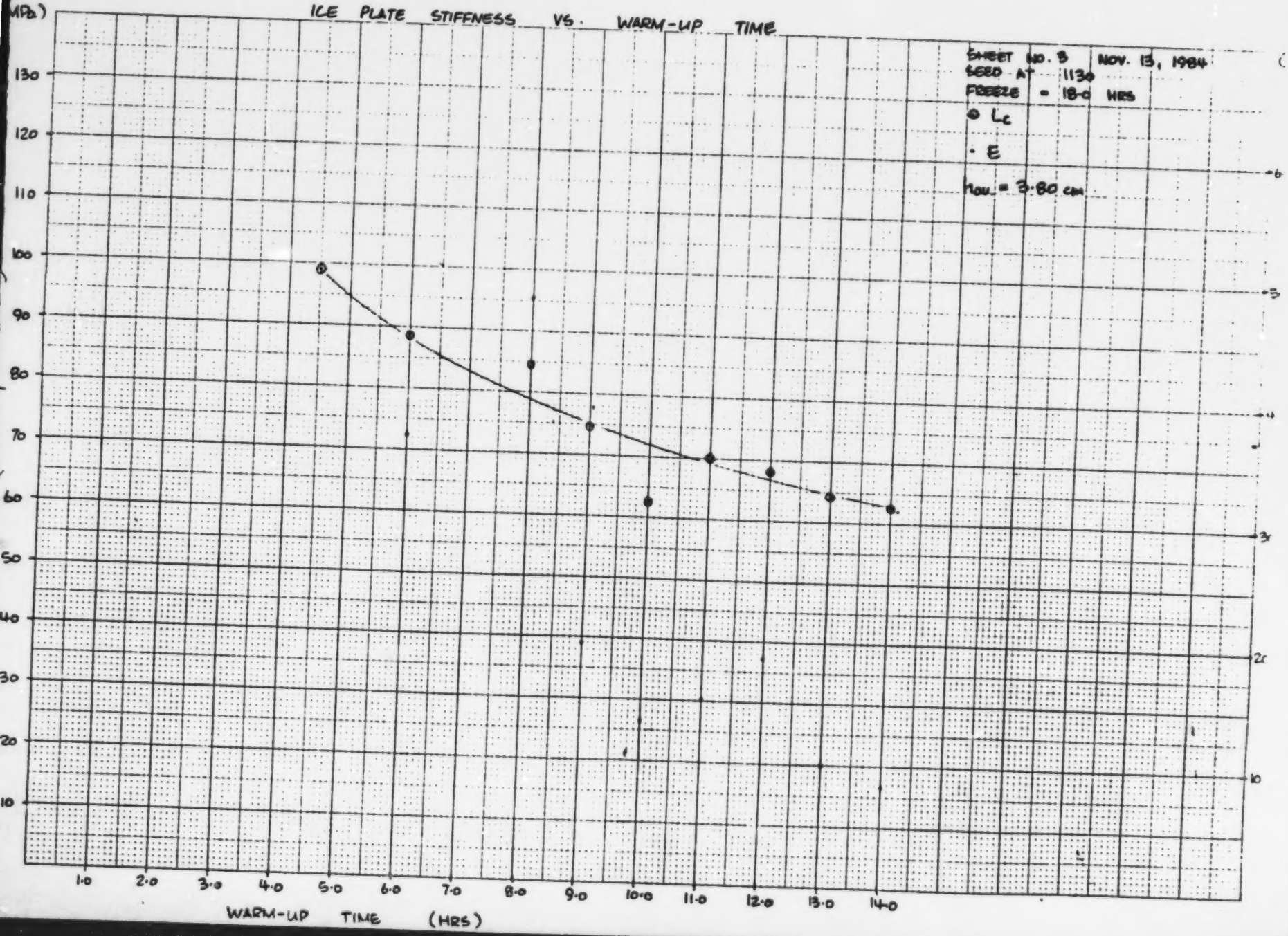
ICE PLATE STIFFNESS VS. WARM-UP TIME
SHEET NO. 3 NOV. 13, 1984
SEED AT 1130
FREEZE = 18.0 HRS
Lc
E
Hou = 3.80 cm
(MPa)
130
120
110
100
90
80
70
60
50
40
30
20
10
1.0
2.0
3.0
4.0
5.0
6.0
7.0
8.0
9.0
10.0
11.0
12.0
13.0
14.0
WARM-UP TIME (HRS)

K·E 10 A 10 TO INCH KEUFFEL & ESSER CO MADE IN U.S.A.

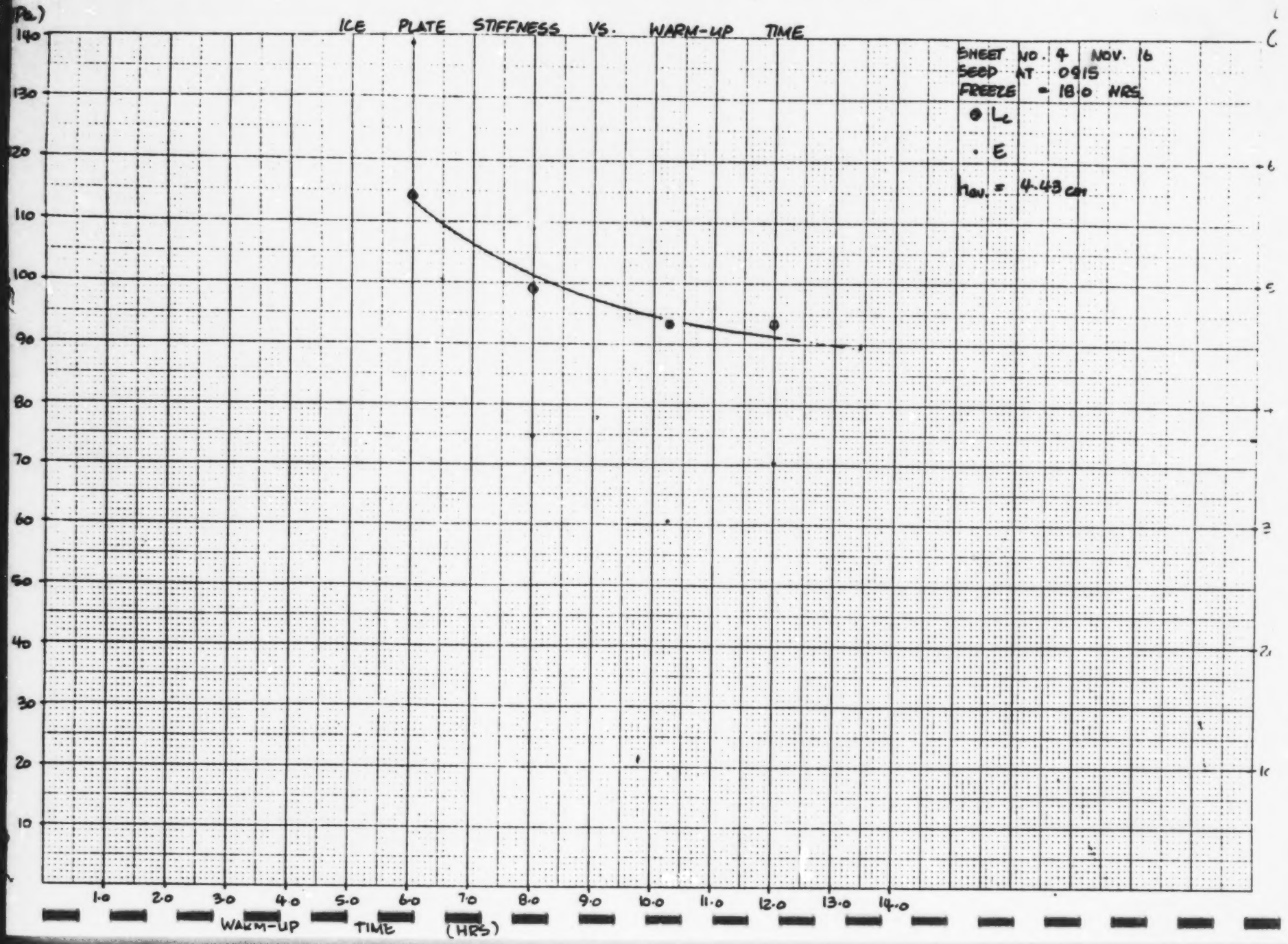

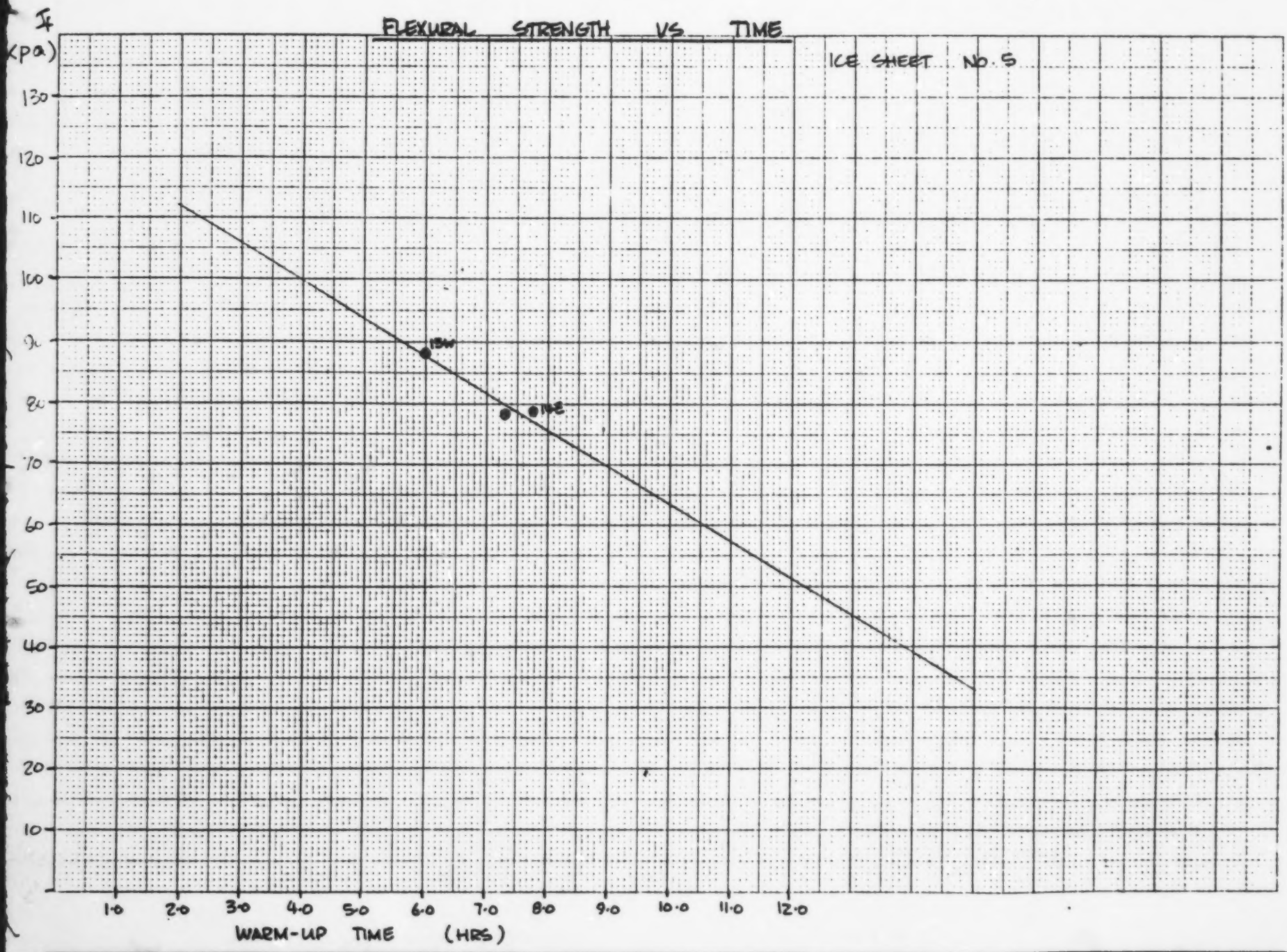
FLEXURAL STRENGTH VS TIME
ICE SHEET NO. 5
If (KPa)
130
120
110
100
90
80
70
60
50
40
30
20
10
1.0
2.0
3.0
4.0
5.0
6.0
7.0
8.0
9.0
10.0
11.0
12.0
WARM-UP TIME (HRS)

K·E 10 T VCH INCH KEUFFEL & ESSER CO. MADE IN U.S.A.

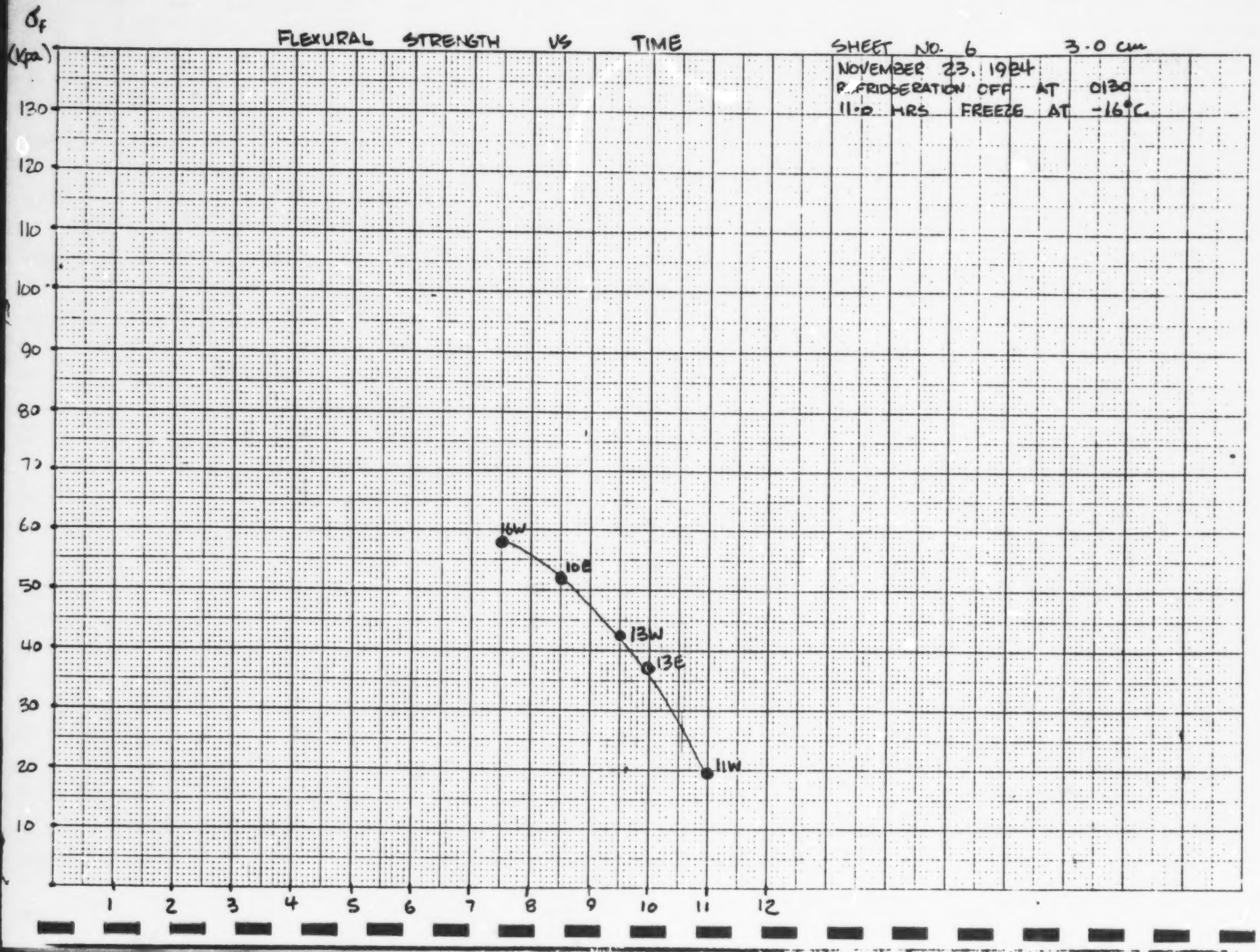

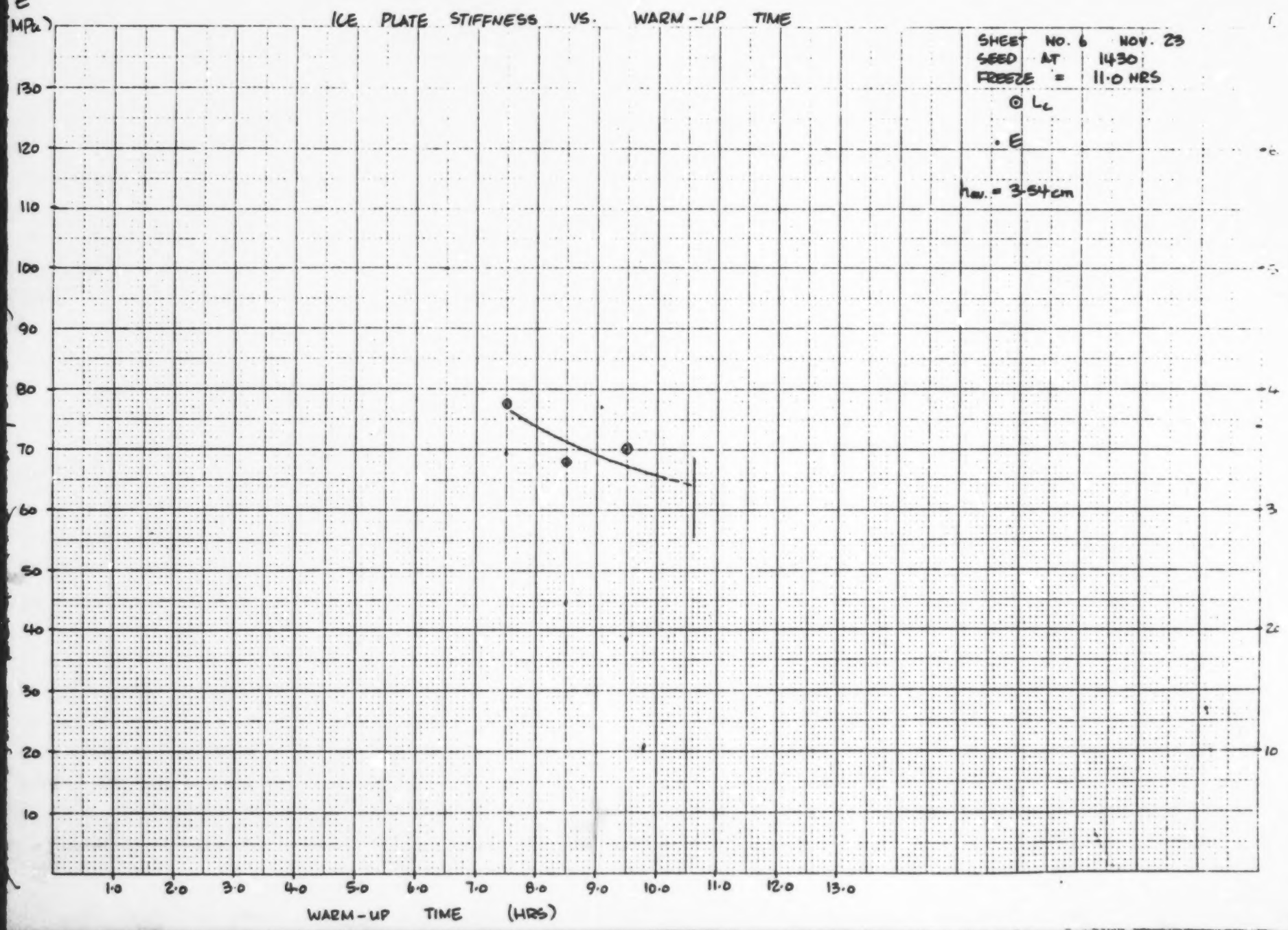
ICE PLATE STIFFNESS VS. WARM-UP TIME
E (MPa)
SHEET NO. 6 NOV. 23
SEED AT 1430
FREEZE = 11.0 HRS
◎ L_c
• E
$h_{av.}$ = 3.54cm
130
120
110
100
90
80
70
60
50
40
30
20
10
1.0
2.0
3.0
4.0
5.0
6.0
7.0
8.0
9.0
10.0
11.0
12.0
13.0
WARM-UP TIME (HRS)
4
3
2
10

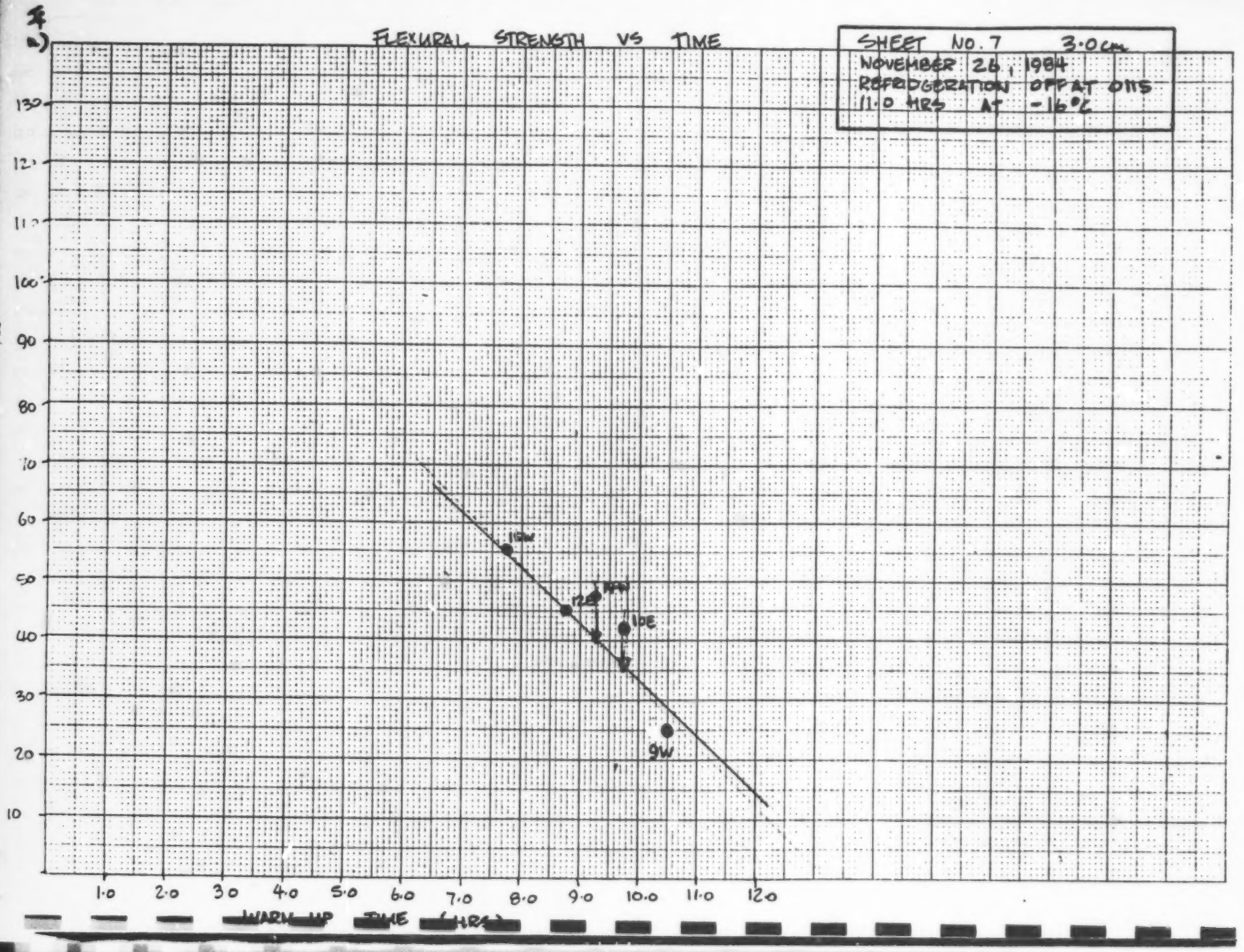
FLEXURAL STRENGTH VS TIME
SHEET NO. 7 3.0 cm
NOVEMBER 26, 1984
REFRIGERATION OFF AT 0115
11.0 HRS AT -16°C
130
120
110
100
90
80
70
60
50
40
30
20
10
1.0
2.0
3.0
4.0
5.0
6.0
7.0
8.0
9.0
10.0
11.0
12.0
WARM UP TIME (HRS)
11W
12W
12E
11E
9W

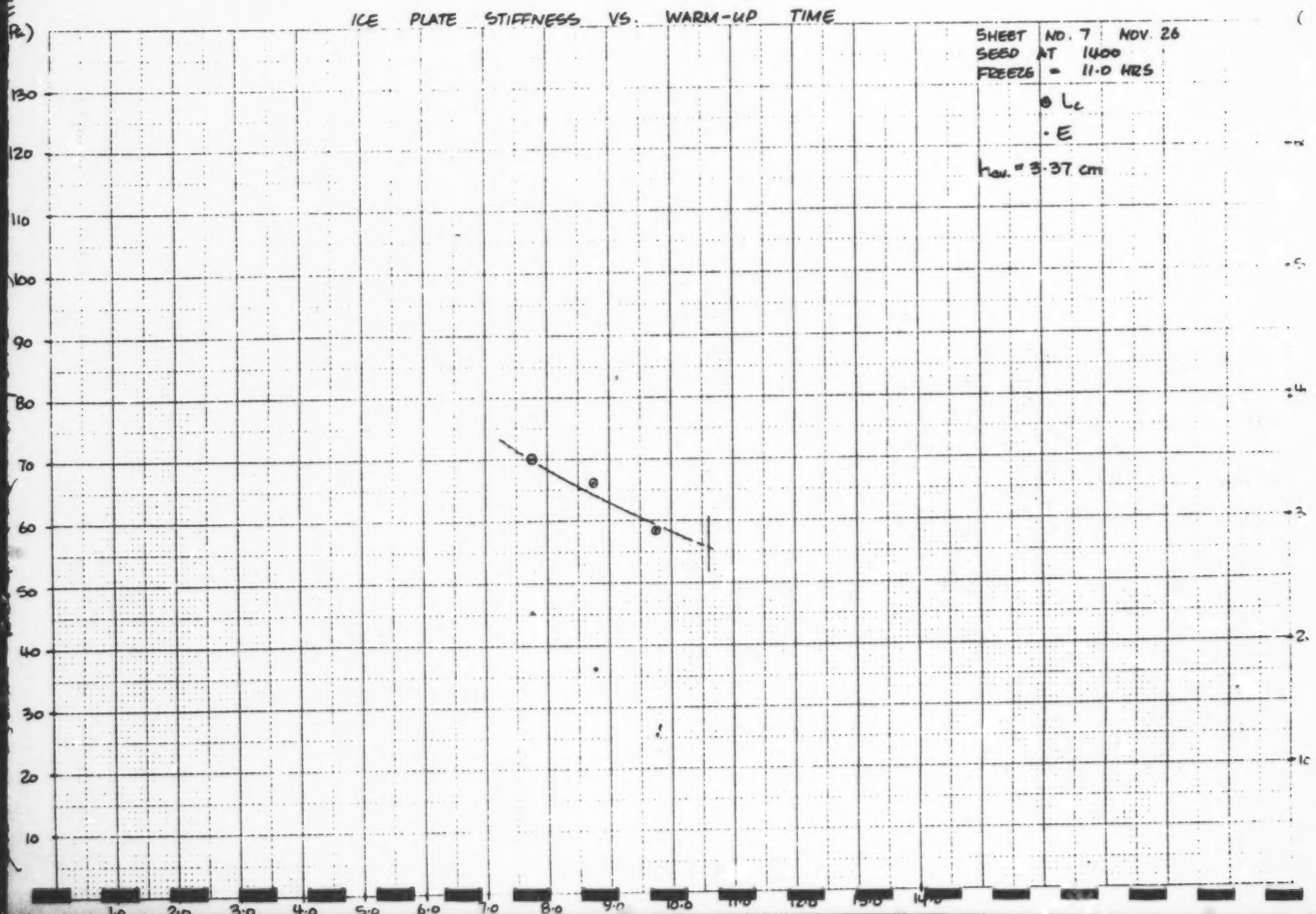
ICE PLATE STIFFNESS VS. WARM-UP TIME
SHEET NO. 7 NOV. 26
SEED AT 1400
FREEZE = 11.0 HRS
Lc
E
hav. = 3.37 cm
(Pa)
130
120
110
100
90
80
70
60
50
40
30
20
10
1.0
2.0
3.0
4.0
5.0
6.0
7.0
8.0
9.0
10.0
11.0
12.0
13.0
14.0

APPENDIX 2

ARCTEC Model Test Report 1904C

ARCTEC CANADA LIMITED 1904C

THE TESTING OF THE SWATH MODEL IN ICE

APRIL 4 1985

BY

D. HOWARD,
L. GOOSSENS,

SUBMITTED TO:

German and Milne,
Suite 300, 4999 St. Catherine St. West,
Montreal, Quebec.
H3Z 1T3

SUBMITTED PY:

Arctec Canada Limited,
311 Legget Drive,
Kanata, Ontario.
K2K 1Z8

LIST OF FIGURES

3.1 MEASUREMENT OF FLEXURAL STRENGTH 5
3.2 MEASURING THE ELASTIC MODULUS OF A SHEET 5
3.3 ICE BASIN ARRANGEMENT FOR TEST NO. 1 10
3.4 ICE BASIN ARRANGEMENT FOR TEST NO. 2 11
3.5 INSTRUMENTATION AND DATA ACQUISITION SYSTEM 12
5.1 SIMULATION OF TWO POINT LOADS ON AN INFINITE ICE SHEET 21

LIST OF TABLES

2.1 MODEL HULL DATA SHEET 3
3.1 TEST MATRIX 9
4.1 MODEL FRICTION COEFFICIENT 15
4.2 ICE RESISTANCE RESULTS FOR SWATH MODEL 16
4.3 ICE RESISTANCE RESULTS FOR STARBOARD SWATH MODEL 16
5.1 DIRECT COMPARISON BETWEEN MODELS 19
5.2 NORMALIZED COMPARISON BETWEEN MODELS AT TARGET CONDITIONS 19

1. INTRODUCTION

Model ice resistance tests were performed on the SWATH (Small Waterplane Area Twin Hull) icebreaking model in the refrigerated ice basin of Arctec Canada Limited in Kanata, Ontario. Two ice sheets were prepared in which four configurations were tested. The first two configurations used the entire model whereas the second two configurations used only one hull. For each of these two model configurations, two ice configurations were tested. For the first ice configuration, a seven metre length of ice was pre-sawn into the approximate size in which the model would break the ice. This scenario would give the sum of the submergence ice resistance, turning ice resistance, frictional ice resistance and hydrodynamic resistance, omitting the force required to break the ice. The second ice configuration was through unbroken ice and measured the total icebreaking resistance. In this scenario, two velocities were tested. This resulted in a total of six data points for two model and two ice configurations.

This report describes the model and test procedures including the results of these tests. Conclusions are drawn from these tests. Appendix A shows the computer plots of all digitized ice resistance data.

2. MODEL DESCRIPTION

Table 2.1 lists the details of the model. For the tests using the entire model, the model was towed from the center of gravity and was restrained in surge, sway, and yaw. For the tests with only the starboard hull, the model was towed from the same lengthwise location, but was towed from just above the deck. This was required because the heavestaff could not fit into the narrow hull. For these tests, the model was restrained in surge, sway, yaw and roll.

ARCTEC CANADA LIMITED

TABLE 2.1

SERIAL #	MODEL HULL DATA SHEET	DESIGNATION
VESSEL NAME & HULL FORM	SWATH ICEBREAKING MODEL (Small Waterplane Area Twin Hull)	SCALE 1:20

*DIMENSIONAL PARAMETERS

L_{BP} = 5.30 m

L_{WL} = 5.35 m

B = 1.20 m (overall)
B = 0.20 m (each hull)
T = 0.53 m
= 0.957 m³
Roll Period = 2.10 sec
Pitch Period = 1.3 sec

C_b = 0.844 (one hull)

C_{bf} =

C_p = 0.865 (one hull)

C_w =

C_{wf} =

C_m = .976 (one hull)

γ_0 = °

β_5 = 0°

**NONDIMENSIONAL PARAMETERS

L/B = 4.458

B/T = 2.264

μ_0 =

η_2 =

FRICTION FACTORS, f:

f = .09

GEOMETRY-FRICTION COEFFICIENTS

f	μ_1	μ_2
0.000		
0.100		
0.200		
0.300		
0.400		
0.500		

FOREBODY WATERPLANE ANGLES

STATION	10 (FP)	9½	9	8½	8	7½	7	6½	6	5½	5
α °											
β °											

3. DATA COLLECTION PROCEDURES

The procedures described herein are standard procedures followed by Arctec Canada Limited for model ship ice resistance tests.

3.1 Model Friction Coefficient

The model friction is determined by measuring the load required to pull a known weight over the surface of the model. The model is cooled down to prevent excess melting during friction tests. The model is then positioned with the aid of a spirit level such that the area of interest is horizontal. The model surface is then liberally coated with water to simulate the ice-water-hull interface which would occur during the model tests. A block of urea ice ranging between 50 and 120 grams is placed on the model and manually pulled over the surface with an instrumented load ring. The length of the run is dependent upon the surface being tested. If there is considerable curvature on the area of the model of interest, the run will be kept short to reduce errors associated with the surface not being horizontal. However, if the curvature is slight, the run is larger to get a more uniform, steady-state measurement. The speed of the test is approximately 0.1 m/sec (1 knot full scale). The test is repeated by loading dead weights onto the ice sample, recording both the total weight (ice sample plus dead weight) and the load required to pull the ice over the surface. The friction coefficient is determined from the slope of the plot of the normal force versus the frictional force.

3.2 Ice Thickness

Ice thickness measurements were made as soon as possible following each level ice test. Using a standard set of calipers, thickness was measured on both sides of the ship track at one metre intervals along the length of the basin. Ice thickness values used in the analysis are the mean values for each run determined from the model position.

3.3 Ice Flexural Strength

Values of ice flexural strength were determined by breaking cantilever beams cut in a surrounding ice sheet. Cantilever beam tests are performed by cutting three of the four sides of a rectangular shape and then loading the free end until failure occurs (See Figure 3.1). A beam is cut to an appropriate size using an ice saw, leaving sufficient clearance on all three sides so as not to restrict deflection. The beam is then loaded until failure and carefully removed to measure its exact dimensions. Load measurements are made using a hand-held calibrated load cell. The load cell velocity was approximately 0.01 m/sec, varying the strain rate from about 3×10^{-2}/sec for a 20 mm ice sheet to about 1.5×10^{-2}/sec for a 40 mm ice sheet. Since ice is a non-homogeneous material and not highly dependent on strain rate, it is more accurate to get a number of measurements by hand rather than a smaller number of measurements at a constant speed. Tests confirming this have been done periodically in the past.

FIGURE 3.1

MEASUREMENT OF FLEXURAL STRENGTH

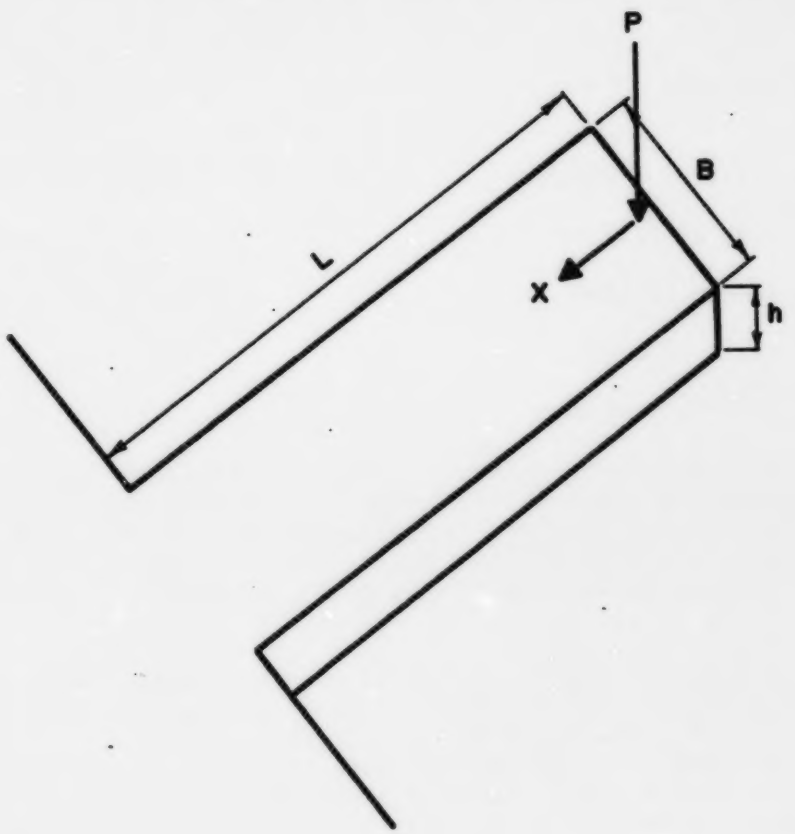

FIGURE 3.2

MEASURING THE ELASTIC MODULUS OF A SHEET

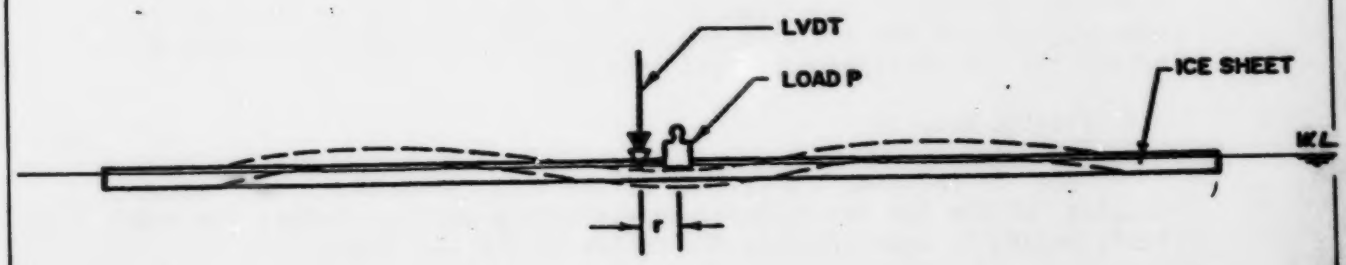

Beams are cut to the dimensions L = 5h; B = 1.5h. Using these dimensions it is possible to neglect the effect of having the beam supported on an elastic foundation, permitting the use of 'classical beam theory'. The error caused by neglecting an elastic foundation is less than five percent if target dimensions are achieved. The flexural strength is given by:

$$\sigma_f = 6\ PL/Bh^2 \qquad (3.1)$$

where σ_f = flexural strength

P = load at failure

L = length of beam

B = width of beam

h = thickness of beam

While the ice sheet is thawing, flexural strength measurements were taken approximately hourly. However, since each measurement requires cutting a hole in the ice, less frequent measurements were taken during the early part of the thaw to preserve an intact ice sheet. During this period the ice sheet is carefully watched by experienced personnel.

While thawing the ice sheet, all flexural strength measurements were taken approximately 0.5 m from the side of the basin. This is to preserve the center of the basin for the ice test. However, following the ice tests the flexural strength data is obtained as close as possible to the channel track. Since flexural strength varies both with time and with location, it is not possible to interpolate to the exact strength at test time unless the same locations are used. However, if flexural strength measurements are obtained close to the test channel before the test, these holes in the ice could influence the resistance results. Therefore, it is felt that it is more precise to only measure flexural strength near the test channel immediately following the resistance test and to use this data as the absolute value for the resistance test. In this manner ice resistance will not be influenced by any holes in the ice. Any errors due to slight drops in flexural strength because of a maximum of a 35 minute delay (or an average 21.5 minutes) between the ice test and the flexural strength measurement will affect the ice resistance by less than 5%.

3.4 Elastic Modulus

Due to the time limitations of the test procedure, the elastic modulus of the ice was measured approximately one hour before the model tests began, in approximately the centre of the ice sheet.

The elastic modulus is determined by applying a load on the ice and simultaneously measuring the deflection of the ice at a nearby location. Ideally, the load should be a point load, but for practical

reasons the load is applied to a "button" of diameter "a". The actual diameter of the button used is 50 mm. The button as well as distributing the load evenly to the ice acts as a thermal insulator between the ice sheet and the load. Even when using the button, the loading device should be approximately the same temperature as the ice so melting through the ice will not occur.

The load is commonly applied with a small "dead weight" set. To prevent errors caused by "creep" while loading the ice, the load is applied and removed in less than thirty seconds. The ice deflection is the difference between the deflection while under load and that immediately following the removal of the load, and is measured using a dial gauge. Although a dial gauge does apply a varying load to the ice sample, this error is of the order of one percent for a 30 mm ice sheet and will be smaller for thicker ice. The deflection measuring device is also placed on a "button" as described above.

Wyman's theories [1], for an infinite free floating plate on elastic foundations are used to calculate the elastic modulus. This theory requires the load and the associated measured deflection at a distance "r" from the load. The distance "r" is kept usually between 0.3 l_c and 0.5 l_c since more accurate modulus of elasticity values were obtained. (See Figure 3.2).

This procedure is followed using a number of different loads, and the data is regressed to give the deflection to load ratio. The deflection to load ratio is then used in Wyman's equation as follows:

$$2\pi\rho g r^2 \left(\frac{\delta(r)}{p}\right) = \left(\frac{r}{l_c}\right)^2 [\text{kei}\ (r/l_c)] \qquad (3.2)$$

Note: The value of "kei" must either be solved numerically or looked up in tables. Listings of "kei" can be found in most mathematical handbooks.

Equation 3.2 is calculated iteratively until an exact value for the characteristic length is found. Once the characteristic length is determined and all the above constraints are satisfied, then the elastic modulus is calculated as follows:

$$E = \frac{12\, g(1 - \nu^2) l_c^4}{h^3} \qquad (3.3)$$

where ν = Poisson's Ratio (assumed = 0.33).

The elastic modulus measurement as described above is measured at one location in the ice sheet. Along with this value is a corresponding flexural strength measurement. From these two parameters, the modulus to strength ratio for each ice sheet is calculated. Due to the length of time required to obtain one modulus measurement, it is assumed that the modulus ratio throughout the ice sheet does not vary with location or time. Therefore, the modulus for each test is obtained by multiplying the local flexural strength by this one ratio. It was found in [2] that this approximation is good as long as the variation of flexural strength around the basin is small and the time lapse is low.

3.5 Ship Resistance Tests

The model resistance tests were performed in two ways. For the first ice sheet, the entire SWATH model as described in Section 2 was used. During these tests, the model was towed from the ship's centre of gravity. It was restrained in surge, sway and yaw leaving the model free to pitch roll and heave. For the second ice sheet, only the starboard hull was used. During these tests the model was towed from the longitudinal centre of gravity. However, since each hull is asymmetric as well as being unstable, for these tests the hull was restrained in surge, sway, yaw and roll leaving only freedom to pitch and heave. Table 3.1 lists the ice resistance test matrix.

For each of the ice sheets, 7 metres of the ice was precut to the size of the broken floes. The dimensions of the pre-sawn ice is shown in Figures 3.3 and 3.4. With the ice already cut to size, it should be possible to separate the icebreaking resistance into its components. The pre-sawn test would measure the sum of the submergence resistance, the ice piece turning resistance, the ice frictional resistance and the hydrodynamic resistance. The breaking resistance would be measured in the following test.

The model resistance is measured with an Arctec Canada Limited designed force block. The force block is a 10 cm cube with strain gauges used to measure load. Prior to the test series the force block was calibrated using identical instrumentation as was used for the test series. Additionally, check calibrations were performed before each test day to insure that the instrumentation was functioning properly. During the ice resistance tests, the model speed and position were measured using a transducer attached to the towing carriage drive mechanism.

3.6 Data Acquisition and Reduction System

The instrumentation system used is shown in Figure 3.5. Both the force block (which was used to measure model resistance) and the load ring (which was used to measure the flexural strength) were conditioned with Vishay series 2100 strain gauge conditioners. The carriage position signal was differentiated to produce carriage velocity. All four of these signals, as well as voice and an event marker, were recorded on an 8 channel FM analog recorder. To ensure that the data was being correctly recorded, the output of the recorder was played live onto an oscillograph chart recorder during all tests. The oscillograph was used only as a real time check of the data acquisition system. All data processing was done with an HP 9816 microcomputer coupled to an Arctec 32 channel A/D unit. This computer system digitized and processed the results of all tests, producing statistics on manually input intervals.

The analysis of the resistance data was done following the tests due to availability of the computer. This data was replayed from the analog tape recorder, filtered through a "low pass" filter at 1 Hz, and then digitized at 16 Hz. The selection of the filtering and digitization frequencies was due to the type of output required. Since

TABLE 3.1

TEST MATRIX

TEST NO.	RUN NO.	TEST DATE	TARGET VELOCITY	TARGET ICE THICKNESS	TARGET FLEXURAL STRENGTH	MODEL USED	COMMENTS
01	01A	25/03/85	V_1	h_1	σ_{f_1}	SWATH	Ice is pre-sawn
01	01B	25/3/85	V_1	h_1	σ_{f_1}	SWATH	Ice is unbroken
01	02	25/3/85	V_2	h_1	σ_{f_1}	SWATH	Ice is unbroken
02	01A	27/3/85	V_1	h_1	σ_{f_1}	Stbd. hull	Ice is pre-sawn
02	01B	27/3/85	V_1	h_1	σ_{f_1}	Stbd. hull	Ice is unbroken
02	02	27/3/85	V_2	h_1	σ_{f_1}	Stbd. hull	Ice is unbroken
02	03A	27/3/85	V_1	h_1	σ_{f_1}	Stbd. hull	Ice is unbroken
02	03B	27/3/85	V_2	h_1	σ_{f_1}	Stbd. hull	Ice is unbroken

Where V_1 = 0.30 m/sec

V_2 = 0.60 m/sec

h_1 = 0.030 m

σ_{f_1} = 30 kPa

Figure 3.3 ICE BASIN ARRANGEMENT for TEST No. 1

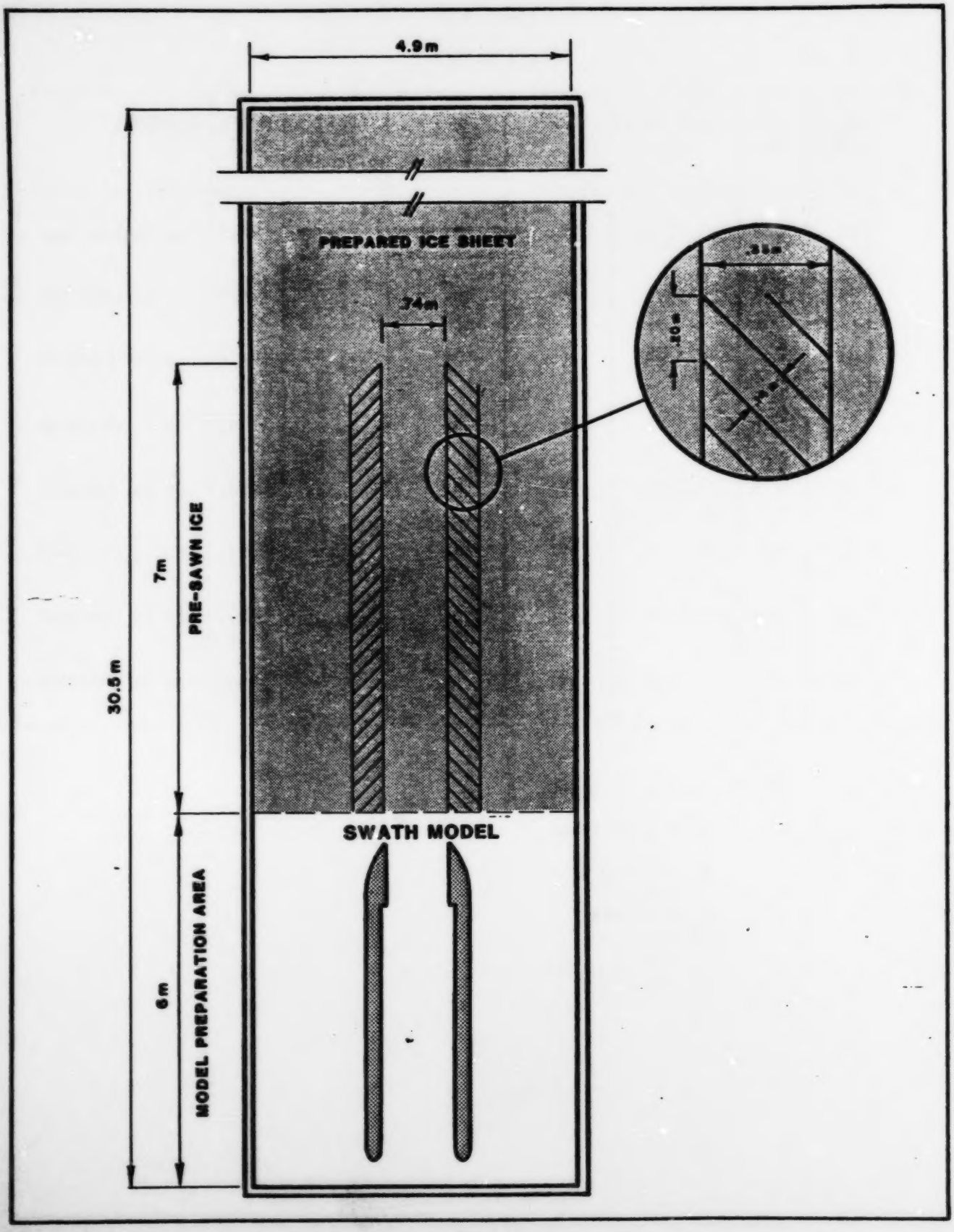

Figure 3.4 **ICE BASIN ARRANGEMENT for TEST No. 2**

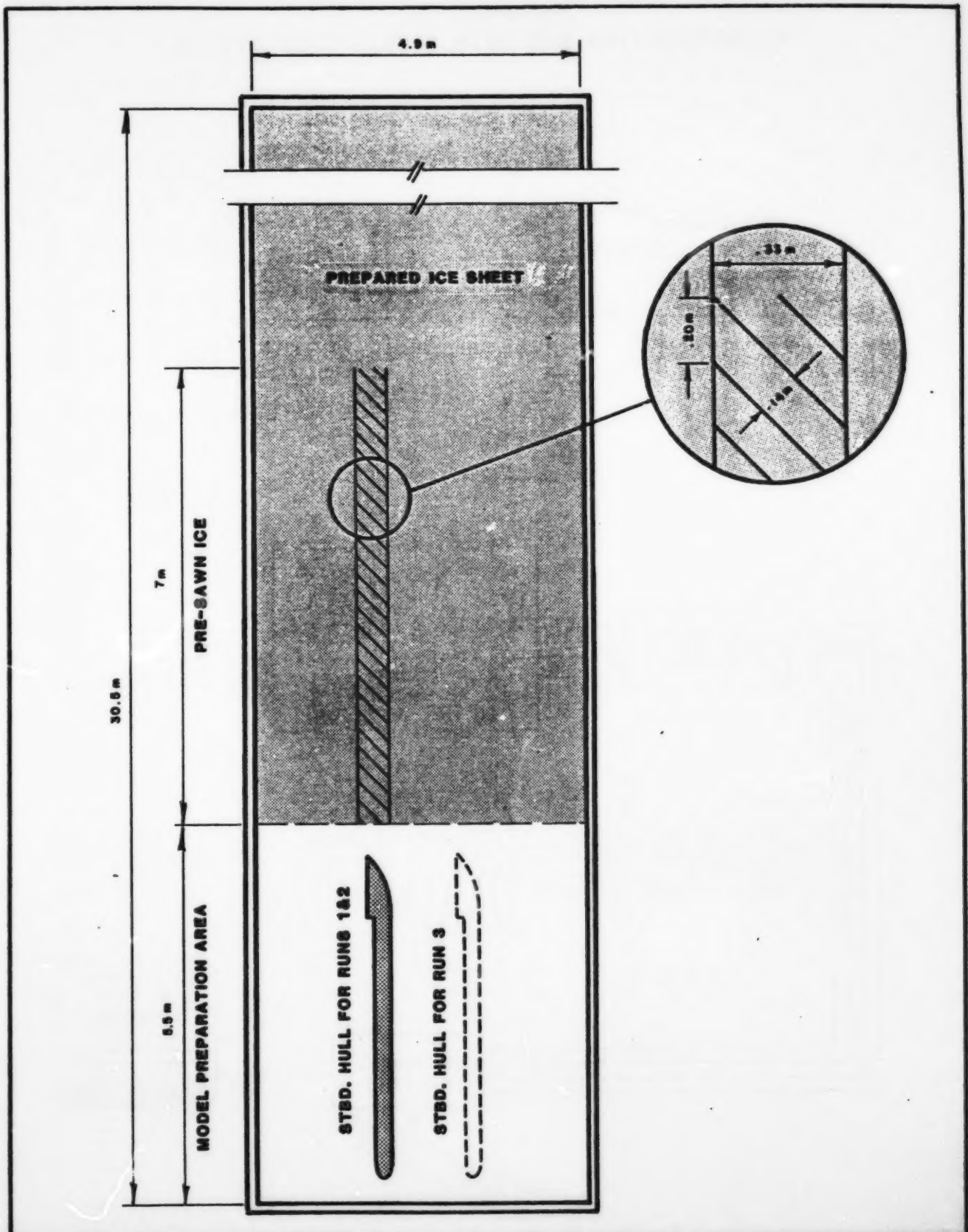

FIGURE 3.5
INSTRUMENTATION AND DATA ACQUISITION SYSTEM

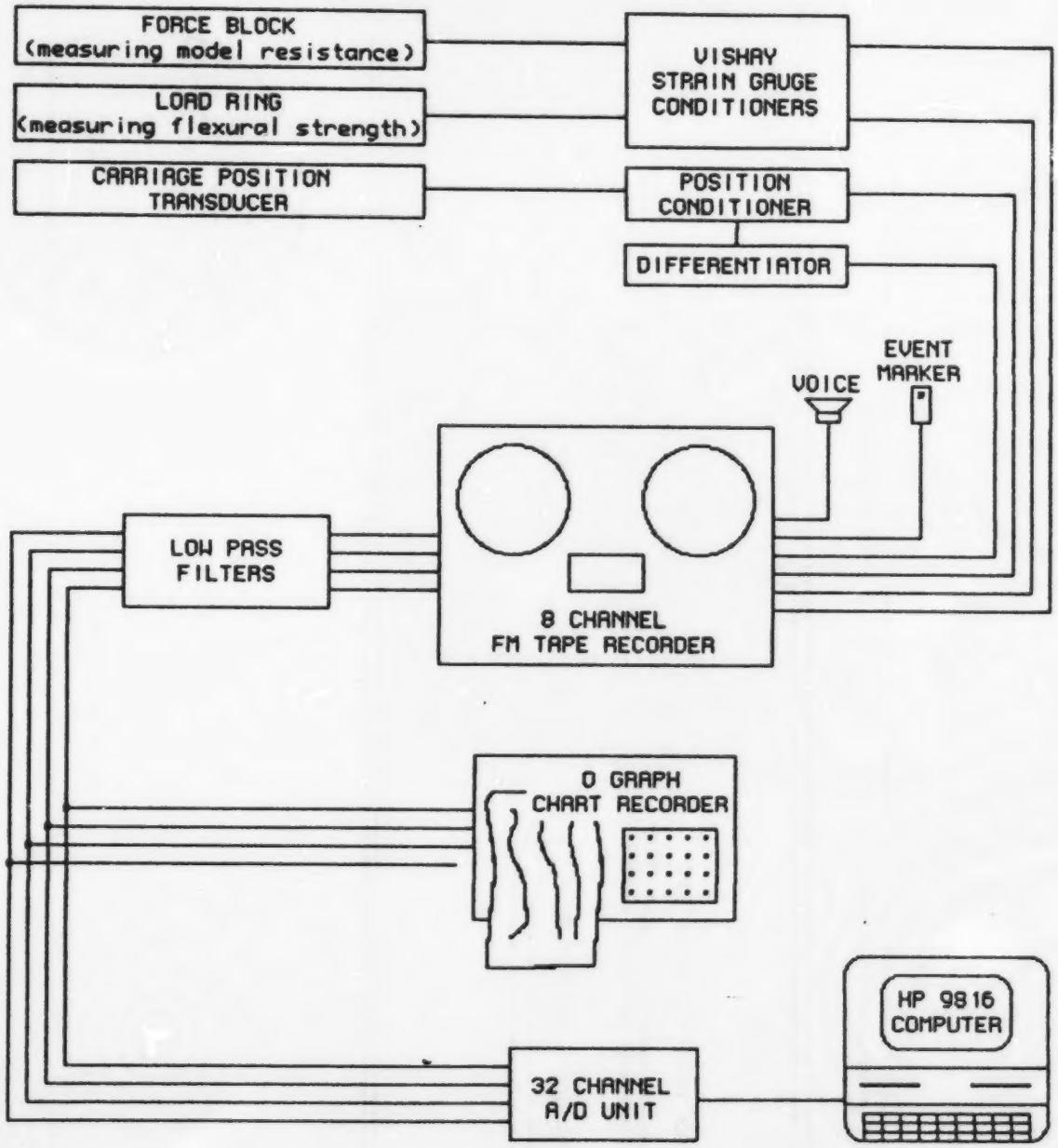

the average model resistance over a 5 to 10 second interval would be the output of each test, there is no need to obtain 50 Hz icebreaking data when this data would only be mathematically filtered by averaging. Therefore the 1 Hz analog filter was selected as producing good icebreaking results over the 5 to 10 second intervals to be averaged.

Once the filtering rate was selected, the digitization rate was determined from the filter rate. In order to adequately reproduce a sinusoidal signal digitally, five samples should be taken per cycle. Therefore the digitization rate should be at least 5 Hz. The digitization frequency of 16 Hz was selected as the next highest frequency on the A/D scanner.

4. TEST RESULTS

4.1 Model Friction Tests

The model/ice friction coefficient as described in Section 3.1 was measured at 8 separate locations along both hulls before the test series began. Since the attempt was to reproduce results obtained at NRC, the friction coefficient was not altered from when NRC had the model. Table 4.1 lists these results. The average hull friction coefficient for these tests was 0.09.

4.2 Ice Resistance Tests

The ice resistance results obtained using the methods discussed in Section 3 are listed in Tables 4.2 and 4.3. Two extra data points than listed in the test matrix (Table 3.1) were obtained due to variations in ice thickness and strength. It should also be noted that all results obtained from ice sheet 2 along the second track (Test 02, Run 03) appear to have boundary effects. This data is to be used cautiously.

TABLE 4.1

MODEL FRICTION COEFFICIENT

LOCATION	FRICTION COEFFICIENT
1 Port Hull bottom	.05
2 Stbd. hull bottom	.05
3 Stbd. hull, stbd. bow	.09
4 Port hull, Port bow	.04
5 Stbd. hull, Port bow	.19
6 Port hull, Stbd. bow	.04
7 Port hull, Port side	.11
8 Stbd. hull, Stbd. side	.14
Average	.09

TABLE 4.2

ICE RESISTANCE RESULTS FOR SWATH MODEL

TEST NO.	RUN NO.	h (m)	V (m/sec)	σ_f (KPa)	E (MPa)	R (N)	COMMENTS
01	01A	.0260	.27	35.4	14.8	10.1	In Pre-sawn ice
01	01B	.0251	.27	34.1	14.3	56.1	
01	01B	.0254	.27	10.3	4.3	47.1	In weak ice
01	02	.0246	.57	8.4	3.5	62.4	In weak ice

TABLE 4.3

ICE RESISTANCE RESULTS FOR STARBOARD SWATH HULL

TEST NO.	RUN NO.	h (m)	V (m/sec)	σ_f (KPa)	E (MPa)	R (N)	COMMENTS
02	01A	.0279	.29	28.9	57.6	6.7	In Pre-sawn ice
02	01B	.0312	.29	26.7	53.2	57.9	
02	02	.0263	.57	25.4	50.6	76.2	
02	03A	.0283	.28	26.6	53.0	75.9	Possible boundary effects
02	03A	.0302	.28	49.1	97.9	139.0	Possible boundary effects
02	03B	.0265	.56	27.2	54.2	59.2	Possible boundary effects

5. DISCUSSION OF THE RESULTS

A comparison of the ice resistance of the starboard hull with that of the entire model is shown in Table 5.1. In the pre-sawn ice, the resistance of the one hull is 66% of the resistance of the entire model. However, in the unbroken ice, the resistance of one hull ranged between 3% larger, to 22% larger than the resistance of the entire model. An explanation of these results is given below.

For the pre-sawn resistance tests, conventional models are influenced by the size of the floe and the model velocity. Although other parameters will affect the model resistance such as the elastic modulus of the floes, the flexural strength of the floes, and the hull friction factor, to name just a few, these are all second (or higher) order affects. Therefore, if an equation was developed which could account for the slight change in velocity and floe size between tests, then the slight change in these parameters could be normalized out to show if any interference between hulls occurred during these tests. However, with only one test performed for each model, the only equation that could be used to account for these parameters is:

$$R' = fn(L, B, h, v) = CLBHv \qquad (5.1)$$

where R' = the sum of submergence, turning, and frictional resistance
L = length of the ice floe
B = width of the ice floe
h = thickness of the ice floe
v = model velocity
C = unknown constant

With length and breadth of the ice floe being constant for both sets of tests, equation 5.1 can be reduced to:

$$R' = C'hv \qquad (5.2)$$

Solving for the unknown constant in equation 5.2 gives:

$$R' = 828\ hv \quad \text{for one hull} \qquad (5.3)$$

and

$$R' = 1439\ hv \quad \text{for two hulls} \qquad (5.4)$$

where R' is in Newtons
h is in metres
v is in m/sec

Therefore, calculating the predicted resistance at the average ice thickness and velocity, results in a resistance of 6.25 N for one hull and 10.86 N for two hulls. These values produce a ratio of 0.58 between

the resistance of two hulls and that of one hull. Although closer to the expected value, it still appears high. Without any further test data, the only conclusion that can be made is that there is a beneficial effect with the second hull.

For the unbroken ice resistance tests, conventional models are influenced by the flexural strength of the ice, the velocity, and the ice thickness. Again other parameters will affect the model resistance but they are all second order affects. Since there is already an approximation to predict the sum of the submergence resistance, turning resistance, and frictional resistance for these models (equation 5.3 and 5.4), the analysis can be more accurately performed with the limited data by removing all knowns and developing a relationship for strictly unknowns. This method combines the results of the pre-sawn tests with those of the unbroken ice and theoretically increases the size of the data base. Therefore if the breaking resistance is defined as:

$$R^{\sim} = R_T - R' \tag{5.5}$$

where $R^{\sim}$ = breaking resistance
R_T = Total resistance (as measured during unbroken ice tests)
R' = as defined above

With only two or three data points to predict the breaking resistance equation (Test 02 Run 03 is not included in this analysis due to suspected boundary effects), the best equation to predict breaking resistance is:

$$R^{\sim} = fn(v, h, \sigma_f) = C_1 v h^2 + C_2 \sigma_f h \tag{5.6}$$

Solving for the unknown constants for the two models and adding the submergence resistance, turning resistance and frictional resistance to the breaking resistance gives:

- For one hull,

$$R_T = 139\ 150\ v h^2 + 13.36\ \sigma_f h + 828\ v h \tag{5.7}$$

- For entire model,

$$R_T = 112\ 240\ v h^2 + 33.96\ \sigma_f h + 1439\ h v \tag{5.8}$$

where R_T = Total Resistance in Newtons
v = velocity in m/sec
h = ice thickness in m
σ_f = flexural strength in KPa

TABLE 5.1

DIRECT COMPARISON BETWEEN MODELS

NO.	TEST CONDITIONS	BOTH HULLS			STBD. HULL			RATIO OF $(\frac{\text{resistance of one hull}}{\text{resistance of model}})$
		TEST NO.	RUN NO.	RESISTANCE (N)	TEST NO.	RUN NO.	RESISTANCE (N)	
1	@ V_1 in Pre-sawn ice	01	01A	10.1	02	01A	6.7	0.66
2	@ V_1	01	01B	56.1	02	01B	57.9	1.03
3	@ V_2	01	02	62.4	02	02	76.2	1.22

TABLE 5.2

NORMALIZED COMPARISON BETWEEN MODELS AT TARGET CONDITIONS

h (m)	ν (m/sec)	σ_f (kPa)	RESISTANCE OF ONE HULL (eq. 5.7) (N)	RESISTANCE OF MODEL (eq. 5.8) (N)	RATIO OF $(\frac{\text{resistance of one hull}}{\text{resistance of model}})$
.030	.30	30	57.05	73.82	0.77
.030	.60	30	102.07	117.08	0.87

Using equation 5.7 and 5.8 to calculate the resistance at the target conditions produces Table 5.2. This table shows that the resistance of one hull ranged between 77 and 87% of the resistance of two hulls. Therefore, it appears that there is a considerable beneficial influence with two hulls. This beneficial influence is primarily from the breaking resistance and only slightly from the submergence, turning and frictional resistance.

The beneficial influence from the second hull is similar to the phenomenon of a point load versus two point loads on an infinite ice sheet. When a single point load is added to an ice sheet, the pressure distribution around that load varies in a manner shown by one of the curves in Figure 5.1a and 5.1c. However, when a second load is applied at a distance of L_0 from the first load, it is found that a higher load is required at both loading points to fail the ice sheet. Figure 5.1b uses superposition to add both stress fields from the two loads in Figure 5.1a, and as a result requires a higher load at each point to break the ice. This scenario would be detrimental to the ice resistance of a SWATH model. However, Figures 5.1c and 5.1d apply the two point loads at a slightly larger distance apart. In this scenario the stress fields produce a considerably higher stress for the same load. Or conversely would require a lower load at each point to fail the ice. Although the SWATH model can not be approximated as two point loads, this can explain why the ice resistance of one hull was 77% to 87% of two. If this is correct, the SWATH model resistance will be very highly dependent upon the elastic modulus of the ice.

Another explanation for this irregularity could be variations of the shear strength of the ice. Although no data is available to substantiate this, from a visual comparison of the icebreaking motion it appeared that the second ice sheet was much "crisper" than the first. The crisper ice sheet is probably due to higher crushing and shear strength of the ice. Since this model sheared the ice along the inside of each hull, the model's resistance is probably dependent upon the shear strength of the ice as well. Therefore if this model is ever tested again, the shear strength of the ice should be measured.

Figure 5.1

SIMULATION of TWO POINT LOADS on an INFINITE ICE SHEET

a) TWO SEPARATE PRESSURE DISTRIBUTIONS AT A SPACING OF L_o

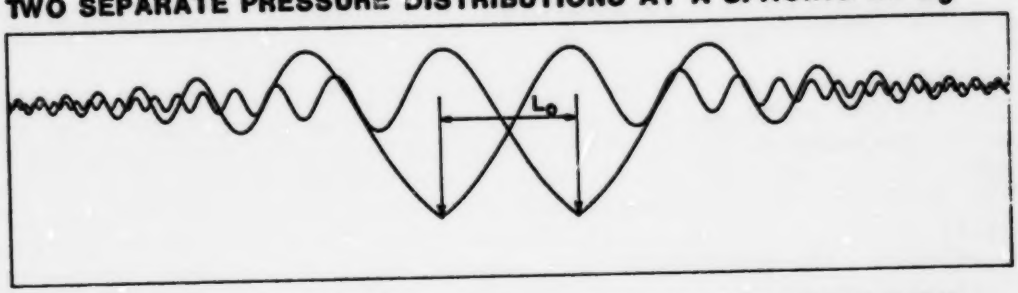

b) USING SUPERPOSITION TO DETERMINE PRESSURE DISTRIBUTION

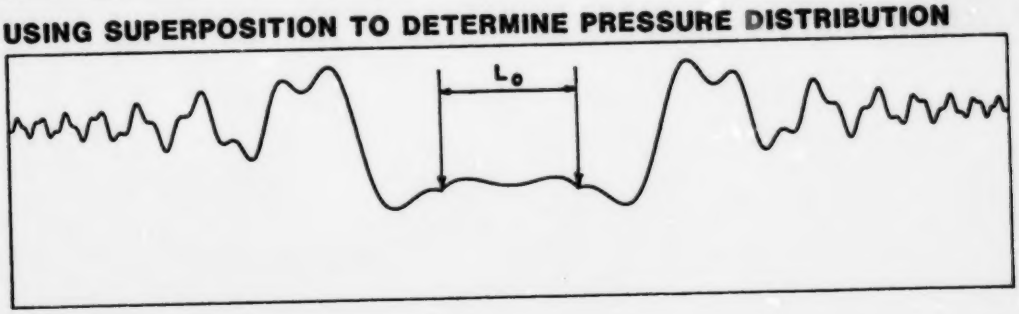

c) TWO SEPARATE PRESSURE DISTRIBUTIONS AT A SPACING OF L_i

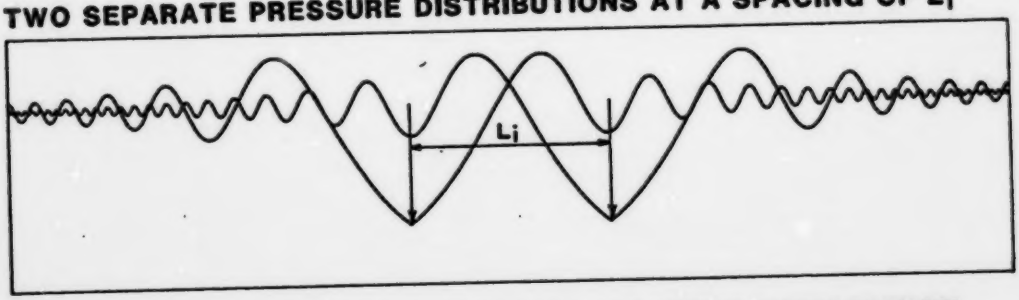

d) USING SUPERPOSITION TO DETERMINE PRESSURE DISTRIBUTION

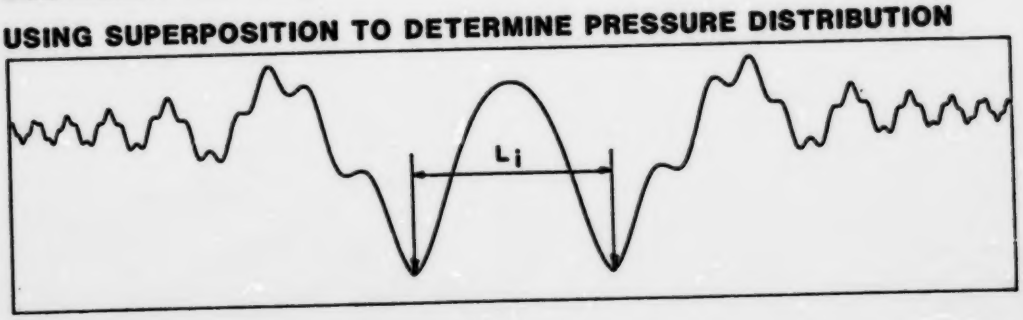

6. CONCLUSIONS AND RECOMMENDATIONS

The pre-sawn ice tests showed that the submergence resistance, turning resistance, and frictional resistance of one hull is 58% of the entire model.

The unbroken ice tests showed that the icebreaking resistance of one hull was only slightly less than for two hulls. Therefore the total resistance of one hull ranged between 77 and 87% of the resistance of two hulls (depending upon speed).

An explanation of the slight increase in resistance when the second hull is added can be shown by examining two point loads on an ice sheet. Depending on the spacing of the two loads, the force required to break the ice can vary considerably. Therefore, it appears that the SWATH model is highly dependent upon the elastic modulus of the ice. If this is correct, considerable savings in ice resistance can be obtained by selecting the appropriate hull spacing for the conditions which the vessel will encounter. A test program is proposed where ice thickness, elastic modulus, model velocity and hull spacing are all varied.

REFERENCES

[1] Wyman, M., "Deflections of an Infinite Plate on an Elastic Foundation", Canadian Journal of Research, Vol. 28, Section 1, 1956.

[2] Howard, D. and Abdelnour, R., "Results of the Implementation of Carbamide Doped Ice in Arctec's Refrigerated Basin", Arctec Canada Limited, Report 1317C, April 1983.

APPENDIX A

MODEL RESISTANCE TEST RESULTS

TEST IDENTIFICATION MATRIX

TEST NO.	RUN NO.	MODEL USED	ICE CONDITION	COMMENT
01	01	SWATH	Pre-sawn and unbroken	This test went continuously from pre-sawn ice to unbroken ice at approximately the 55 second mark
01	02	SWATH	Unbroken	One test
02	01	Stbd. hull	Pre-sawn and unbroken	This test went continuously from pre-sawn ice to unbroken ice at approximately the 45 second mark
02	02	Stbd. hull	Unbroken	One test
02	03	Stbd. hull	Unbroken	This test was the entire length of the tank along the west side of the basin. Two velocities were tested. During run, boundary effects are seen.

SWATH Model Resistance Tests

TEST Ø1 RUN Ø1

DATA DIGITIZED ON: 26 MAR 1985
DIGITIZING RATE: 16 Hz/CHANNEL
FILTER FREQUENCY: 1 HZ

INTERVAL STATISTICS

INTERVAL 1 START: 41.9375 END: 47.75

CHANNEL	MINIMUM	MAXIMUM	MEAN VALUE	STAN. DEV
Resistance	-23.25	50.ØØ9	9.665	18.67
Velocity	.2555	.2775	.2672	.ØØ58654
Position	3.364	4.926	4.148	.469

INTERVAL 2 START: 47.75 END: 54.25

CHANNEL	MINIMUM	MAXIMUM	MEAN VALUE	STAN. DEV
Resistance	-7.Ø76	33.835	1Ø.14	9.Ø99
Velocity	.2628	.2775	.27Ø1	.ØØ34678
Position	4.926	6.83	5.9	.535

INTERVAL 3 START: 41.9375 END: 54.25

CHANNEL	MINIMUM	MAXIMUM	MEAN VALUE	STAN. DEV
Resistance	-23.25	5Ø.ØØ9	9.987	14.44
Velocity	.2555	.2775	.2687	.ØØ49685
Position	3.364	6.83	5.Ø73	1.Ø1

INTERVAL 4 START: 63.9375 END: 68.625

CHANNEL	MINIMUM	MAXIMUM	MEAN VALUE	STAN. DEV
Resistance	25.27	1ØØ.43	56.143	19.37
Velocity	.26Ø4	.2775	.27Ø1	.ØØ466Ø8
Position	9.614	1Ø.83	1Ø.2	.38

INTERVAL 5 START: 68.625 END: 73.25

CHANNEL	MINIMUM	MAXIMUM	MEAN VALUE	STAN. DEV.
Resistance	18.61	72.843	47.Ø66	15.61
Velocity	.2579	.275	.2677	.ØØ48ØØ7
Position	1Ø.83	12.15	11.49	.385

INTERVAL 6 START: 63.9375 END: 73.25

CHANNEL	MINIMUM	MAXIMUM	MEAN VALUE	STAN. DEV.
Resistance	18.61	1ØØ.43	51.5Ø6	18.17
Velocity	.2579	.2775	.269	.ØØ48889
Position	9.614	12.15	1Ø.84	.753

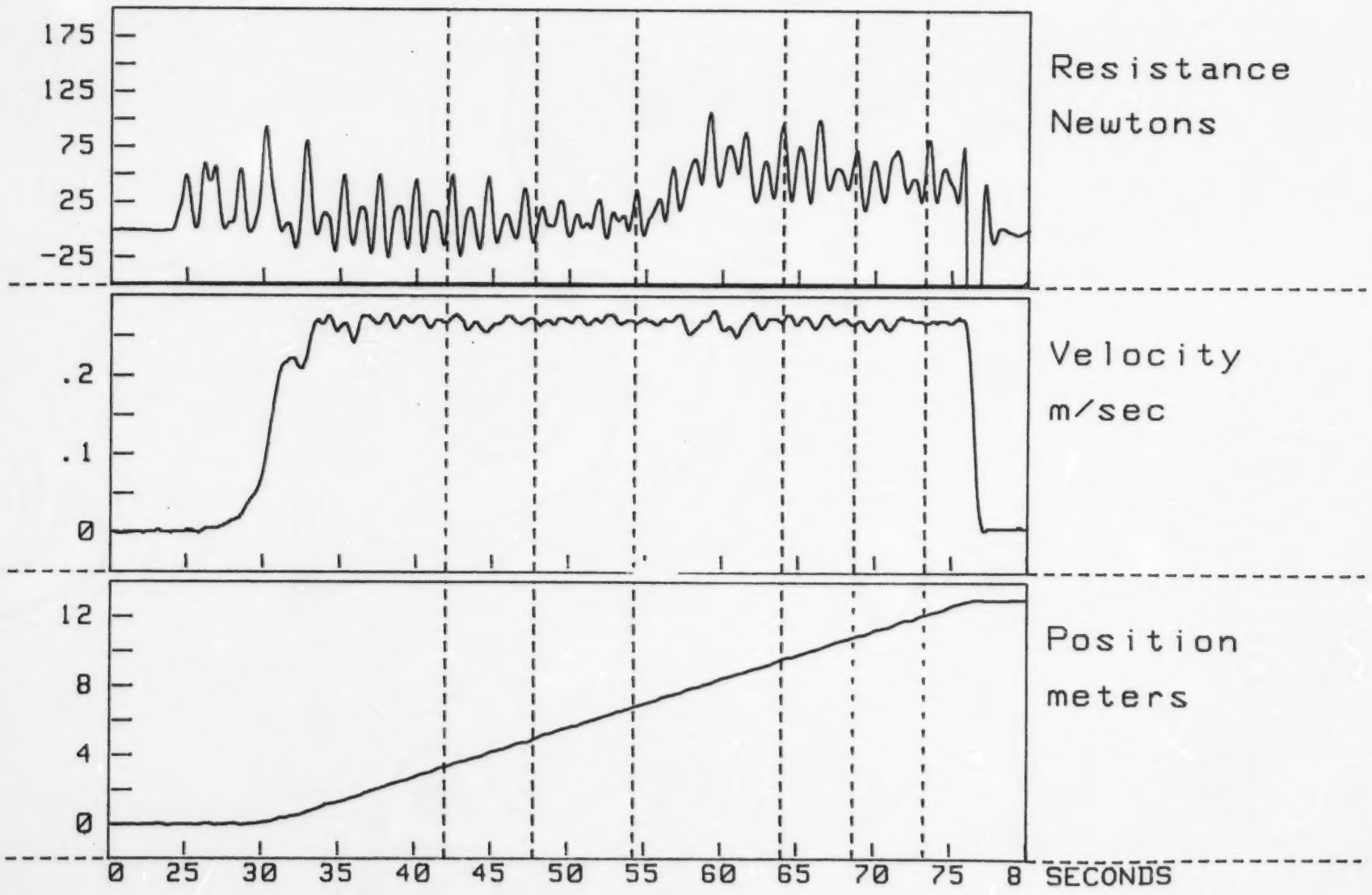
SWATH Model Resistance Tests
TEST 01 RUN 01
175
125
75
25
-25
Resistance
Newtons
.2
.1
0
Velocity
m/sec
12
8
4
0
Position
meters
0 25 30 35 40 45 50 55 60 65 70 75 8
SECONDS

SWATH Model Resistance Tests

TEST Ø1 RUN Ø2

DATA DIGITIZED ON: 26 MAR 1985
DIGITIZING RATE: 16 Hz/CHANNEL
FILTER FREQUENCY: 1 HZ

INTERVAL STATISTICS

INTERVAL 1 START: 31.Ø625 END: 35.625

CHANNEL	MINIMUM	MAXIMUM	MEAN VALUE	STAN. DEV.
Resistance	29.Ø7	82.351	53.449	14.9
Velocity	.547	.584	.569	.ØØ89888
Position	4.291	7.Ø75	5.678	.797

INTERVAL 2 START: 35.625 END: 4Ø.125

CHANNEL	MINIMUM	MAXIMUM	MEAN VALUE	STAN. DEV.
Resistance	35.732	97.574	62.449	16.72
Velocity	.552	.579	.567	.ØØ81631
Position	7.Ø75	9.711	8.374	.781

INTERVAL 3 START: 31.Ø625 END: 4Ø.125

CHANNEL	MINIMUM	MAXIMUM	MEAN VALUE	STAN. DEV.
Resistance	29.Ø7	97.574	57.8Ø3	16.45
Velocity	.547	.584	.568	.ØØ85997
Position	4.291	9.711	7.Ø16	1.57

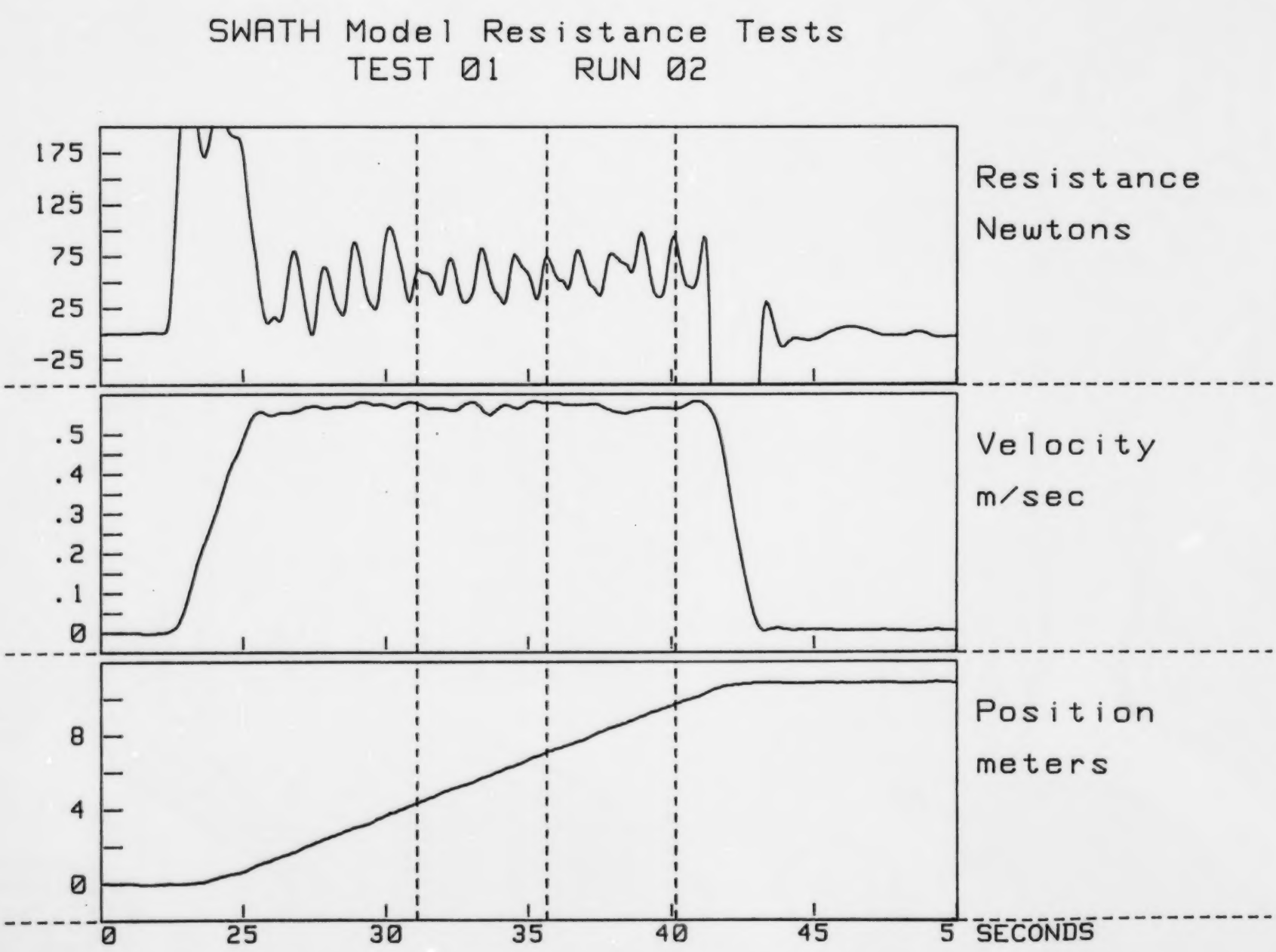
SWATH Model Resistance Tests
TEST 01 RUN 02
175
125
75
25
-25
Resistance
Newtons
.5
.4
.3
.2
.1
0
Velocity
m/sec
8
4
0
Position
meters
0
25
30
35
40
45
5
SECONDS

SWATH Model Resistance Tests

TEST Ø2 RUN Ø1

DATA DIGITIZED ON: 27 MAR 1985
DIGITIZING RATE: 16 Hz/CHANNEL
FILTER FREQUENCY: 1 HZ

INTERVAL STATISTICS

INTERVAL 1 START: 28.4375 END: 37

CHANNEL	MINIMUM	MAXIMUM	MEAN VALUE	STAN. DEV.
Resistance	-1Ø.Ø4	28.Ø1	6.338	8.876
Velocity	.2735	.2955	.2851	.ØØ49361
Position	2.Ø4	4.631	3.357	.756

INTERVAL 2 START: 37 END: 43.9375

CHANNEL	MINIMUM	MAXIMUM	MEAN VALUE	STAN. DEV.
Resistance	-3.383	18.5	6.657	4.912
Velocity	.28Ø8	.2979	.2866	.ØØ42394
Position	4.631	6.731	5.7Ø5	.615

INTERVAL 3 START: 28.4375 END: 43.9375

CHANNEL	MINIMUM	MAXIMUM	MEAN VALUE	STAN. DEV.
Resistance	-1Ø.Ø4	28.Ø1	6.478	7.385
Velocity	.2735	.2979	.2857	.ØØ47Ø26
Position	2.Ø4	6.731	4.4Ø8	1.36

INTERVAL 4 START: 55.125 END: 61.625

CHANNEL	MINIMUM	MAXIMUM	MEAN VALUE	STAN. DEV.
Resistance	26.11	1Ø6.98	52.542	17.45
Velocity	.2784	.2979	.2857	.ØØ46138
Position	1Ø.1	12	11.Ø7	.552

INTERVAL 5 START: 61.625 END: 66.8125

CHANNEL	MINIMUM	MAXIMUM	MEAN VALUE	STAN. DEV.
Resistance	35.625	88.9Ø4	57.87	14.Ø2
Velocity	.28Ø8	.2979	.2894	.ØØ41177
Position	12	13.57	12.82	.449

INTERVAL 6 START: 55.125 END: 66.8125

CHANNEL	MINIMUM	MAXIMUM	MEAN VALUE	STAN. DEV.
Resistance	26.11	1Ø6.98	54.8Ø5	16.21
Velocity	.2784	.2979	.2874	.ØØ47ØØ6
Position	1Ø.1	13.57	11.85	1.Ø1

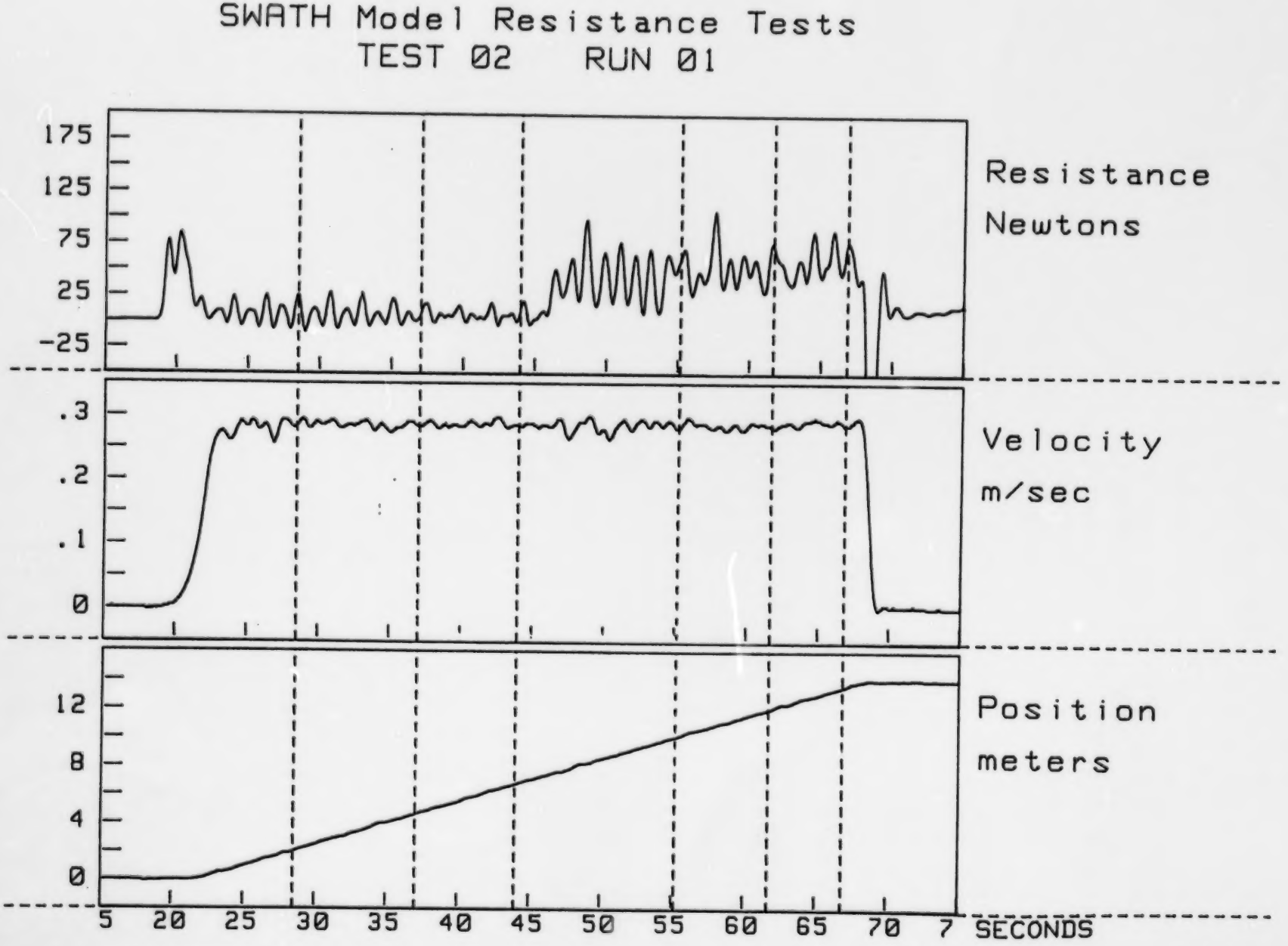
SWATH Model Resistance Tests
TEST 02 RUN 01
175
125
75
25
-25
Resistance
Newtons
.3
.2
.1
0
Velocity
m/sec
12
8
4
0
Position
meters
5 20 25 30 35 40 45 50 55 60 65 70 7
SECONDS

SWATH Model Resistance Tests

TEST Ø2 RUN Ø2

DATA DIGITIZED ON: 27 MAR 1985
DIGITIZING RATE: 16 Hz/CHANNEL
FILTER FREQUENCY: 1 HZ

INTERVAL STATISTICS

INTERVAL 1 START: 26.4375 END: 29.25

CHANNEL	MINIMUM	MAXIMUM	MEAN VALUE	STAN. DEV
Resistance	38.318	120.14	71.597	22.75
Velocity	.549	.585	.568	.Ø1Ø561
Position	3.31	4.97	4.116	.492

INTERVAL 2 START: 29.25 END: 34.25

CHANNEL	MINIMUM	MAXIMUM	MEAN VALUE	STAN. DE
Resistance	39.27	112.53	76.269	18.4
Velocity	.553	.585	.57	.Ø1Ø534
Position	4.97	7.949	6.447	.856

INTERVAL 3 START: 26.4375 END: 34.25

CHANNEL	MINIMUM	MAXIMUM	MEAN VALUE	STAN. DE
Resistance	38.318	120.14	74.397	2Ø.19
Velocity	.549	.585	.569	.Ø1Ø564
Position	3.31	7.949	5.6Ø8	1.35

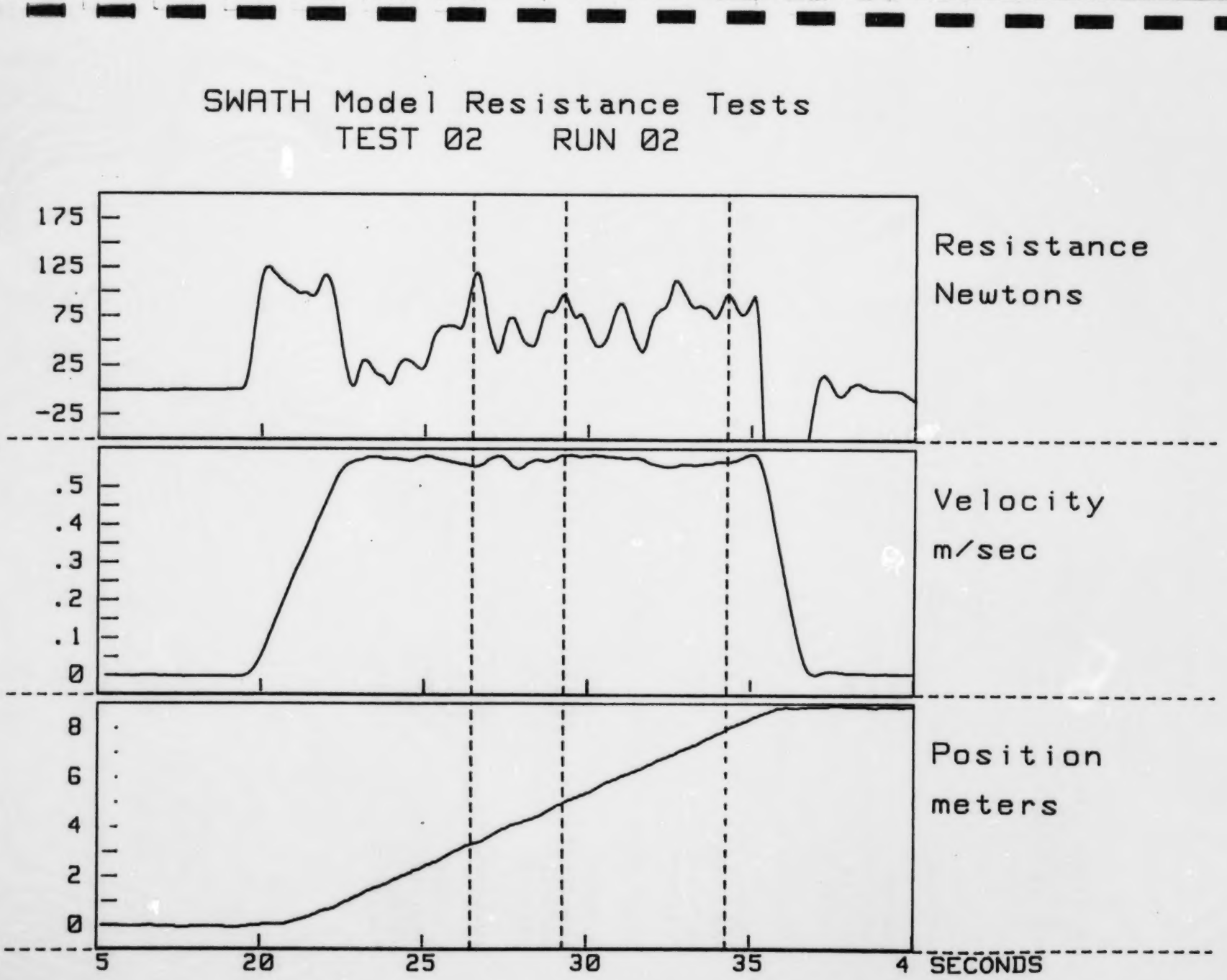
SWATH Model Resistance Tests
TEST 02 RUN 02
175
125
75
25
-25
Resistance
Newtons
.5
.4
.3
.2
.1
0
Velocity
m/sec
8
6
4
2
0
Position
meters
5
20
25
30
35
4
SECONDS

SWATH Model Resistance Tests

TEST 02 RUN 03

DATA DIGITIZED ON: 27 MAR 1985
DIGITIZING RATE: 16 Hz/CHANNEL
FILTER FREQUENCY: 1 HZ

INTERVAL STATISTICS

INTERVAL 1 START: 33.5625 END: 37.1875

CHANNEL	MINIMUM	MAXIMUM	MEAN VALUE	STAN. DEV
Resistance	13.9	129.02	60.935	24.12
Velocity	.2656	.2851	.2753	.006293
Position	3.11	4.138	3.631	.3052

INTERVAL 2 START: 37.1875 END: 40.8125

CHANNEL	MINIMUM	MAXIMUM	MEAN VALUE	STAN. DEV
Resistance	58.613	103.33	75.868	12.26
Velocity	.2656	.2851	.2758	.0055195
Position	4.138	5.212	4.685	.3114

INTERVAL 3 START: 46.1875 END: 51

CHANNEL	MINIMUM	MAXIMUM	MEAN VALUE	STAN. DEV
Resistance	105.23	179.44	139.01	17.89
Velocity	.2607	.29	.2764	.0059356
Position	6.823	8.19	7.495	.4

INTERVAL 4 START: 59.6875 END: 72.3125

CHANNEL	MINIMUM	MAXIMUM	MEAN VALUE	STAN. DEV
Resistance	26.27	110.94	59.237	18.71
Velocity	.537	.573	.558	.0089002
Position	12.19	19.47	15.87	2.13

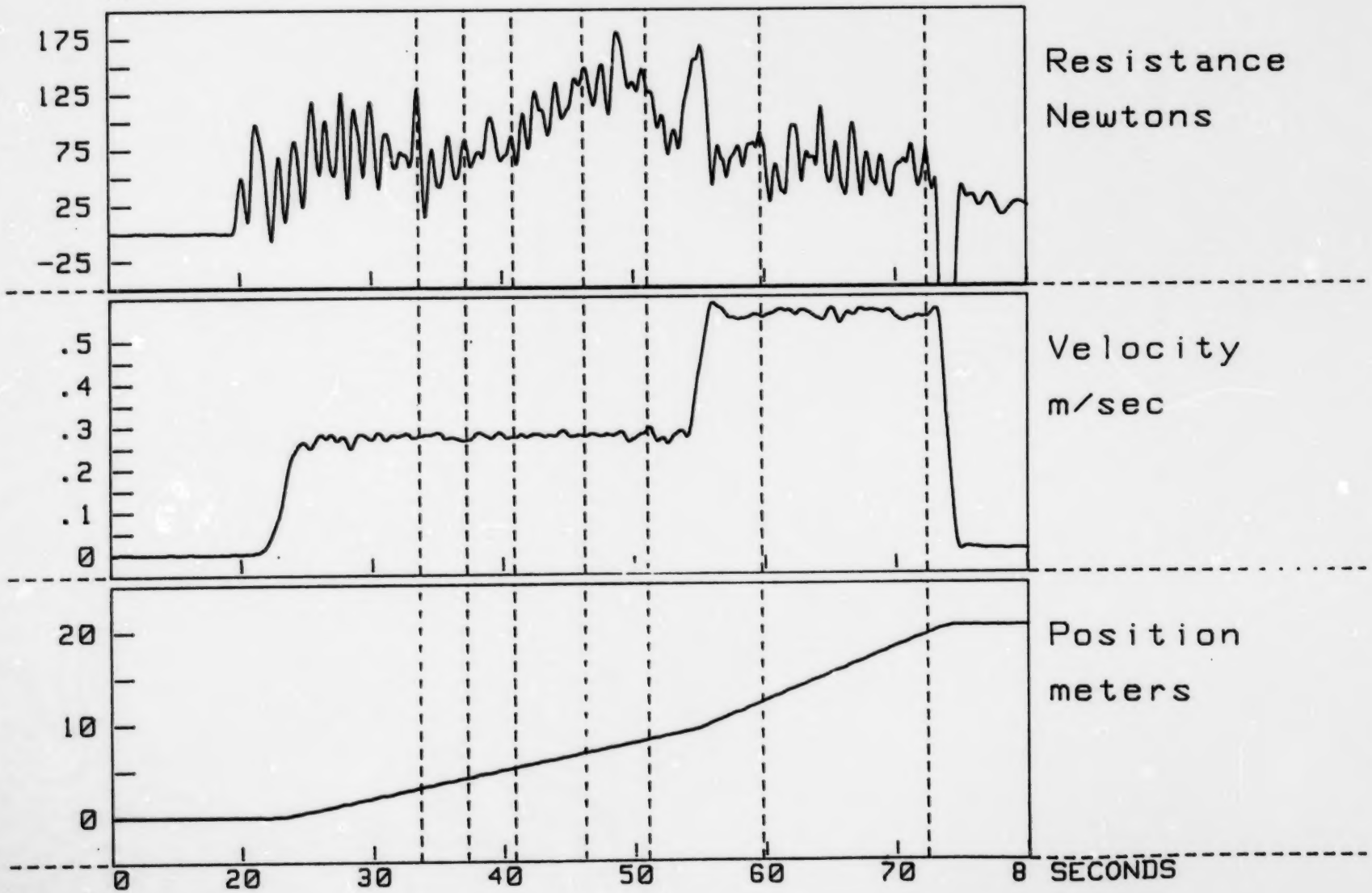
SWATH Model Resistance Tests
TEST 02 RUN 03
175
125
75
25
-25
Resistance
Newtons
.5
.4
.3
.2
.1
0
Velocity
m/sec
20
10
0
Position
meters
0
20
30
40
50
60
70
8
SECONDS

APPENDIX 3

NRC Model Test Report LTR-SH-383

REPORT
RAPPORT

PAGES 20

FIG.
DIAG. 10

TABLES 10

Institute for Marine
Dynamics
(IMD)

Institut de dynamique marine
(IDM)

REPORT
RAPPORT LTR-SH-383

DATE October 1984

LAB ORDER
COMM. LAB. _____

FILE
DOSSIER 7860

FOR INTERNAL
POUR

REFERENCE

LTR-SH-383

"R" CLASS ICEBREAKING EXPERIMENTS WITH MODEL 327 AND COMPARISON WITH 1:40 SCALE AND FULL SCALE RESULTS

SUBMITTED BY
PRESENTE PAR
Section Head
Chef de section

AUTHOR
AUTEUR
S. NEWBURY

APPROVED
APPROUVE
N.E. JEFFREY

This report may not be published wholly or in part without the written consent of the IMD.

Ce rapport ne doit pas être reproduit, ni en entier ni en partie, sans une autorisation écrite de l'IDM.

Copy No. 11

TABLE OF CONTENTS

		Page
	LIST OF TABLES	ii
	LIST OF FIGURES	iii
	LIST OF SYMBOLS	iv
1.0	INTRODUCTION	1
2.0	THE MODEL	2
3.0	ICE-HULL FRICTION COEFFICIENT	3
4.0	MEASUREMENT OF ICE PROPERTIES	4
5.0	EXPERIMENTAL PROCEDURES	6
6.0	ANALYSIS OF TEST RESULTS	8
7.0	COMPARISON OF 1:20 AND 1:40 SCALE MODELS	10
8.0	COMPARISON OF FIELD TRIALS AND MODEL PREDICTIONS	11
9.0	COMPARISON WITH OTHER ICE MODEL BASINS	14
10.0	CONCLUSIONS	16
11.0	ACKNOWLEDGEMENTS	18
12.0	REFERENCES	19

LIST OF TABLES

	Table
Hydrostatic Particulars	1 - 4
Details of Rudder and Stern Arrangement	5
Ice-Hull Friction Values	6
1:20 Scale Model Results	7
1:40 Scale Model Results	8
Full Scale Trial Results	9
Full Scale and Predicted Level Ice Resistance	10

LIST OF FIGURES

	Figure
Body Plan	1
Bow and Stern Lines	2
Stern Arrangement	3
Example of Force and Motion Records	4
1:20 Scale Dimensionless Resistance as Functions of Cn and Fn	5
1:20 and 1:40 Scale Dimensionless Resistance as a Function of Cn x Fn	6
Comparison between Predicted and Full Scale Level Ice Resistance	7
1:20 Scale, Predicted, and Full Scale Dimensionless Ice Resistance as a Function of Cn x Fn	8
Nondimensionalized Resistance Comparison With Other Ice Tanks	9
Resistance Comparison With Other Ice Tanks Using the IMD Regression Equation	10

LIST OF SYMBOLS

B	Maximum ship beam at waterline, m
c	Ratio of prototype to model fluid density
Cn	Dimensionless bending strength; Cauchy number = $\sigma_f/\gamma h_i$
E	Modulus of elasticity, MPa
f	Coefficient of friction
Fn	Dimensionless velocity; Froude number = $V/\sqrt{gh_i}$
f.w.	Fresh water
g	Acceleration of gravity, m/sec^2
GM	Metacentric Height, m
h_i	Ice thickness, m
h_s	Snow cover thickness, m
l	Characteristic length of ice sheet, m
L	Length of cantilever beam, m
LPP	Ship length between perpendiculars, m
N	Normal force, N
P	Load applied to ice, kg
R_i	Level ice resistance, N
R_{it}	Total resistance in ice, N
R_{ow}	Resistance in ice-free water, N
R_s	Resistance due to snow cover, N
s.w.	Salt water
t	Thrust deduction coefficient
T	Tangential force, N

LIST OF SYMBOLS

T_A	Measured thrust, N
V	Ship speed, m/sec or knots
W	Width of cantilever beam, m
δ	Deflection of ice sheet, in
γ	Specific weight of water, kN/m^3
λ	Model scale factor
μ	Poisson's ratio
ρ	Mass density of water, kg/m^3
σ_f	Flexural strength, kPa

1.0 INTRODUCTION

This report presents the results of resistance experiments in ice-covered waters with a 1:20 scale model of the Canadian R-class icebreakers CCGS Radisson, Franklin, and des Groseilliers. The tests were carried out at the Hydraulics Laboratory ice tank, on loan to the Institute for Marine Dynamics (IMD), in May and June 1984. Models of the same ships were also tested at other ice model basins (References 1 to 6) under a program developed by the Committee on Ships in Ice-covered Waters of the International Towing Tank Conference (ITTC).

A 1:40 scale R-class model was previously tested in ice at the IMD and a comparison of those results has been made with the 1:20 scale model results. Field trials were also carried out with the CCGS Franklin in 1980 (Reference 7) and the trial results are compared to model predictions. The 1:20 scale model was tested in ice-free water at the IMD in 1980 (Reference 8) to obtain resistance and propulsion data.

2.0 THE MODEL

The 1:20 scale model, designated 327, was made of fiberglass complete up to the weather deck but with no superstructure fitted. A body plan and bow and stern lines are shown in Figures 1 and 2 respectively. The model was fitted with twin propeller shafts with fairing cones and shaft bossings, a single centerline rudder and an ice guard (Figure 3).

The model was ballasted to a displacement of 956.9 kg f.w., which is equivalent to 7846.5 tonnes s.w. for the full scale ship. Since the model was too large to fit in the balance frame the distribution of ballast weights was arranged while the model was floating in the water.

The pitch and roll periods were obtained by the use of empirical formulae and the assumption that the radius of gyration for pitching is 0.25 LPP from the longitudinal center of gravity, and the added mass for rolling is 20 percent of the actual displacement of the model (Reference 9).

The ballast weights were adjusted until the measured pitch and roll periods (1.39 sec and 2.10 sec respectively) were within approximately 2 percent of the calculated periods (1.37 sec and 2.05 sec), and the transverse GM was 0.125 m (2.5 m full scale).

Hydrostatic particulars for the hull are listed in Tables 1 to 4, and details of the rudder are given in Table 5.

3.0 ICE HULL FRICTION COEFFICIENT

The coefficient of dynamic friction between the ice and the model was determined experimentally. A 16 x 16 cm ice sample was cut from the ice sheet in the test basin and inserted into an ice sample holder. The sample was placed on the hull bottom, which had previously been levelled, and loaded with a normal force N of 86.7 N. The sample was then manually pulled along the hull at about 1 cm/sec through a push-pull gauge. The pulling force T was recorded and the coefficient of friction was calculated by:

(1) $$f = T/N$$

Both top and bottom surfaces of the ice were tested, under wet and dry conditions, with little variation in the resulting coefficient of friction (friction values are listed in Table 6). The overall average friction factor was 0.091. This value is very low because of the very smooth surface of the fibreglass model's hull. The full scale ship is likely to have a much higher friction factor of approximately 0.3 to 0.4.

4.0 MEASUREMENT OF ICE PROPERTIES

The flexural strength, σ_f, and ice thickness, h_i, were monitored during the ice warm-up period prior to testing. A set of five small cantilever beams (beam length L equal to 5 to 7 times the ice thickness, and beam width W equal to about twice the thickness) were cut in the ice at various locations about 1 m from the tank walls. The load P on the beam was applied manually with a hand held push-pull gauge and failure occurred in about 1 sec. The flexural strength was calculated from the following formula:

$$\sigma_f = \frac{6\ PL}{Wh_i^2} \qquad (2)$$

where P is the load at failure. The ice thickness was measured with a precision caliper with a resolution of 0.01 mm.

The effective modulus of elasticity was also measured during the ice warm-up. A load P was applied near the center of the ice sheet and the resulting deflection δ was measured by a dial indicator. The characteristic length of the ice was determined by considering the ice sheet as an elastic plate on an elastic foundation, which leads to the following formula (Reference 10):

$$l = \left(\frac{1}{2\pi\rho g}\ k_{ei}\ (r/l)\right)^{\frac{1}{3}}\ (P/\delta)^{\frac{1}{3}} \qquad (3)$$

where k_{ei} (r/l) is a modified Bessel function equal to $\pi/4$ if the deflection is measured at the point of load application. For the particular units P in kg, δ in inches, and l in cm, which were specifically given by the instruments used in the Hydraulics Laboratory, this equation then reduces to:

$$(4) \qquad l = 7\sqrt{P/\delta}$$

The effective modulus may then be obtained by:

$$(5) \qquad E = \frac{12\ \rho g\ (1-\mu^2) l^4}{h_i^3}$$

where μ is Poisson's ratio and is assumed to be 1/3 for ice. This equation can be simplified to :

$$(6) \qquad E = 0.0011\ \frac{l^4}{h_i^3}$$

for h_i in cm, l in cm, and E in MPa.

5.0 EXPERIMENTAL PROCEDURES

The ice tank at the Hydraulics Laboratory measures 20 x 7 x 1 m. Since the 1:20 scale model is about 5 m long the useable length of each ice sheet was about 12 m, and therefore, to ensure at least two model lengths for each test only one run per ice sheet could be made. A total of nine runs was completed: three runs at each of the three speeds (0.15, 0.30, 0.60 m/s, or 1.3, 2.6, 5.2 knots full scale), at nominal thicknesses and flexural strengths of 3.5 cm, 40 kPa; 3.5 cm, 20 kPa; and 2.25 cm, 40 kPa.

The model was attached to the carriage through a towing system which allowed it freedom to roll, pitch and heave. The pitch and roll axes were located at the centers of gravity of the model. The model was restrained in sway and surge by the towing post, which had a natural frequency of 2.1 hz. The yaw restraint consisted of a vertical pole, attached to the carriage, which extended down into the bow section of the model between two roller guides fixed to the model. The stiffness of this system is not very important since the ice tends to have a stabilizing effect on yaw motion if the model enters the ice sheet on a straight course.

A 100 lb. capacity force block was used to measure model resistance. The resistance and model motions, pitch angle, roll angle, and heave displacement, were sampled at a rate of 100 samples per second. The voltage signals from the model were digitized and then recorded on magnetic tape for later analysis. Typical force and motion records are shown in Figure 4.

The model's resistance is largely a function of ice thickness, so immediately after each run the thickness was measured at 1 m intervals along both sides of the model's path.

6.0 ANALYSIS OF TEST RESULTS

The results obtained from tests with the 1:20 scale model are presented in Table 7. R_{it} is the total resistance in ice, taken as the average measured resistance over a selected time interval of the run. Different intervals selected from the same run gave a maximum variation in R_{it} of about 10 percent. The longest time interval with the least force variation was then chosen for use in the final analysis. The test distance for each time interval is about one and one-half model lengths (between 6 and 9 m).

R_{ow} is the resistance in ice-free water taken from the test results given in Reference 8. This open-water resistance is a very small part, 1 to 7 percent, of the total resistance in ice. The percentage of open-water resistance to total ice resistance increases with increasing Froude number, but is not dependent on the Cauchy number.

The level ice resistance, R_i, was calculated as $R_i = R_{it} - R_{ow}$. This ice resistance was normalized by $\gamma B h_i^2$ where γ is the specific weight of water, equal to 9.84 kN/m^3, B is the model's maximum waterline beam, equal to 0.969m, and h_i is the ice thickness. The ice thickness used in the analysis is the average of thicknesses at 1 m intervals on each side of the model's path within the time interval previously selected for the average measured resistance.

The dimensionless ice resistance is considered to be a function of the dimensionless bending strength or Cauchy number, $C_n = \sigma_f/\gamma h_i$, and the dimensionless velocity or Froude number, $Fn = V/\sqrt{gh_i}$. In Figure 5 the dimensionless resistance is plotted as functions of the Froude and Cauchy numbers and polynomial curves are fitted to the data points by the least squares method. The polynomial coefficients are given in the following equation, which may be used to predict the dimensionless resistance for a given Froude and Cauchy number within the range of the experimental data:

(7) $$R_i/\gamma B h_i^2 = 4.9821 + 0.4131\ Fn - 0.0065\ Cn + 0.0403\ FnCn$$

with a standard deviation of 0.2893.

7.0 COMPARISON OF 1:20 AND 1:40 SCALE MODELS

The test data obtained from the 1:40 scale model tests is given in Table 8. A comparison between the 1:20 and 1:40 scale test results was made by plotting the dimensionless ice resistance as a function of the product Cn x Fn. This graph, Figure 6, shows that there is a fairly good agreement between the two models although the resistance obtained from the 1:20 scale tests is, on the average, a little greater than that from the 1:40 scale tests, for the same Cn x Fn.

The reason for the difference in resistance may be due to differences in the hull surface finishes. The measured ice-hull friction coefficient for the 1:20 scale model was 0.09 while that of the 1:40 scale model was 0.05. Another factor which may have led to some difference in the resistance is a scale effect in the breaking component of the ice resistance.

8.0 COMPARISON OF FIELD TRIALS AND MODEL PREDICTIONS

Full scale data from field trials on the CCGS Franklin in Lake Melville, Labrador, is given in Table 9. Only the data within the range of the experimental parameters (V, h_i, σ_f), or nearly so, was used for comparison with the model predictions.

The major difference between the field trials and the model tests was the presence of a snow cover which was not modelled in the laboratory tests. This snow cover added another resistance component, R_s, to the full scale trials due to increased frictional effects on the ship's hull. For lack of a better predictor the following formula, proposed by Carter (Reference 1), was used to calculate the resistance due to snow cover:

(8) $$R_s = kh_s$$

where $k = 900$ when R_s is in kN and h_s, the snow cover thickness, is in m.

This snow resistance makes up a large part of the total resistance in ice (up to about 50 percent for 50 cm of snow, using Carter's formula), so it is very important to have an accurate estimator for this resistance. Therefore more and better full scale data is needed in order to assess the effect of snow cover on the ship's performance.

The level ice resistance for the ship was calculated as $R_i = R_{it} - R_{ow} - R_s$. R_{ow} was obtained from the open water resistance tests on model 327 (Reference 8), and R_{it} was calculated from the field trial data:

(9) $$R_{it} = T_A(1 - t)$$

where T_A is the total measured thrust and t is the thrust deduction coefficient which was estimated from data obtained from model propulsion tests in ice-free water (Reference 8).

The full scale ice resistance predicted by the model tests is equal to, under the Froude scaling law, $c\lambda^3$ times the model resistance, where λ is the model scale factor and c is the ratio of prototype to model fluid density. The model's dimensionless resistance for the full scale Froude and Cauchy numbers was calculated from equation 7 and then multiplied by $\gamma B h_i^2 \times c\lambda^3$ to obtain the predicted level ice resistance for the ship.

The level ice resistance calculated from the field trials and that predicted for the full scale from model results are listed in Table 10 and are compared in Figure 7. As can be seen from this graph, the predicted resistance is higher than the calculated resistance by an average of 18.6 percent.

In Figure 8 the dimensionless resistance calculated from the field trials data is compared to the model test results and the predicted full scale results (from equation 7) by plotting dimensionless resistance against Cn x Fn. As can be seen from this plot, the resistance from the field trials is, on the average, slightly less than that predicted from the model results.

9.0 COMPARISON WITH OTHER ICE MODEL BASINS

A comparison of the IMD test results and those from the other ice model basins (CRREL, ARCTEC, NHL, AARI, SRI, and WADAM; References 1, 2, 3, 4, 5, 6) was made by nondimensionalizing the ice resistance, R_i, by γBh_i^2 and plotting this against Cn x Fn. The data for the comparisons was taken from the measured model data, except for that from the AARI and NHL tanks. At these two tanks a correction factor for the ice strength was incorporated in the analysis, so the data from their full scale predictions was used for comparison purposes. The plot of $R_i/\gamma Bh_i^2$ vs Cn x Fn, Figure 9, shows that there is fairly good agreement between most of the data plotted. The resistance obtained from the SRI tank seems to be significantly less than the main group of data points, while most of the data from the NHL tank is much greater.

As another form of comparison, the regression equation obtained from the IMD data, $R_i/\gamma Bh_i^2 = 4.9821 + 0.4131Fn - 0.0065Cn + 0.0403FnCn$, was used to predict the resistance from the other ice tanks, given the variables h_i, σ_f, and V. This predicted ice resistance was then plotted against the measured ice resistance for each tank (except for the AARI and NHL tanks where the model ice resistance was calculated from the full scale predictions) to which a straight line was fit by the least squares method. This graph, Figure 10, shows that the IMD regression equation predicts resistance values which are in very good agreement, though they are slightly overpredicted, with those from the CRREL, ARCTEC, AARI, and WADAM model ice basins. The

regression equation greatly overpredicts the resistance for the SRI tank and underpredicts the resistance for the NHL tank. This indicates that the resistance measured at SRI was much less, and that measured at NHL much greater, than that from the other tanks for the same ice and ship conditions.

There were some small differences in ice and model conditions between the ice tanks which could have led to some differences in the resulting resistance data. The ice-hull friction values were approximately the same at all the ice tanks (about 0.05) except for the AARI and NHL tanks, which reported friction values of about 0.08 and 0.11 respectively, and the IMD which measured 0.091. The difference in friction values between the IMD and the CRREL, ARCTEC, and WADAM tanks could account for the slight overprediction in resistance values for these three tanks.

All tanks used a 1:20 scale model except for the AARI and NHL tanks which tested the smaller 1:40 scale model. The type of ice used for the model tests also differed between the ice tanks. The IMD and CRREL tanks used urea ice (at slightly different urea concentrations) and very similar ice management techniques. The ARCTEC, WADAM, SRI, and AARI tanks all used saline ice and, though not documented in the reports, probably used different salinities and ice management procedures. NHL is the only tank which used an artificial ice material. All tanks used similar analysis for calculation of the ice resistance.

10.0 CONCLUSIONS

1. The level ice resistance predicted by the 1:20 scale model tests for the full scale ship was, on the average, 18.6 percent greater than that calculated from the field trial measurements. This is a very good agreement but considering that the model's ice-hull friction coefficient, as measured after the ice tests, was significantly lower than that estimated for the full scale ship, it is probably not quite as good as it first seems. The discrepancy between the model and full scale results could be due to several reasons:

   a. different methods and results of ice property measurements between the model and full scale;

   b. scale effects in the breaking component of the ice resistance between the model and full scale, due to incorrect modelling of the ice fracture toughness (fracture toughness of urea model ice is two to three times greater than the corresponding value for sea ice, Reference 12);

   c. incorrect thrust deduction coefficients, as these were estimated from propulsion tests in ice-free water;

   d. an inaccurate formula for the calculation of resistance due to snow cover, or;

   e. a combination of the above.

2. The 1:40 scale model results show a dimensionless resistance which is a little less than that from the 1:20 scale tests. This could be due to a lower ice-hull friction coefficient for the 1:40 scale than for the 1:20 scale model.

3. Much more and better data from full scale trials is needed. Methods and procedures for the measurement of ice properties and ship performance and responses should be standardized so that the full scale data can be analyzed more easily and compared to model predictions. The effect of snow cover should also be investigated in both full scale and model experiments.

11.0 ACKNOWLEDGEMENTS

I wish to acknowledge the cooperation of the Hydraulics Laboratory in supplying the ice tank facility, and the support of Mr. Rob Bowen for managing the ice sheet production. I also wish to thank all those who participated in the model preparations and in carrying out the experiments.

12.0 REFERENCES

1. Tatinclaux, Jean-Claude
"Model Tests in Ice of a Canadian Coast Guard R-Class Icebreaker", U.S. Army Corps of Engineers, Cold Regions Research and Engineering Laboratory, Hanover, New Hampshire, Special Report 84-6, April 1984.

2. Bulat, V. and Glen, I.F.
"The Testing of a Ship Model in Ice for the National Research Council", Arctec Canada Limited, Kanata, Ontario, Report FR335C-4, August 1981.

3. Herfjord, Kjell
"Model Tests in Ice on Canadian Coast Guard R-Class Icebreaker", Norwegian Hydrodynamic Laboratories, Ship and Ocean Laboratory Division, Trondheim, Norway, Report NHL 181096, May 1981.

4. "Model Test Results in the AARI Ice Tank of Canadian R-Class Icebreaker", The Arctic and Antarctic Research Institute, Leningrad, 1981.

5. Kitagawa, K.
"Test Results with R-Class Icebreaker Model in Level Ice", Ship Research Institute, Japan, September 1983.

6. Heideman, Torsten
"Model Tests in Level Ice with the Canadian Arctic R-Class Icebreaker", Wartsila Helsinki Shipyard, Wartsila Arctic Design and Marketing, December 1982.

7. Michailidis, M., and Murdey, D.C.
"Performance of CCGS Franklin in Lake Melville, 1980", Paper No. 24, The Society of Naval Architects and Marine Engineers Spring Meeting/STAR Symposium, Ottawa, June 17 - 19, 1981.

8. Murdey, D.C.
"Resistance and Propulsion Experiments with Model 327-1 and Propellers 66L and 66R", Marine Dynamics and Ship Laboratory, Report LTR-SH-269, March 1980.

9. Bhattacharyya, Rameswar
Dynamics of Marine Vehicles, John Wiley & Sons, New York, 1978, pp. 63 - 84.

10. Sodhi, D.S., Kato, K., Haynes, F.D., and Hirayama, K.
"Determining the Characteristic Length of Model Ice Sheets", Cold Regions Science and Technology 6, 1982.

11. Carter, D.
"Ship Resistance to Continuous Motion in Level Ice", Transport Canada Research and Development Centre, Report TP-3679E, March 1983.

12. Timco, G.W.
"Flexural Strength and Fracture Toughness of Urea Model Ice", Hydraulics Laboratory, National Research Council of Canada, Proc. 4th International Symposium on Offshore Mechanics and Arctic Engineering, Dallas, February, 1985.

Table 1

LTR-SH-383

MODEL 327
R-CLASS ICE BREAKER
ITTC TEST DRAFTS

HYDROSTATIC PARTICULARS FOR MODEL OF SCALE 1/20 WITHOUT APPENDAGES

LENGTH BETWEEN PERPENDICULARS (LPP), M	4.397
LENGTH ON WATERLINE (LWL), M	4.650
WATERLINE BEAM AT MIDSHIPS, M	0.968
WATERLINE BEAM AT MAXIMUM SECTION, M	0.968
MAXIMUM WATERLINE BEAM, M	0.969
DRAFT AT MIDSHIPS, M	0.347
DRAFT AT MAXIMUM SECTION, M	0.349
DRAFT AT AFT PERPENDICULAR, M	0.358
DRAFT AT FORWARD PERPENDICULAR, M	0.335
EQUIVALENT LEVEL KEEL DRAFT, M	0.347
MAXIMUM SECTION FORWARD OF MIDSHIPS, M	-0.370
PARALLEL MIDDLE BODY, FROM, AFT OF MIDSHIPS, M	0.370
TO, FORWARD OF MIDSHIPS, M	-0.370
AREA OF MAXIMUM STATION, SQ. M	0.309
CENTER OF BUOYANCY FORWARD OF MIDSHIPS (LCB), M	0.016
CENTER OF BUOYANCY ABOVE KEEL, M	0.194
WETTED SURFACE AREA, SQ. M	5.339
VOLUME OF DISPLACEMENT, CU. M	0.954
DISPLACEMENT, KG OF FRESH WATER	953.7
CENTER OF FLOATATION FORWARD OF MIDSHIPS (LCF), M	-0.035
CENTER OF FLOATATION ABOVE KEEL, M	0.347
AREA OF WATERLINE PLANE, SQ. M	3.598
TRANSVERSE METACENTRIC RADIUS (BM), M	0.244
LONGITUDINAL METACENTRIC RADIUS (BML), M	4.800
CENTER OF AREA OF PROFILE PLANE FORWARD OF MIDSHIPS (CLR), M	-0.039
CENTER OF AREA OF PROFILE PLANE ABOVE KEEL, M	0.179
AREA OF PROFILE PLANE, SQ. M	1.405

INCLUDING BOSSINGS, ICE HORN AND RUDDER

VOLUME OF DISPLACEMENT, CU. M	0.957
DISPLACEMENT, KG OF FRESH WATER	956.9
CENTER OF BUOYANCY FORWARD OF MIDSHIPS	-0.023

Table 2

LTR-SH-383

MODEL 327
R-CLASS ICEBREAKER
ITTC TEST DRAFTS

HYDROSTATIC PARTICULARS FOR A FULL SIZED SHIP WITHOUT APPENDAGES

LENGTH BETWEEN PERPENDICULARS (LPP), M	87.93
LENGTH ON WATERLINE (LWL), M	93.00
WATERLINE BEAM AT MIDSHIPS, M	19.36
WATERLINE BEAM AT MAXIMUM SECTION, M	19.36
MAXIMUM WATERLINE BEAM, M	19.37
DRAFT AT MIDSHIPS, M	6.93
DRAFT AT MAXIMUM SECTION, M	6.97
DRAFT AT AFT PERPENDICULAR, M	7.16
DRAFT AT FORWARD PERPENDICULAR, M	6.71
EQUIVALENT LEVEL KEEL DRAFT, M	6.94
MAXIMUM SECTION FORWARD OF MIDSHIPS, M	-7.39
PARALLEL MIDDLE BODY, FROM, AFT OF MIDSHIPS, M	7.39
TO, FORWARD OF MIDSHIPS, M	-7.39
AREA OF MAXIMUM STATION, SQ. M	123.41
CENTER OF BUOYANCY FORWARD OF MIDSHIPS (LCB), M	-0.33
CENTER OF BUOYANCY ABOVE KEEL, M	3.88
WETTED SURFACE AREA, SQ. M	2135.52
VOLUME OF DISPLACEMENT, CU. M	7629.27
DISPLACEMENT, TONNES OF SALT WATER	7820.00
CENTER OF FLOATATION FORWARD OF MIDSHIPS (LCF), M	-0.69
CENTER OF FLOATATION ABOVE KEEL, M	6.94
AREA OF WATERLINE PLANE, SQ. M	1439.10
TRANSVERSE METACENTRIC RADIUS (BM), M	4.89
LONGITUDINAL METACENTRIC RADIUS (BML), M	96.00
CENTER OF AREA OF PROFILE PLANE FORWARD OF MIDSHIPS (CLR), M	-0.77
CENTER OF AREA OF PROFILE PLANE ABOVE KEEL, M	3.57
AREA OF PROFILE PLANE, SQ. M	562.05

MODEL 327
R-CLASS ICE BREAKER
ITTC TEST DRAFTS

COEFFICIENTS OF FORM FOR NAKED HULL

COEFFICIENTS BASED ON: LENGTH ON WATERLINE
MAXIMUM BEAM
EQUIVALENT LEVEL KEEL DRAFT

L/B	4.802
L/T	13.407
B/T	2.792
LCB %L FORWARD OF MIDSHIPS	-0.355
LCF %L FORWARD OF MIDSHIPS	-0.743
CLR %L FORWARD OF MISHIPS	-0.832
CB	0.611
CMAX	0.918
CP	0.665
CW	0.799
CIX	0.662
CIY	0.564
BM/B	0.252
BML/L	1.032
KB/T	0.560
BEAM - DISPLACEMENT RATIO (CIRCB)	0.984
DRAFT - DISPLACEMENT RATIO (CIRCT)	0.352
LENGTH - DISPLACEMENT RATIO (CIRCM)	4.724
WETTED SURFACE - DISPLACEMENT RATIO (CIRCS)	5.510
BM - DISPLACEMENT RATIO	0.248
BML - DISPLACEMENT RATIO	4.876
AREA OF PROFILE PLANE/LT	0.871

Table 4
LTR-SH-383

MODEL 327
R-CLASS ICE BREAKER
ITTC TEST DRAFTS

SUMMARY OF NORMALIZED STATION DATA

STATION	AREA	BEAM	DEPTH
0	0.023	0.246	0.146
1	0.132	0.518	0.767
2	0.341	0.709	0.997
3	0.567	0.830	0.994
4	0.759	0.903	0.991
5	0.880	0.948	0.987
6	0.948	0.980	0.984
7	0.987	0.998	0.981
8	0.999	1.000	0.978
9	0.999	1.000	0.975
10	0.995	0.999	0.971
11	0.990	0.999	0.968
12	0.981	0.999	0.965
13	0.960	0.997	0.962
14	0.919	0.988	0.959
15	0.848	0.961	0.955
16	0.736	0.904	0.952
17	0.565	0.801	0.949
18	0.331	0.632	0.921
19	0.097	0.399	0.422
20	0.008	0.127	0.131

AFT END OF WATERLINE IS AT -0.395
FORWARD END OF WATERLINE IS AT 20.758

AREA IS STATION AREA / MAXIMUM SECTION AREA
BEAM IS STATION BEAM / MAXIMUM WATERLINE BEAM
DEPTH IS STATION DEPTH / MAXIMUM DRAFT

Table 5
LTR-SH-383

MODEL 327
DETAILS OF RUDDER AND STERN ARRANGEMENT

RUDDER DETAILS

Chord, m	0.192
Span at stock, m	0.206
Thickness/chord ratio	0.143
Area (projected), m^2	0.041

LOCATION OF RUDDER STOCK

Forward of A.P., m	0.195

LOCATION OF PROPELLER CENTERS

Above keel, m	0.122
Forward of A.P., m	0.102
Out from centerline, m	0.221

Table 6
LTR-SH-383

MODEL 327
ICE-HULL FRICTION VALUES
(JUNE 1984)

Test Condition	Normal Force	Tangential Force	Friction Coefficient
	N	T	f=T/N
	(N)	(N)	
Ice Top Dry	86.7	7.89	0.091
	86.7	7.60	0.088
	86.7	7.36	0.085
	86.7	7.75	0.089
Ice Bottom Dry	86.7	7.31	0.084
	86.7	8.53	0.098
	86.7	7.60	0.088
	86.7	7.65	0.088
Ice Top Wet	86.7	6.28	0.072
	86.7	9.12	0.105
	86.7	7.99	0.092
	86.7	8.58	0.099
Ice Bottom Wet	86.7	7.40	0.085
	86.7	8.83	0.102
	86.7	8.63	0.099
	86.7	8.04	0.093

Overall average friction coefficient f=0.091

Table 7
LTR-SH-383

1:20 Scale Model Results

V (m/s)	h_i (cm)	σ_f (kPa)	R_{it} (N)	R_{ow} (N)	R_i (N)
0.15	3.64	37	75.5	0.6	74.9
0.6	3.61	40	121.6	4.3	117.3
0.15	3.73	15	66.8	0.6	66.2
0.3	3.33	42	78.0	1.5	76.5
0.3	2.46	38	52.5	1.5	51.0
0.3	4.08	25	97.0	1.5	95.5
0.6	2.47	30	61.1	4.3	56.8
0.6	3.77	20	85.0	4.3	80.7
0.15	2.19	36	36.7	0.6	36.1

Table 8
LTR-SH-383

1:40 Scale Model Results

V (m/s	h_i (cm)	σ_f (kPa)	R_{it} (N)	R_{ow} (N)	R_i (N)
0.08	2.85	48	14.0	0	14.0
0.40	3.07	48	27.9	0.3	27.6
0.22	2.89	48	16.9	0.1	16.8
0.22	2.46	50	11.6	0.1	11.5
0.3	2.90	35	30.9	0.2	30.7
0.3	2.80	27	19.4	0.2	19.2
0.3	3.10	29	24.0	0.2	23.8
0.3	3.10	42	37.9	0.2	37.7
0.3	2.70	43	20.5	0.2	20.3
0.3	2.60	43	14.5	0.2	14.3
0.3	2.60	45	19.8	0.2	19.6

TABLE 9
LTR-SE-303

Full Scale Trial Results

V (m/s)	h_i (cm)	σ_f (kPa)	h_s (cm)	T_A* (kN)
1.12	70.4	510	8	578
2.38	62.0	480	13	648
2.77	67.4	460	9	707
2.08	67.6	460	15	827
1.82	73.8	300	52	1177
0.99	75.4	300	48	1094

*Total measured thrust

LEVEL ICE RESISTANCE
FULL SCALE AND PREDICTED VALUES

Full Scale							Predicted
Fn	Cn	t	$R_{it}=T_A(1-t)$ (kN)	R_s (kN)	R_{ow} (kN)	$R_i=R_{it}-R_s-R_{ow}$ (kN)	R_i (kN)
0.426	72.44	0.075	535	72	12	451	570
0.965	77.42	0.090	590	117	29	444	588
1.077	68.25	0.090	643	81	37	525	700
0.808	68.05	0.092	751	135	23	593	628
0.676	40.65	0.093	1068	468	20	580	644
0.364	39.79	0.062	1026	432	8	586	601

Table 10
LTR-SI-383

MODEL 327

BODY PLAN

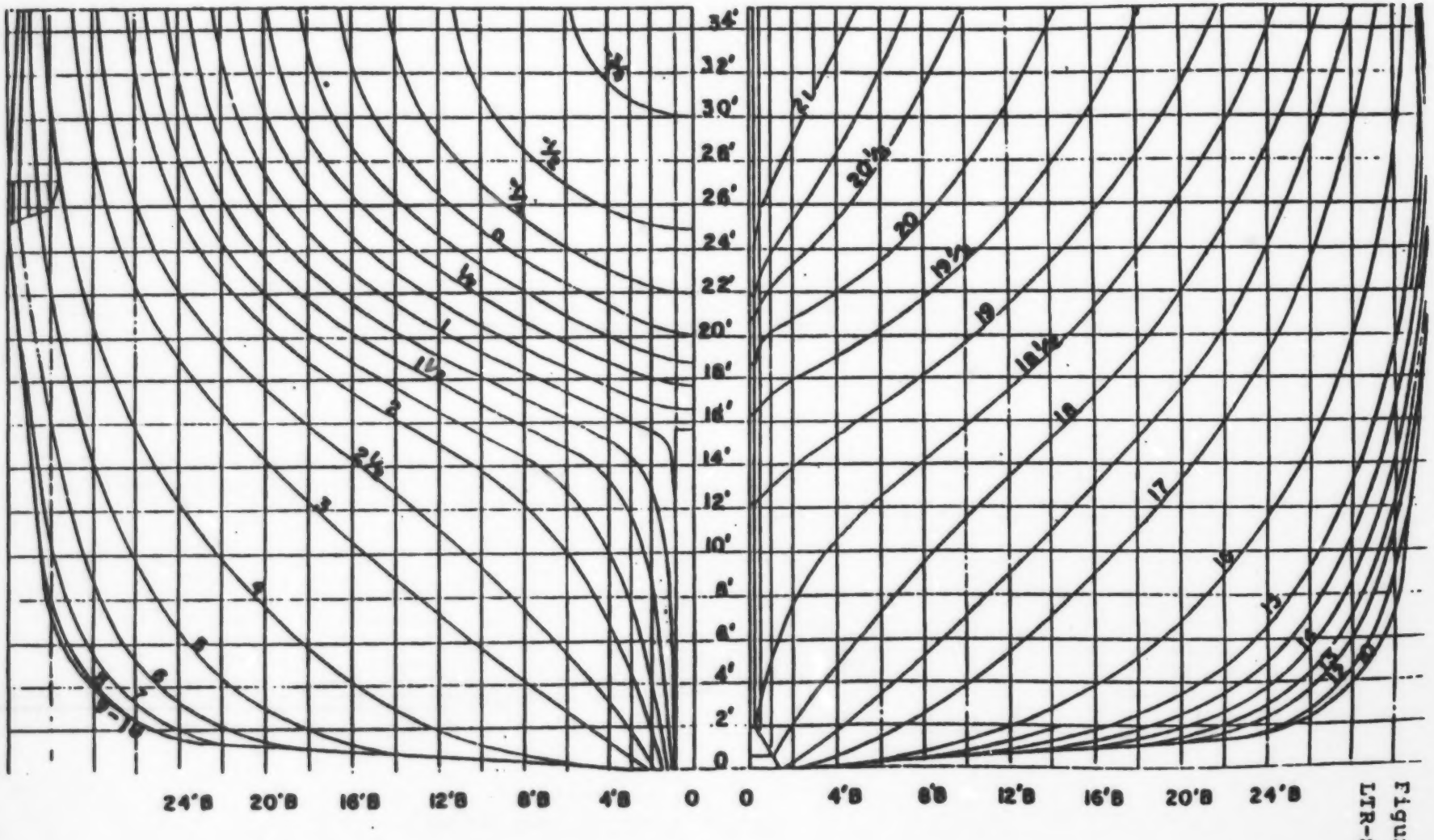

Figure 1
LTR-SH-383

BOW AND STERN LINES
MODEL 327

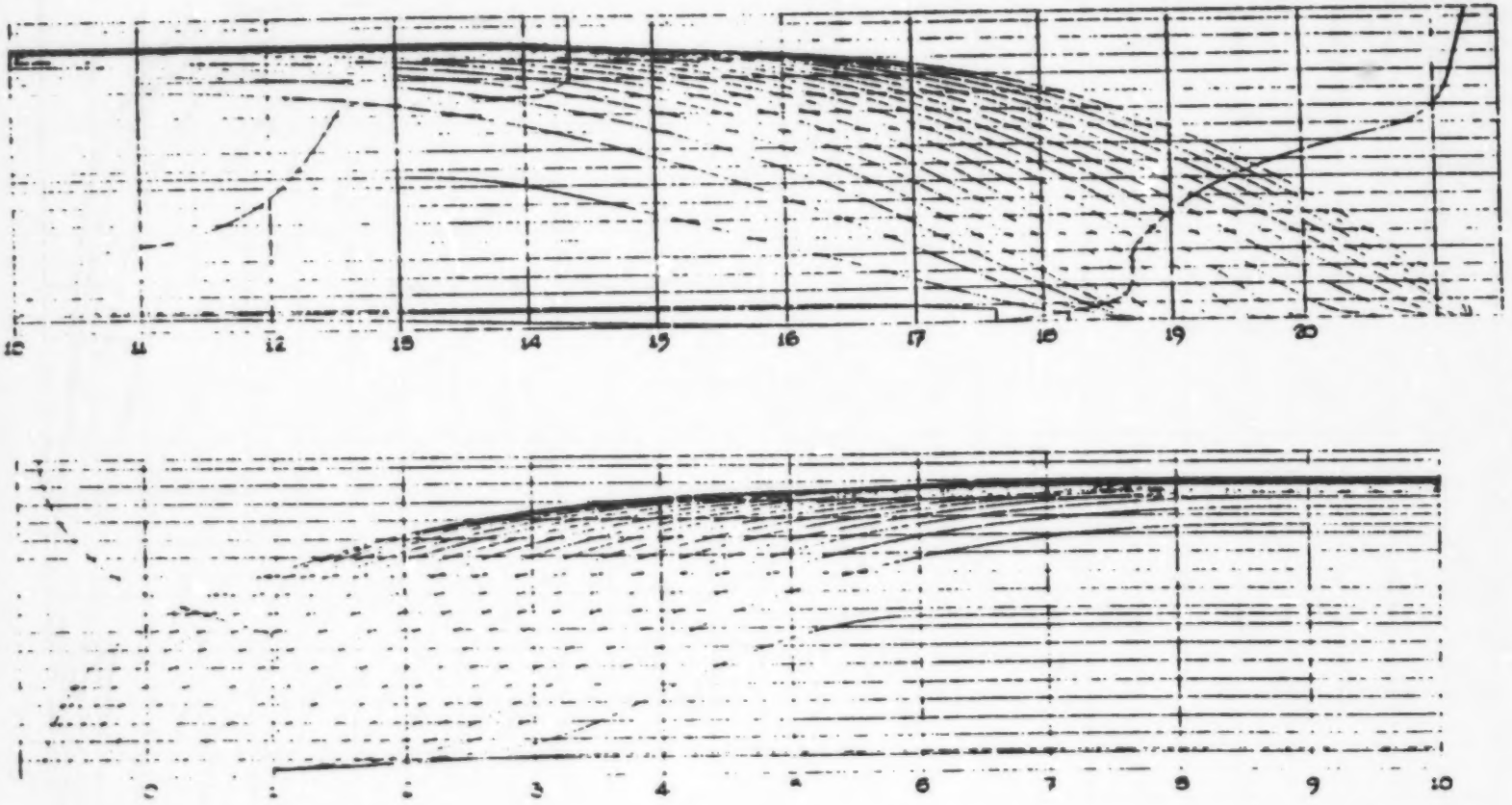

Figure 2
LTR-SH-383

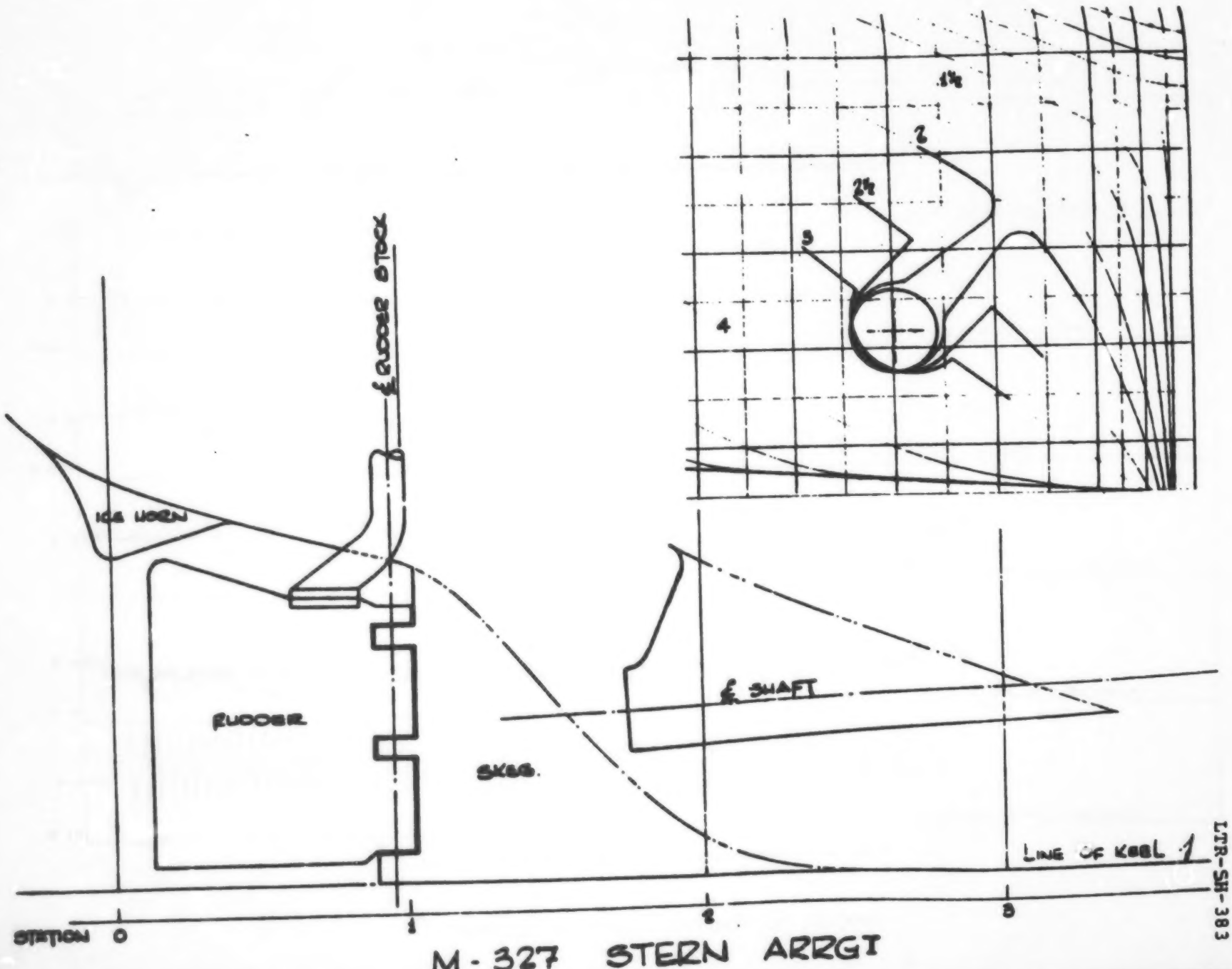

M-327 STERN ARRGT

Figure 3
LTR-SH-383

EXAMPLE OF FORCE AND MOTION RECORDS

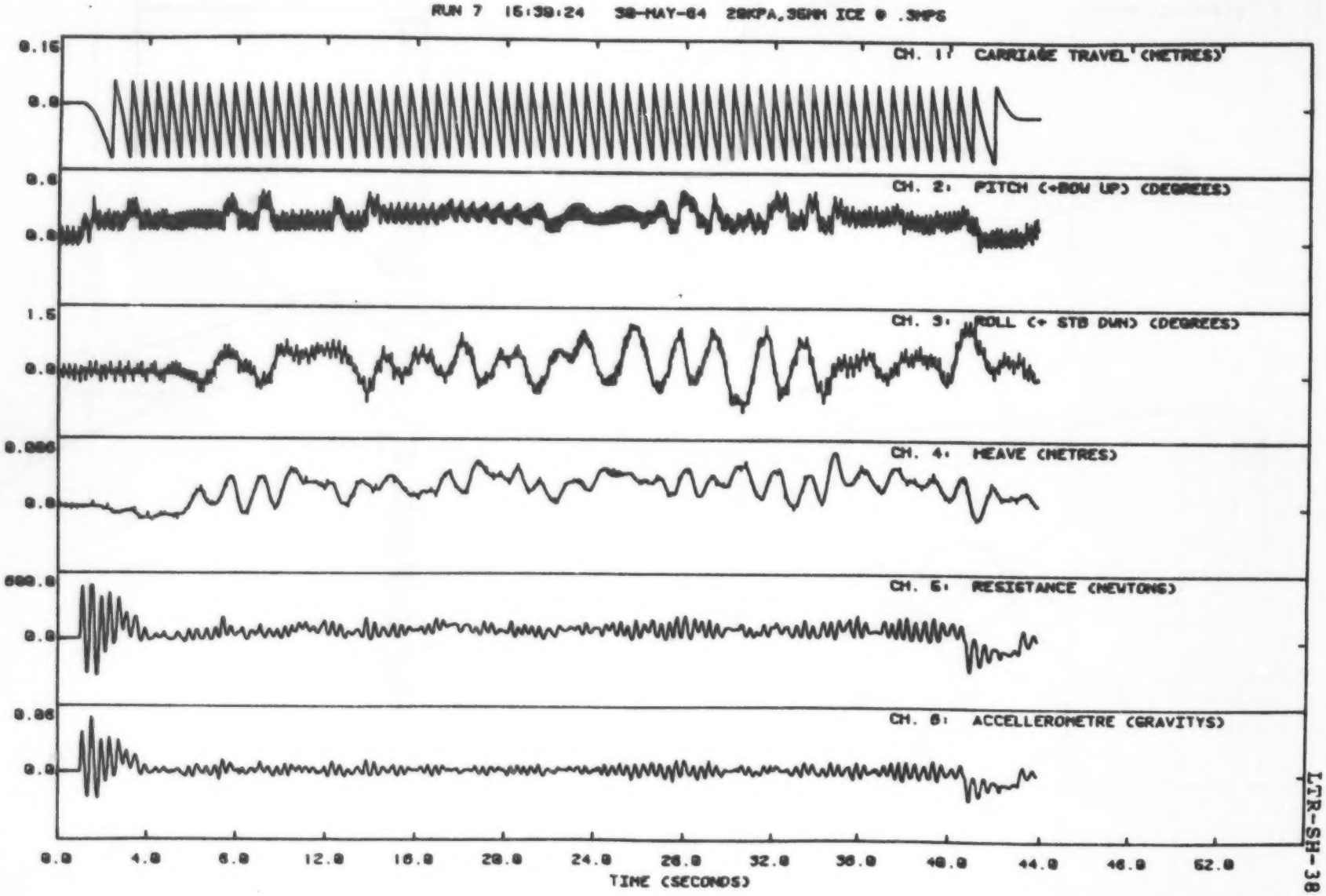

Figure 4
LTR-SH-383

1:20 SCALE DIMENSIONLESS RESISTANCE
AS FUNCTIONS OF Cn AND Fn

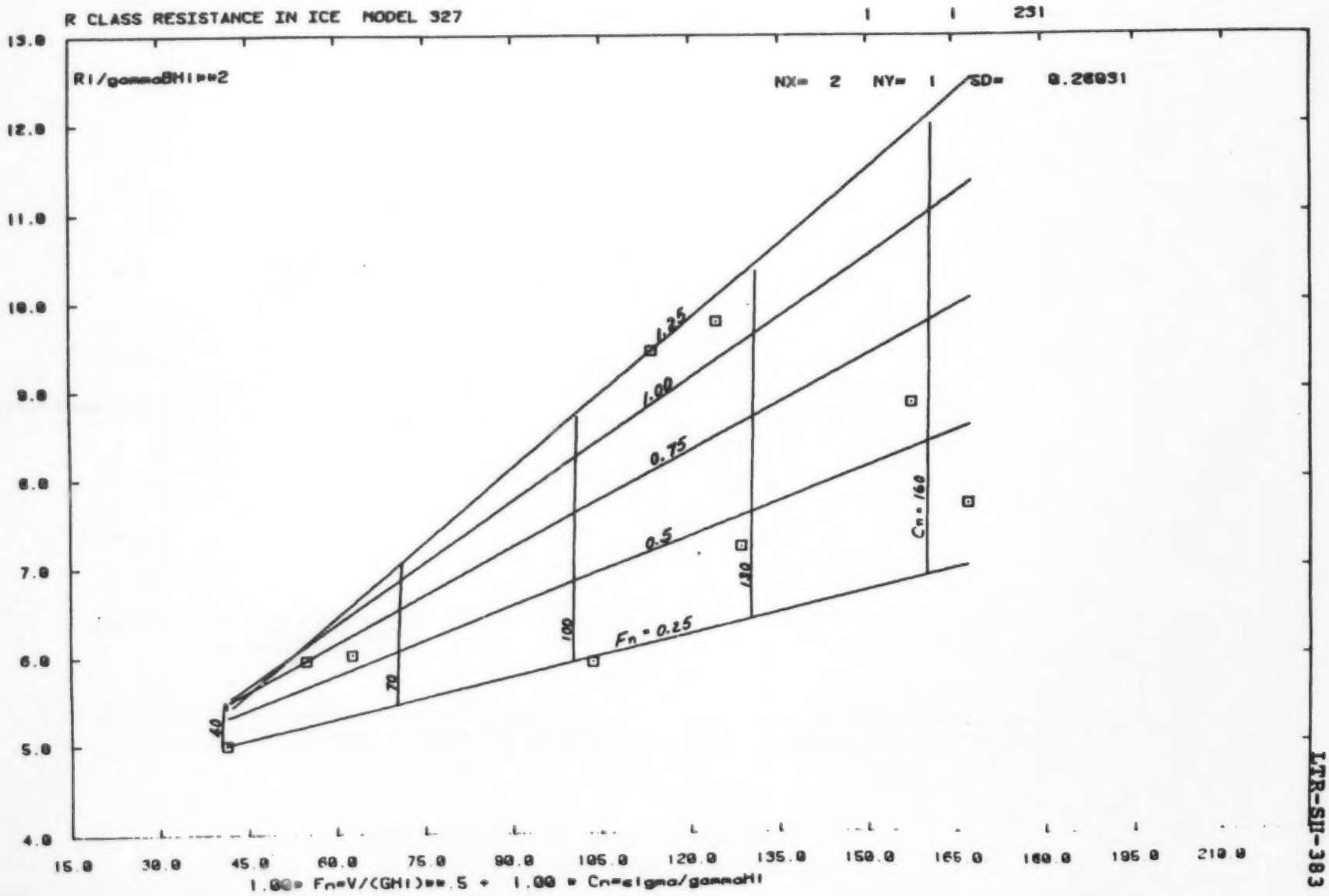

Figure 5
LTR-SH-383

1:20 AND 1:40 SCALE DIMENSIONLESS
RESISTANCE AS A FUNCTION OF Cn x Fn

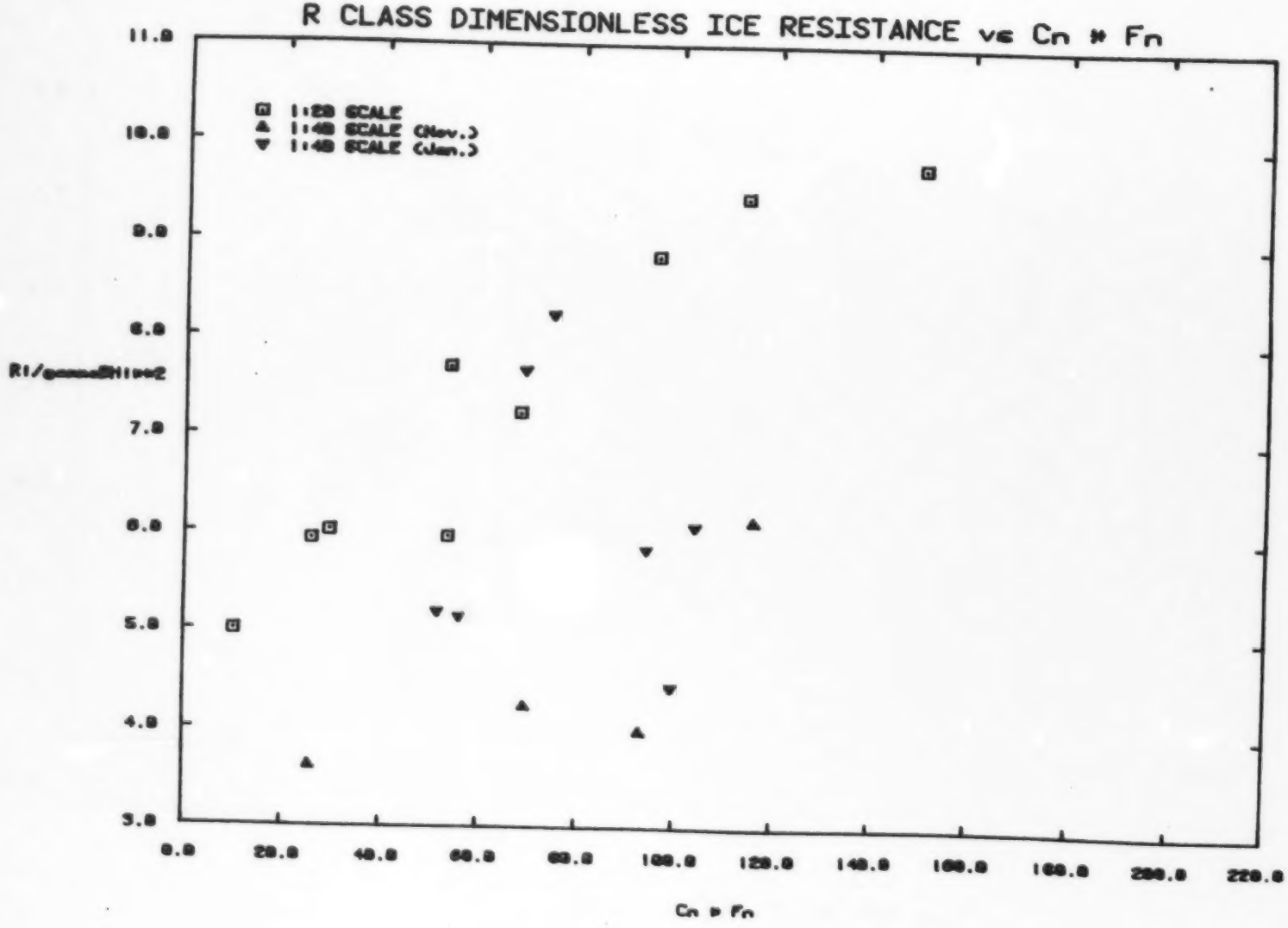

Figure 6
LTR-SH-383

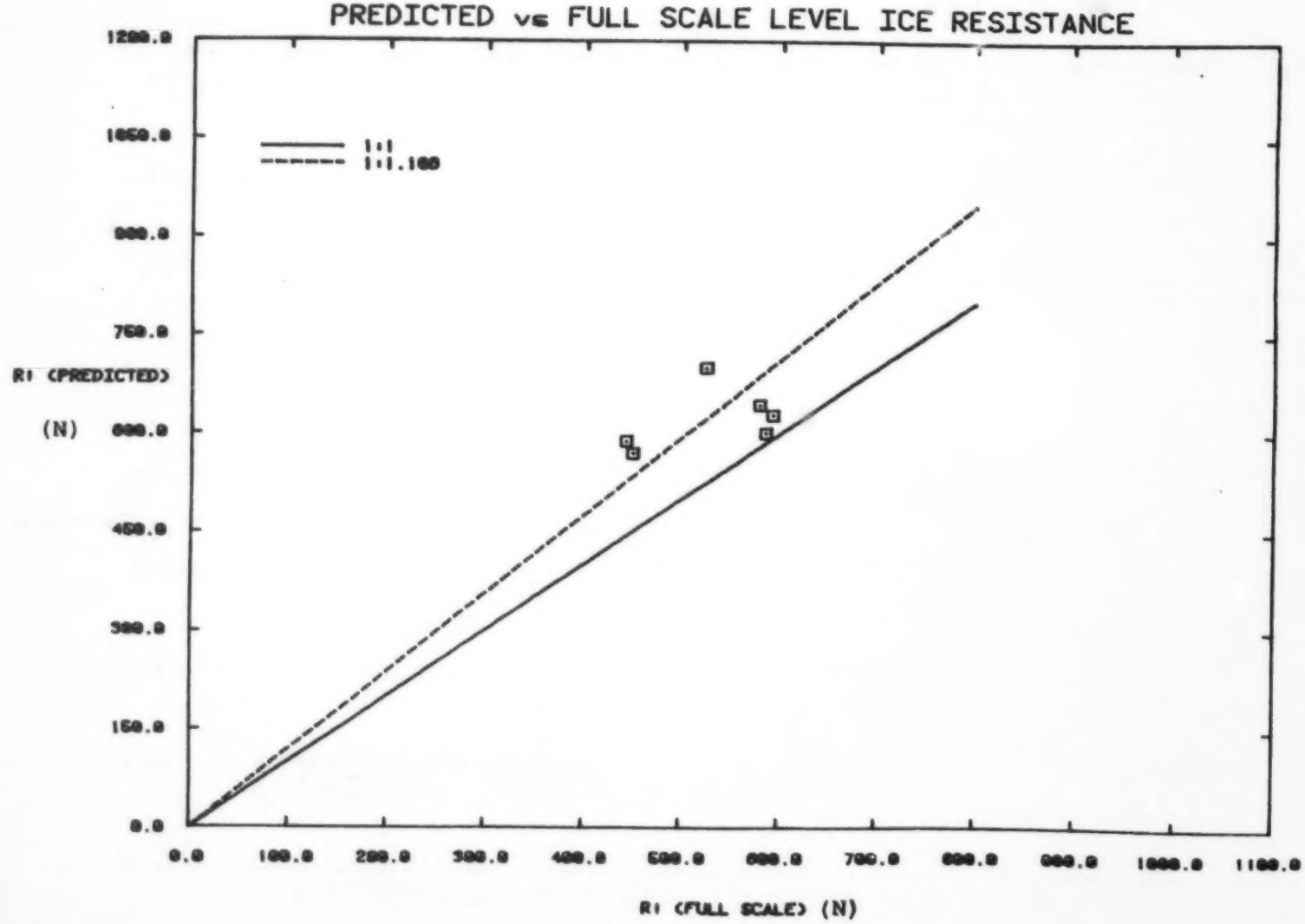

Figure 7
LTR-SE-333

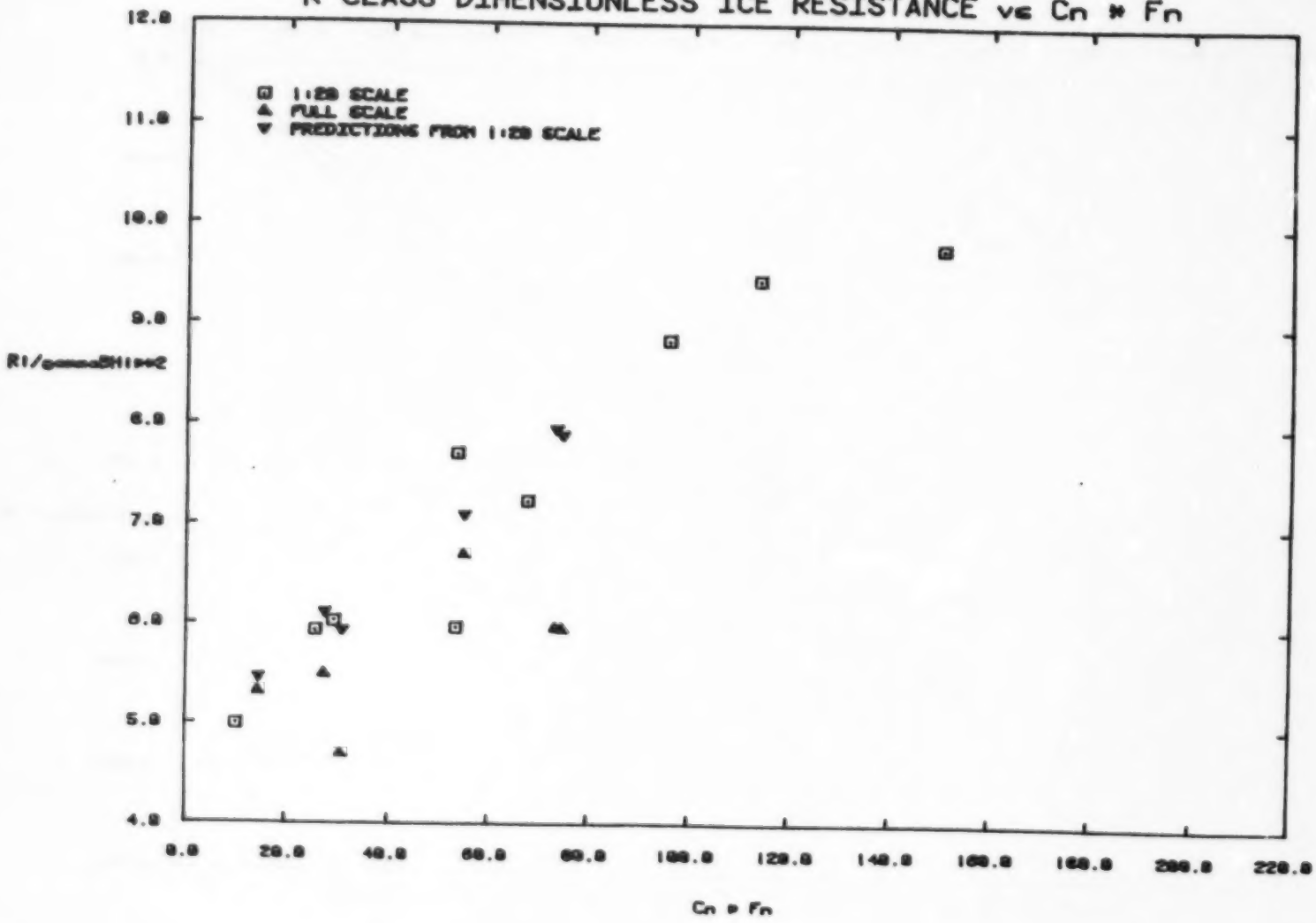

Figure 8
LTR-ST-333

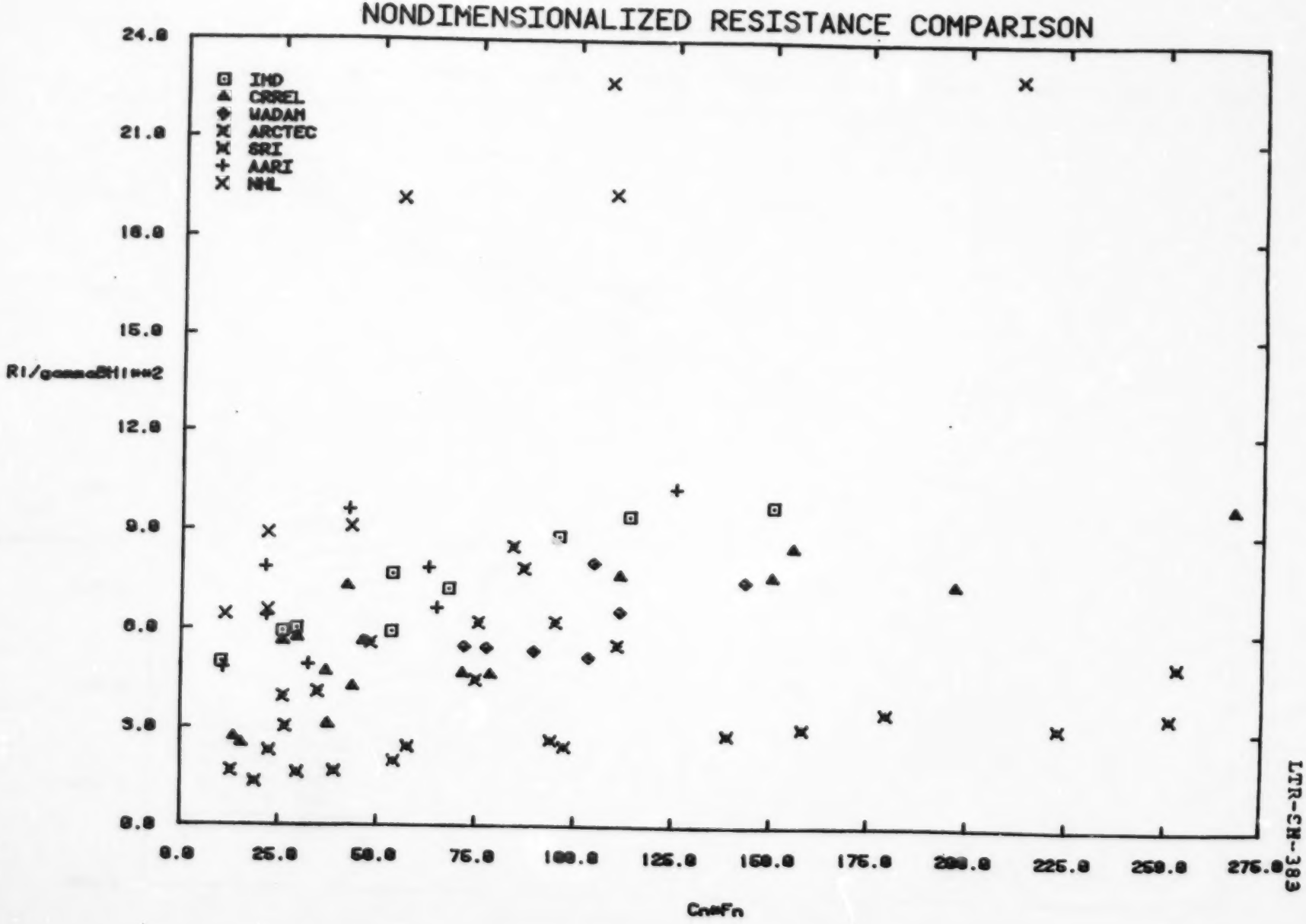

Figure 9
LTR-SN-383

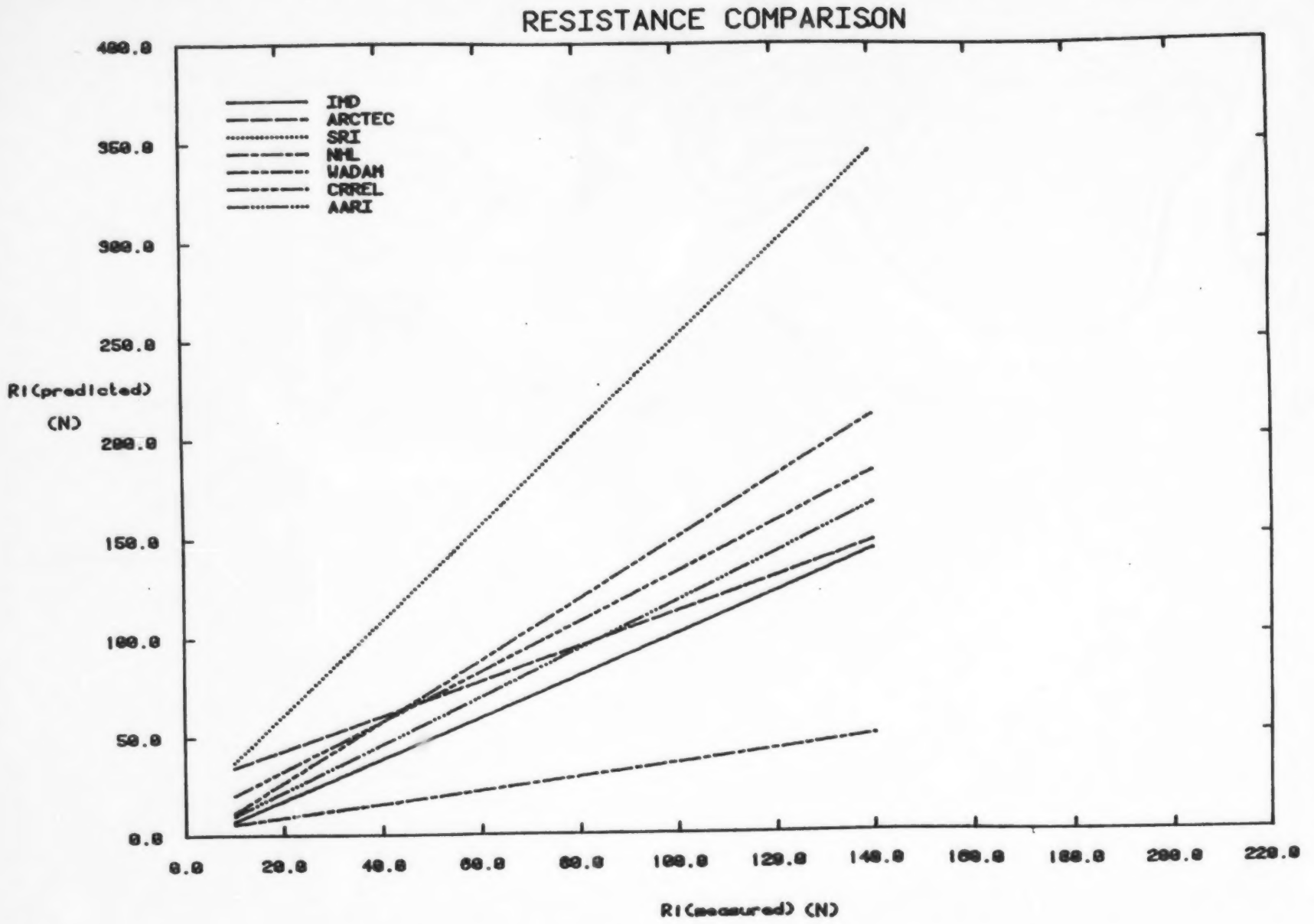

Figure 10
LTR-SH-383